DOT/FAA/TC-12/40

Federal Aviation Administration
William J. Hughes Technical Center
Aviation Research Division
Atlantic City International Airport
New Jersey 08405

Smart Patch System to Detect Fatigue Cracks and Damage in Rotorcraft Structures

February 2014

Final Report

This document is available to the U.S. public through the National Technical Information Services (NTIS), Springfield, Virginia 22161.

This document is also available from the Federal Aviation Administration William J. Hughes Technical Center at actlibrary.tc.faa.gov.

U.S. Department of Transportation
Federal Aviation Administration

NOTICE

This document is disseminated under the sponsorship of the U.S. Department of Transportation in the interest of information exchange. The U.S. Government assumes no liability for the contents or use thereof. The U.S. Government does not endorse products or manufacturers. Trade or manufacturers' names appear herein solely because they are considered essential to the objective of this report. The findings and conclusions in this report are those of the author(s) and do not necessarily represent the views of the funding agency. This document does not constitute FAA policy. Consult the FAA sponsoring organization listed on the Technical Documentation page as to its use.

This report is available at the Federal Aviation Administration William J. Hughes Technical Center's Full-Text Technical Reports page: actlibrary.tc.faa.gov in Adobe Acrobat portable document format (PDF).

Technical Report Documentation Page

1. Report No.	2. Government Accession No.	3. Recipient's Catalog No.
DOT/FAA/TC-12/40		

4. Title and Subtitle	5. Report Date
SMART PATCH SYSTEM TO DETECT FATIGUE CRACKS AND DAMAGE IN ROTORCRAFT STRUCTURES	February 2014
	6. Performing Organization Code
7. Author(s)	8. Performing Organization Report No.
Shawn Beard, Amrita Kumar, and Roy Ikegami	
9. Performing Organization Name and Address	10. Work Unit No. (TRAIS)
Acellent Technologies, Inc. 835 Stewart Drive Sunnyvale, CA 94089	
	11. Contract or Grant No. DTFACT-05-C-00022
12. Sponsoring Agency Name and Address	13. Type of Report and Period Covered
U.S. Department of Transportation Federal Aviation Administration Southwest Region—Aircraft Certification Service, Rotorcraft Directorate 2601 Meacham Blvd. Fort Worth, TX 76137	Final Report
	14. Sponsoring Agency Code ASW-112

15. Supplementary Notes

The Federal Aviation Administration William J. Hughes Technical Center Aviation Research Division COR was Traci Stadtmueller.

16. Abstract

Monitoring the continued health of aircraft subsystems and identifying problems before they affect airworthiness has been a long-term goal of the aviation industry. This project demonstrated a Smart Patch System (SPS) that could be used for the in-service health monitoring of new and existing commercial rotorcraft structures. The objectives of this project were to:

- Develop, validate, and demonstrate SPS technologies, including advanced software, algorithms, and methodologies for structures and dynamic components to (1) detect fatigue cracks and damages before exceeding critical threshold or incipient failure and (2) characterize fatigue cracks and damages.
- Develop preliminary certification compliance requirements and a framework for certification of an SPS that would be integrated into a Health and Usage Monitoring System for fatigue crack monitoring of commercial rotorcraft structures per the guidelines provided in Federal Aviation Administration Advisory Circular 29-2C, Section MG-15.

This report describes the work conducted during a 5-year project. It presents the details on the tasks that were conducted toward the development, validation, and potential certification of an SPS for a specific structural application.

17. Key Words	18. Distribution Statement
Fatigue cracks, Health and Usage Monitoring System Software, Sensors, Functional hazards assessment	This document is available to the U.S. public through the National Technical Information Service (NTIS), Springfield, Virginia 22161. This document is also available from the Federal Aviation Administration William J. Hughes Technical Center at actlibrary.tc.faa.gov.

19. Security Classif. (of this report)	20. Security Classif. (of this page)	21. No. of Pages	22. Price
Unclassified	Unclassified	126	

Form DOT F 1700.7 (8-72) Reproduction of completed page authorized

TABLE OF CONTENTS

			Page
EXECUTIVE SUMMARY			x
1.	INTRODUCTION		1
	1.1	Objective	1
	1.2	Background	1
	1.3	Basic Approach for SPS Certification	3
2.	SMART PATCH SYSTEM		6
	2.1	Selection of Airframe Application	6
	2.2	The SPS Design—System Design and Optimization for Rotorcraft	15
	2.2.1	Smart Patch Design	16
	2.2.2	Sensor Optimization and Layout	19
	2.2.3	Damage Detection Software Development	23
	2.2.4	Reliability Issues—POD and False Alarm Rates, Sensor Reliability, and System Reliability	51
3.	TESTING AND VALIDATION FOR THE SPS SYSTEM		52
	3.1	Coupon Tests	52
	3.2	Component Tests	58
	3.3	Flight Tests	61
4.	IMPLEMENTATION AND TECHNOLOGY TRANSFER PLAN		67
	4.1	Intended Functions and Use	68
	4.2	Maturation	68
	4.3	System Development	70
	4.3.1	Determination of System Requirements	70
	4.3.2	Determination of System Criticality	70
	4.4	System Installation	74
	4.5	Certification for SPS	75
	4.5.1	Design Approval	75
	4.5.2	Production Approval	76

4.5.3 Installation Approval 76
4.5.4 Instructions for Continued Airworthiness 76

4.6 Benefit/Credit Validation 76

5. CONCLUSIONS 77

6. REFERENCES 79

APPENDICES

A—Functional Hazard Assessment
B—Coupon Test Report

LIST OF FIGURES

Figure		Page
1	Acellent's Basic SMART Layer SHM System	2
2	Functioning of the Active Sensing System	2
3	The SPS Certification Approach Framework	5
4	The S-76 Dynamic Components	6
5	Transmission Beam and Frame	8
6	Representative Frame and Beam Joint	9
7	Bulkhead	9
8	Fitting	10
9	Skins and Stringers	11
10	The MR Spindle	11
11	The TR Horn	12
12	Sensor Locations on the TR Horn	14
13	Gearbox Middle-Housing Clevis Fitting	14
14	The SPS	15
15	Example of Smart Patch	16
16	Smart Patch Components	17
17	Properties of the Piezoelectric Materials Used in the Smart Patch	19
18	Required Signal Path to Detect Notch on Opposite Side of 0.5″ and 1.0″ Plates	20
19	Determining Sensor Layout	21
20	Relationship Between Sensor Spacing, Structure Thickness, and Detectable Crack Size on the Opposite Face	22
21	The SPS Design for Gearbox Middle Clevis Fitting	23
22	Software Overview	25

23	The SPS System Diagram	27
24	The SPS Architecture	28
25	Sensor Layout Windows	30
26	Windows for DAQ Setup	31
27	Windows for Signal Path Definition	31
28	Window for Data Collection	32
29	Interface Displaying 3D Geometry	33
30	Self-Diagnostic Reasoning Process Compares Signals on Paths Going Directly Through Affected Sensors	34
31	Data Collection Based on Predefined Trigger	36
32	Temperature Calibration Process	37
33	Baseline Data and the Current Data File Selections	40
34	Selecting the Direct Path Image from the Applications Menu	40
35	Imaging Window	40
36	Controls to Adjust Threshold for Imaging	41
37	Controls to Select Analysis Methodologies	42
38	Controls to Select Time Windows for Imaging	43
39	Controls to Select Frequencies for Imaging	44
40	Controls to Select Paths for Imaging	45
41	Interface for Selecting and Ignoring Paths	45
42	Flowchart for Empirical-Based Damage Quantification Scheme	46
43	Window for Inputting Parameters	47
44	Damage Index Curves for Each Path	48
45	Damage Size Estimates and Uncertainty Values	49
46	Calibration for Both Environmental Compensation and Damage Quantification	50

47	Example of Signal-to-Noise Ratio for Usable Data	53
48	Test Specimens for Bolted Joint Test	54
49	Workspace of Data Acquisition Software	55
50	Test Setup	55
51	Image Highlighting Location of Structural Changes in Specimen 1	56
52	Image Highlighting Location of Structural Changes in Specimen 2	56
53	Damage Index vs. Cycles for Path 12 to 20 on Specimen 2	57
54	Detection Results for Specimen 3	57
55	Smart Patch Layers Installed on the Right-Hand Triplex Clevis on Gearbox Housing	59
56	Expected Crack Locations and Monitored Areas	59
57	Reflection-Based Analysis Highlighting Crack Area	60
58	Damage Index vs. Cycles Plot Showing the Reflection-Based Damage Index	61
59	SMART Layers Installed at Crack-Prone Area on Tailboom	62
60	All SMART Layers Are Connected to a Single Connector	62
61	Sensor Data Collected From EH-60L Black Hawk Flight Tests	63
62	Diagnostic Images From Tailboom	63
63	The Raptor-90 URV Airframe Component Chosen for Flight Tests	64
64	Seeded Faults on Sideframe	65
65	The Raptor-90 Airframe Component	65
66	The Raptor-90 Flight Test Stand	66
67	The SPS Sensor Layers Mounted on URV Component	67
68	The SPS Certification Process for Benefit/Credit Validation	68

LIST OF TABLES

Table		Page
1	The SPS Component Selection	13
2	Required Inputs to the Sensor Layout Module	30
3	Event Messages for HUMS Interface	51
4	Department of Defense TRL Definitions	69

LIST OF ACRONYMS

3D	Three-dimensional
AC	Advisory Circular
API	Application program interface
ARL	Army Research Laboratory
ASCOPE	Automated Simultaneous Constraint Optimized Parameter Extraction
CAD	Computer-aided design
CRADA	Cooperative Research and Development Agreement
DA	Design authority
DAQ	Data acquisition
EDM	Electrical discharge machining
FAA	Federal Aviation Administration
FHA	Functional Hazard Assessment
FMEA	Failure Mode and Effects Analysis
FMECA	Failure Mode, Effects, and Criticality Analysis
FTA	Fault Tree Analysis
HUMS	Health and Usage Monitoring System
ICA	Instructions for Continued Airworthiness
MR	Main rotor
MSA	Mean signal amplitude
NDI	Nondestructive inspection
OEM	Original equipment manufacturer
POD	Probability of detection
PZT	Lead zirconate titanate
QA	Quality assurance
SAC	Sikorsky Aircraft Corporation
SHM	Structural Health Monitoring
SMART	Stanford Multi-Actuator-Receiver Transduction
SPS	Smart Patch System
TR	Tail rotor
TRL	Technology Readiness Level
TSE	Total signal energy
URV	Unmanned rotorcraft vehicle

EXECUTIVE SUMMARY

Monitoring the continued health of aircraft subsystems and identifying problems before they affect airworthiness has been a long-term goal of the aviation industry. Because in-service conditions experienced by structures are generally complex and unknown, conservative calendar-based maintenance practices can be overly time-consuming, labor-intensive, and very expensive. Furthermore, as structures age, maintenance service frequency and costs increase while performance and availability decrease. Built-in sensor networks on the structure can provide crucial information regarding the condition and damage state of the structure. Diagnostic information from sensor data can be used to facilitate better decision making processes with respect to inspection and repair, e.g., repair versus no repair or replacement. Asset management can be performed based on the actual health and usage of the structure, thereby minimizing in-service failures and maintenance costs, while maximizing reliability and readiness.

The intent of this project was to develop a Smart Patch System (SPS) that can be used for the in-service monitoring of the health of new or existing commercial rotorcraft structural components. The overall goals of the system are as follows:

- Reduce the total structural inspection costs for rotorcraft structures.
- Avoid unplanned structural inspection/maintenance and catastrophic failures.
- Provide maintenance credit by reducing the number of maintenance activities when the structural condition assessment shows no need for the scheduled work.

The objectives of this project were to:

- Develop, validate, and demonstrate SPS technologies consisting of advanced software, algorithms, and methodologies for structures and dynamic components to (1) detect fatigue cracks and damages before exceeding critical threshold or incipient failure and (2) characterize fatigue cracks and damages.
- Develop preliminary certification compliance requirements and a framework for certification of an SPS that can be an integral part of a Health and Usage Monitoring System for the fatigue crack monitoring of commercial rotorcraft structures per the guidelines provided in Federal Aviation Administration Advisory Circular AC 29-2C, Section MG-15.

This report describes the details of the tasks conducted toward the SPS development and validation with focus on fatigue crack monitoring in rotorcraft structures. This report also provides information on the development of the system application to a specific rotorcraft structural component, certification compliance procedures and requirements, Functional Hazard Assessment with respect to the rotorcraft structural application, and details on three test levels conducted to validate the system at coupon-level, component-level, and inflight.

1. INTRODUCTION.

1.1 OBJECTIVE.

The objective of this effort was to develop, validate, and demonstrate damage-detection technologies, including advanced software, algorithms, and methodologies for structures and dynamic components to (1) detect fatigue cracks and damages before exceeding critical threshold or incipient failure and (2) characterize fatigue cracks and damages. Particularly, this effort supports Advisory Circular (AC) 29-2C, Section MG-15 [1].

1.2 BACKGROUND.

AC 29-2C, Section MG-15 addresses airworthiness approval of Health and Usage Monitoring System (HUMS). The AC provides guidance for achieving airworthiness approval for installation, credit validation, and Instructions for Continued Airworthiness (ICA) for a full range of HUMS applications. Installation includes all the equipment needed for the end-to-end application that is associated with acquiring, storing, processing, and displaying the HUMS application data, such as airborne- and ground-based equipment. Credit validation includes evidence of effectiveness for the developed algorithms, acceptance limits, trend-setting data, tests, and demonstration methods employed. A plan, which includes the methods used, is needed to ensure continued airworthiness of those parts that could change with time or usage. The AC establishes an acceptable means, but not the only means, of certifying rotorcraft HUMS.

HUMS are used for rotor track and balance, exceedance monitoring, engine and drive train diagnostics, and structural usage monitoring. HUMS typically consist of a variety of onboard sensors, algorithms, and data acquisition systems. The acquired data may be processed onboard the rotorcraft or on a ground station (or a combination of both) providing the means to measure against defined criteria and to generate instructions for the maintenance staff and flight crew for intervention.

Most HUMS technologies focus on monitoring the conditions in terms of measurements of vibration, not structural damage, cracks, or failures. Because fatigue damage of rotorcraft components in service is a major concern, development, validation, and demonstration of a system for crack detection and crack growth monitoring is critically needed.

This project developed the concept for a Smart Patch System (SPS) for the detection of cracks and damages in commercial rotorcraft structures. The system includes sensors, hardware, and damage detection software. Acellent Technologies, Inc. developed a sensor network-based Structural Health Monitoring (SHM) system (see figure 1) that uses a network of distributed piezoelectric sensors or actuators embedded on a thin, dielectric carrier film called the Standard Multi-Acuator-Receiver Transduction (SMART) Layer® to query, monitor, and evaluate the condition of a structure [2-7]. A portable diagnostic unit called the SMART Suitcase™ processes diagnostic signals obtained from a structure during monitoring. With appropriate diagnostic software, the signals can be analyzed to ascertain the integrity of the structure being monitored. The SMART Layer technology has both active and passive sensing capabilities using the same

piezoelectric sensors for structural health monitoring purposes. The piezoelectric material is lead zirconate titanate (PZT). In the active sensing mode, the SMART Suitcase can be used to automatically instruct actuators to generate preselected diagnostic signals and transmit them to neighboring sensors. These sensors' responses can then be interpreted in terms of damage location and size or material property changes. A comparison is then made between the current sensor response and the baseline taken when the structure was undamaged, as shown in figure 2. In the passive sensing mode, the SMART Layer sensors can be used as continuously monitored sensors to detect anomalous structural events such as impacts. Both modes permit real-time structural analysis and evaluation along with constant collection of structural data and information while the structure/vehicle is in service; however, for the quantification of actual damage in structures required for this project, only the active sensing mode capabilities are required.

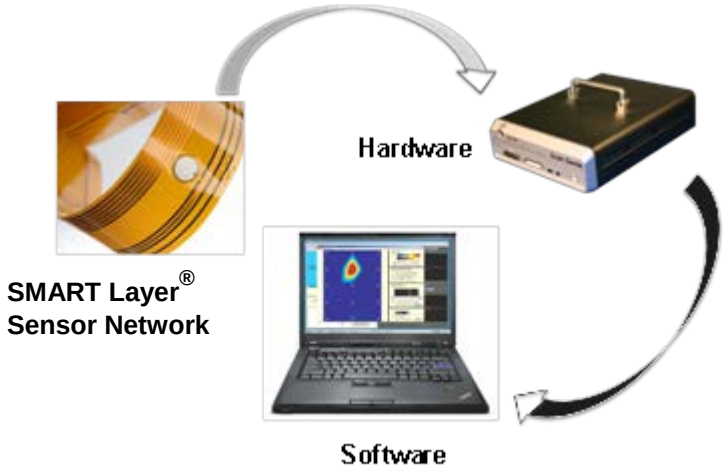

Figure 1. Acellent's Basic SMART Layer SHM System

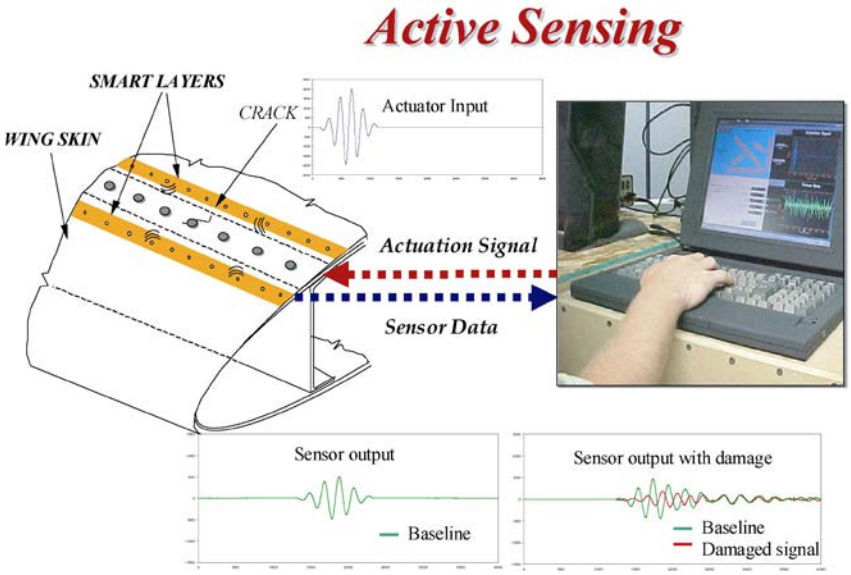

Figure 2. Functioning of the Active Sensing System

The design and validation of an SPS to be certified for use on a specific commercial rotorcraft structural application is described in section 2.2. The system will provide the following capabilities:

- Obtain real-time information on the integrity of a structure during service.
- Identify visible and invisible damage in metal and composite structures.
- Assess fatigue cracks in highly loaded metallic fittings.
- Characterize and monitor damage growth.
- Provide an easy-to-use inspection tool for maintenance personnel to assess the integrity of damaged structures and take preventive action.
- Reduce inspection and structural maintenance costs.

1.3 BASIC APPROACH FOR SPS CERTIFICATION.

The three aspects for the certification of HUMS outlined in AC29-2C [1] were used as the basic approach to SPS certification. They are:

1. Installation—including all equipment needed for the end-to-end application of the SPS to rotorcraft airframe structural components that is associated with acquiring, storing, processing, and displaying the SPS data, which includes both airborne and ground-based data.

2. Credit Validation—including evidence of effectiveness for the developed algorithms, acceptance limits, trend setting data, tests, and the demonstration methods employed.

3. ICA—including a plan to ensure continued airworthiness of those parts that could change with time or usage and the methods used to ensure continued airworthiness.

The end-to-end SPS could be an integral part of the rotorcraft HUMS by providing in-service information regarding the health of new and existing rotorcraft airframe structures. Built-in sensor networks on the airframe structural components provide data regarding the condition and damage state of the structure. Data acquisition hardware and algorithms process sensor data to provide diagnostic information in the form of location and size of damage. The diagnostics information is displayed and used to facilitate better decision-making processes with respect to inspection and repair (e.g., repair versus no repair or replacement). Rotorcraft asset management could then be performed based on HUMS data representing the actual health or usage of the structure, thereby minimizing in-service failures and maintenance costs and maximizing reliability and readiness.

Figure 3 shows the basic approach for SPS certification for application to a specific rotorcraft airframe structural component. The process steps shown in the certification approach framework

were developed based on the guidance provided in AC 29-2C, Section MG-15. For this project, Sikorsky Aircraft Corporation (SAC) was selected as the original equipment manufacturer (OEM) partner. SAC assisted with the selection of a suitable airframe application and development of the requirements for the SPS design. A Functional Hazard Assessment (FHA) was performed to determine the end-to-end criticality level for the SPS application. The FHA is a top-down analysis that identifies the hazards to the rotorcraft and traces these hazards to the component level in the airframe structures affected by the SPS application. SAC performed the assessment for the rotorcraft structural component and Acellent performed the assessment for the various components of the SPS. The intent for the end-to-end SPS application was to obtain maintenance credit in that it will add to, replace, or intervene in existing rotorcraft maintenance practices or flight operations. The optimized design, which includes the sensor network, data acquisition and processing algorithms, software, and electronic hardware, of the SPS for the specific selected application was then developed. Two types of validation tests were performed at SAC test facilities: coupon tests to determine the system sensitivity and robustness, and component tests to validate system functionality, performance, and reliability when applied to the full-scale component under actual design load levels. Mitigating actions and certification limitations were determined based on the system performance assessment. Flight tests were performed on a Sikorsky EH-60 Black Hawk helicopter and a Raptor-90 unmanned rotorcraft vehicle (URV) under a cooperative research agreement with the U.S. Army Research Laboratory (ARL). The purpose of the tests was to develop direct evidence for system validation in the actual rotorcraft flight environment. In the final step, implementation and technology transfer plans were developed. This approach addressed the three basic aspects for certification of the SPS as a part of a rotorcraft HUMS as specified in the AC.

Specifically, the goal of an SPS is to:

- Reduce the total structural inspection costs for rotorcraft structures.
- Avoid unplanned structural failure and, possibly, catastrophic failures.
- Provide maintenance credit by reducing the number of maintenance activities when the structural condition assessment shows no need for the scheduled work.

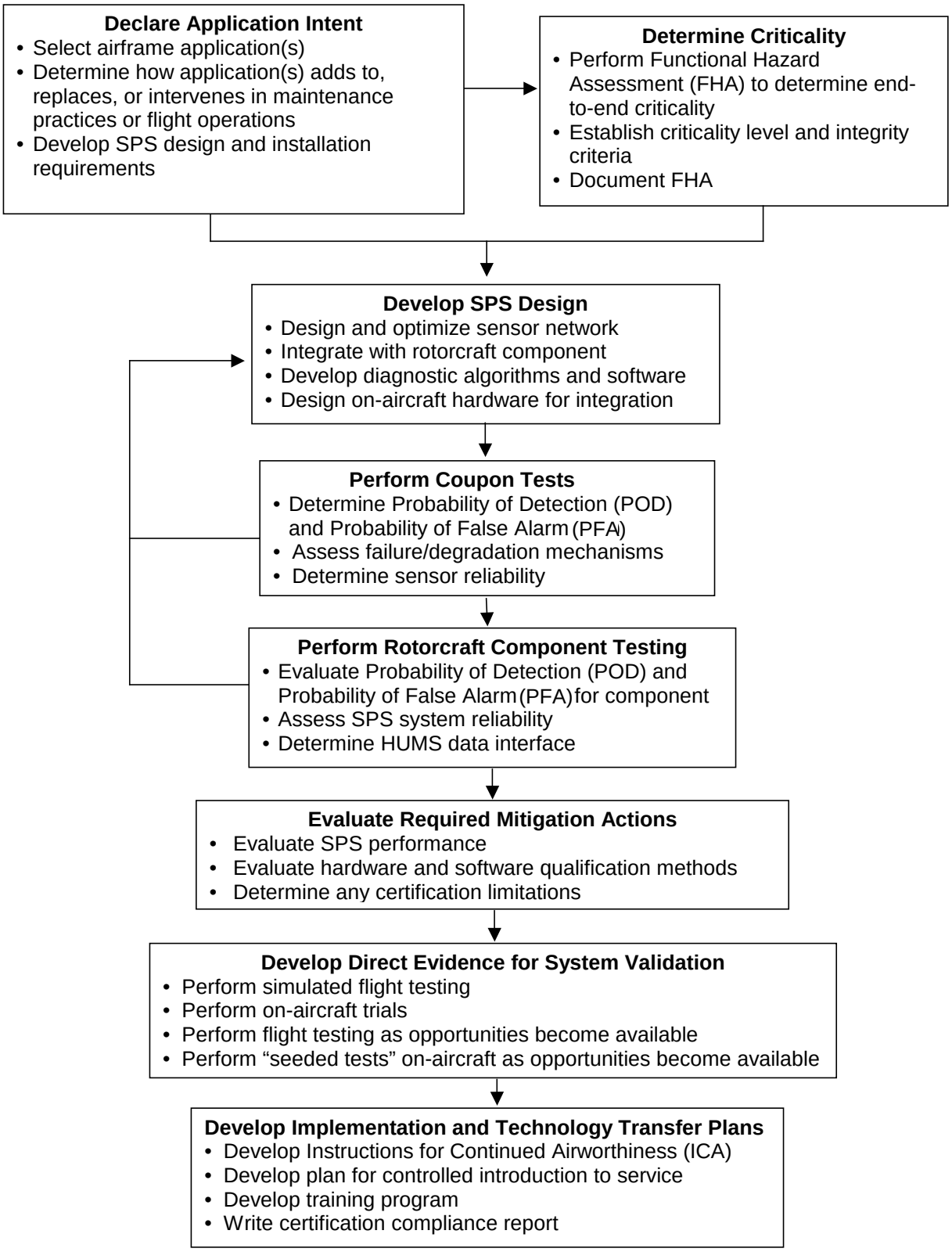

Figure 3. The SPS Certification Approach Framework

2. SMART PATCH SYSTEM.

2.1 SELECTION OF AIRFRAME APPLICATION.

The primary goal for the selection of a suitable airframe application was to identify potential critical components that can benefit from the use of the SPS. A secondary goal was to identify the component most suitable for SPS testing and validation.

In collaboration with SAC, an assessment of rotorcraft component families on airframe and dynamic systems was performed. The assessment considered criteria such as structural criticality, fatigue sensitivity, complexity, sensor feasibility, component testability, component availability, and benefits. Generic component data were also collected to aid in the selection of a demonstration/test component.

Based on the assessment criteria, both airframe and dynamic components (see figure 4) were identified as potential components that can benefit from the SPS. A list of the components chosen for further review is detailed below.

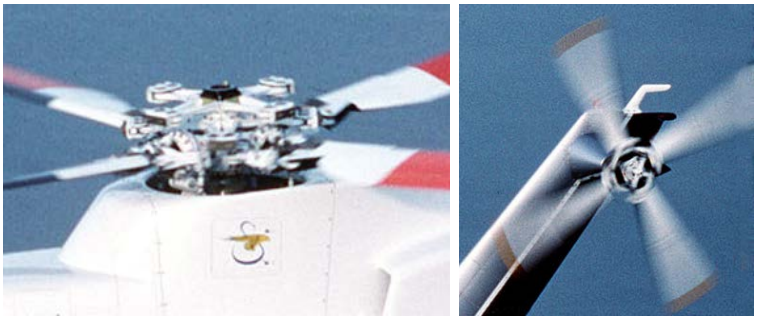

Figure 4. The S-76 Dynamic Components

- Airframe Elements
  - Frame
  - Transmission beam (upper deck)
  - Bulkhead
  - Beams
  - Attachments or lugs
  - Stringers
  - Skins
- Dynamic Components
  - Main rotor (MR) spindle
  - Tail rotor (TR) horn

A matrix was developed to rate the identified rotorcraft components. The matrix consisted of the identified rotorcraft components versus the key components of the assessment criteria. The following key components govern the assessment criteria:

- Structural Criticality and Fatigue Sensitivity—Evidence that site has potential for crack in laboratory testing. Significance of the component to maintaining safety.

- Complexity—Determine challenges in understanding loading, fatigue behavior, and geometry features that influence demonstration results. Higher complexity for rotating components and complex joints.

- Sensor Feasibility—Determine feasibility to apply sensor system to detect damage in laboratory and projected service aircraft.

- Component Availability and Testability—Determine ease of building test setup in laboratory environment. Planned ground test evaluations are preferred to leverage existing fatigue testing.

- Benefits—The ability to inspect is low because of location and would require more than a walk-around. Monitoring the structural health using the SPS would allow reduced inspection and repair costs.

The objective was to rate the rotorcraft components relative to each other per each criterion and determine which components would be the best for testing and validating the SPS. The rating metrics were standardized to low (1 point), medium (3 points), and high (5 points). Each criterion was weighted and added together to create an overall rating per component. The selection was based on finding components with overall ratings that were greater than or equal to 1 sigma above the mean.

The evaluation criteria are as follows:

- Structural Criticality
  - Site has potential for crack
  - Component is critical for maintaining safety

- Complexity
  - Simplicity of geometry (ability to model or test)
  - Simplicity of loading (ability to model or test)

- Sensor Feasibility
  - Capability to place sensor for detection in laboratory environment
  - Capability to place sensor for detection in service
  - Accessibility to data and transfer

- Component Testability

  - Ground test is planned
  - Ease in building test setup

- Benefit

  - Component inspection is more difficult
  - Monitoring will reduce inspection time
  - Monitoring will reduce repair cost
  - Cost of repair is low

Examples of the selected airframe and dynamic components are presented below with details of their configurations highlighted.

- Example 1: Transmission Beam/Frame

  The transmission beam/frame (see figure 5) is a metallic component (aluminum) with a built-up assembly of fasteners and joints. Early detection of damage in this component prevents major repair. The beam has fatigue sensitive locations transmitting rotor loads to airframe.

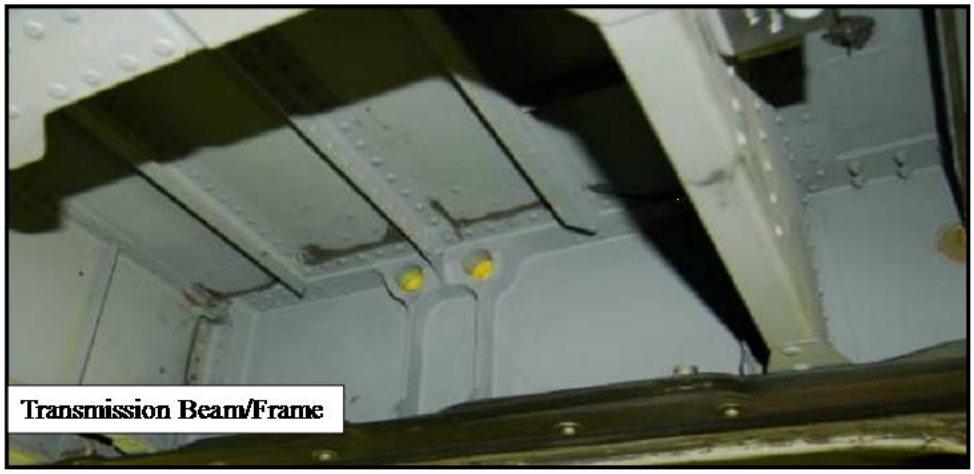

Figure 5. Transmission Beam and Frame

- Example 2: Frame/Beam Joint

  This is a key airframe structure with fatigue concern. The representative structure, as shown in figure 6, has a complicated load path and geometry as well as difficult installation. In critical sites, the cracks are visible, so early detection provides only a limited opportunity to save repair.

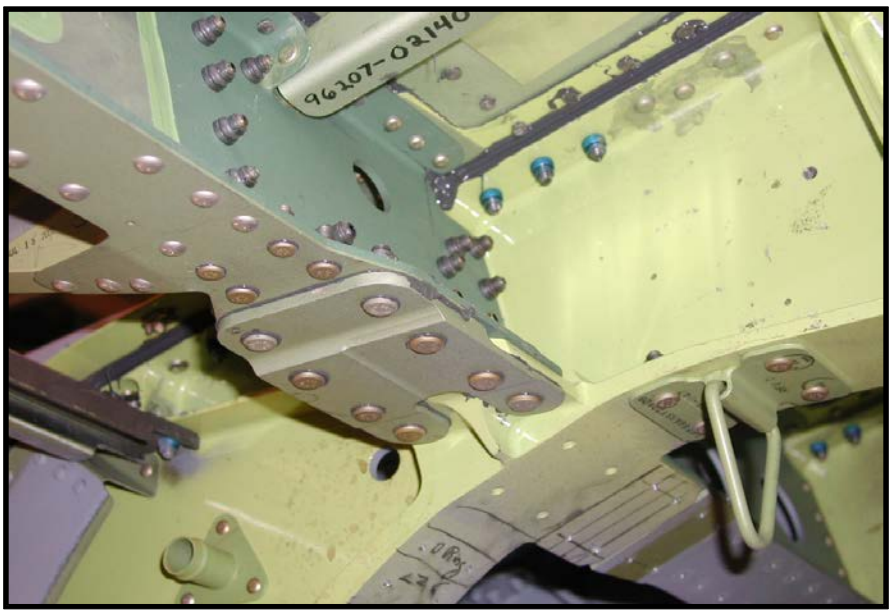

Figure 6. Representative Frame and Beam Joint

- Example 3: Bulkhead

  The bulkhead, shown in figure 7, has fatigue-sensitive locations. Early detection provides limited benefit in reducing repair costs. Visual inspection is possible.

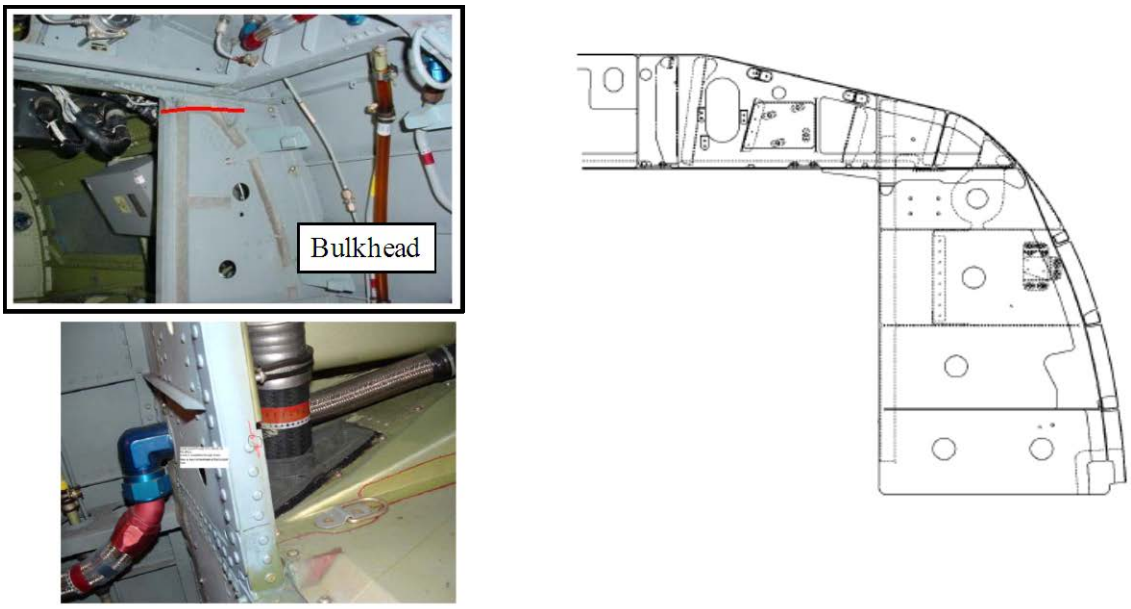

Figure 7. Bulkhead

- Example 4: Fitting

  The fitting, shown in figure 8, is the primary loaded structure for attachment of a tail rotor gearbox, stabilator, etc. Early detection mitigates safety risks. The cost of repair is low.

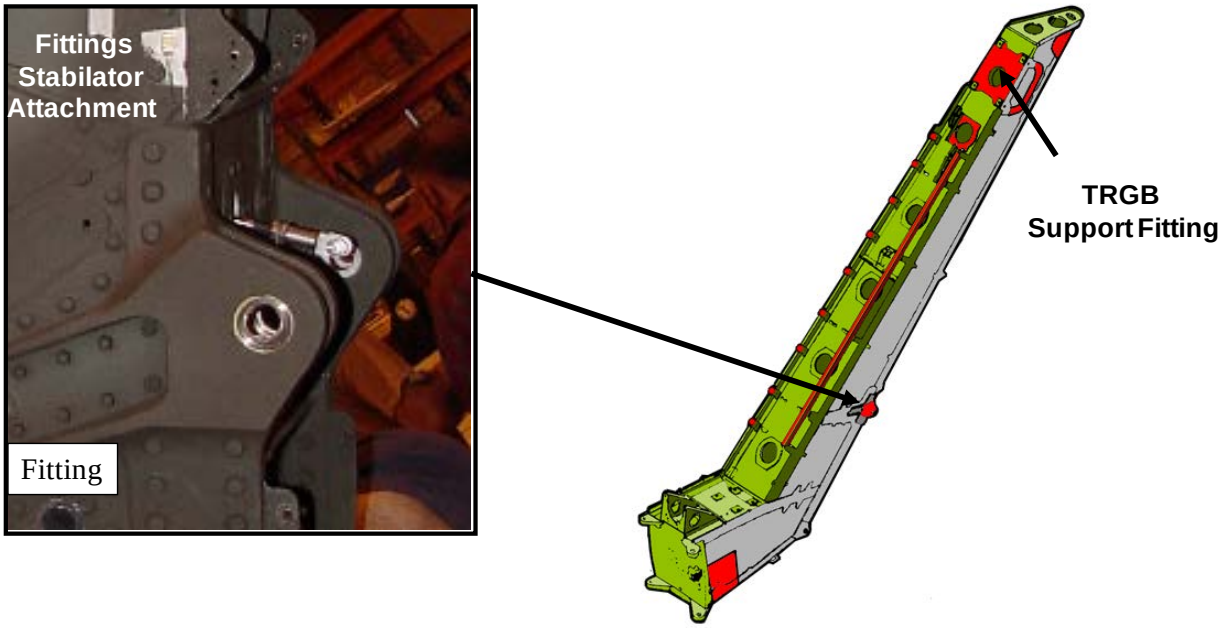

Figure 8. Fitting

- Example 5: Skins/Stringers

  Fatigue and corrosion can be present in skins, as shown in figure 9. Repair is performed more directly with less disassembly than beams and frames. Structure is not critical for maintaining safety. The cost of repair is low.

Figure 9. Skins and Stringers

- Example 6: The MR Spindle Lugs

The MR spindle, shown in figure 10, is a dynamic metallic component (aluminum) that has an MR blade attachment. It has low complexity in features and is critical for maintaining safety; however, sensor placement is a challenge.

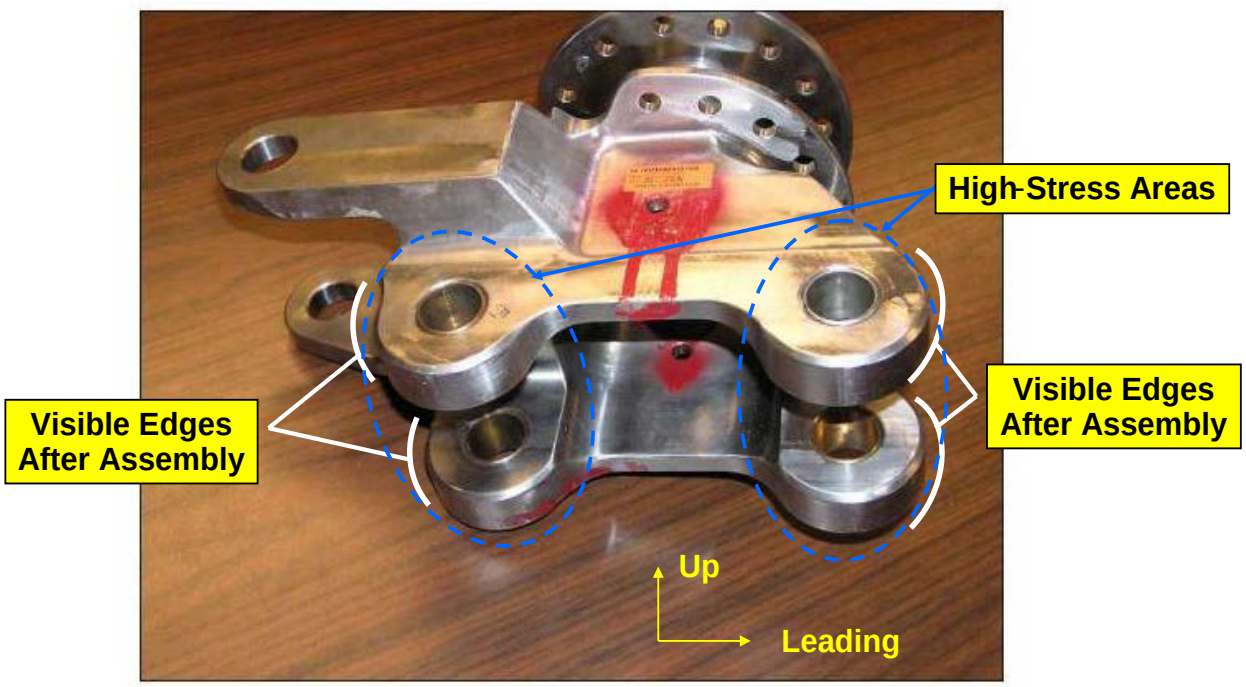

Figure 10. The MR Spindle

- Example 7: TR horn

  This aluminum component, shown in figure 11, is a TR blade attachment. Although it has simple features, the TR horn structure is critical for maintaining safety.

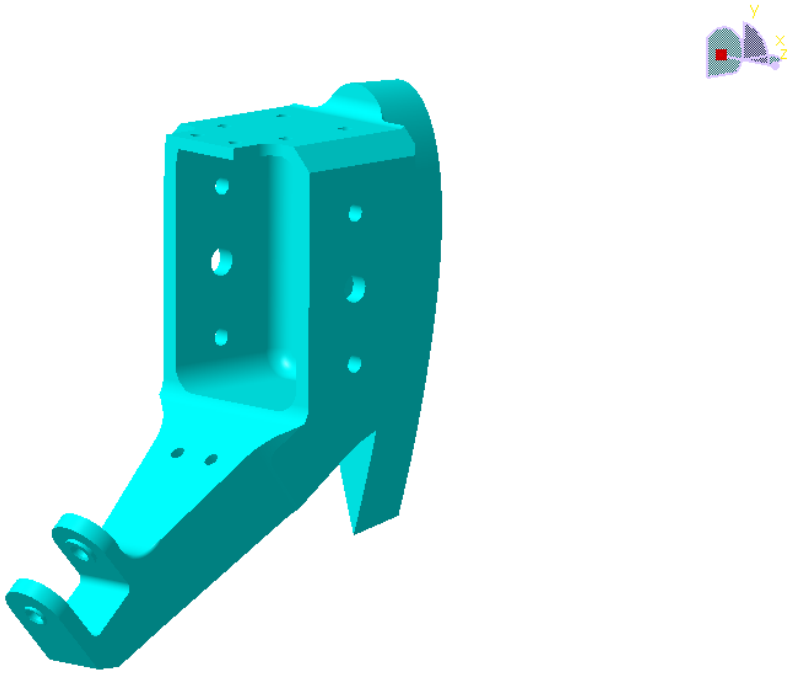

Figure 11. The TR Horn

The rotorcraft components were evaluated against the assessment criteria to determine the most appropriate components to test the SPS. The selection matrix is provided in table 1. Each individual criterion was not weighted; however, the combined criteria for component testability were weighted by a factor of 2. The rationale for increasing the weight on this factor was to account for the objective of testing and validating the SPS on actual components.

The selection matrix resulted in a mean of 45.9 with a standard deviation of 9.8. The chosen component should have a value of 55.6 or higher to be statistically significant. The TR horn was the only component that was above 55.6, with a value of 63.

Based on the selection matrix, the TR horn was initially chosen as the candidate to test the SPS. The SPS design for application to the TR horn was started; however, due to vendor manufacturing issues, SAC decided to forgo any further development effort on this TR horn design. For reference, the proposed SPS sensor locations for the TR horn are provided in figure 12. The proposed sensor locations are based on the locations of the high-stress areas and the ability to install and monitor sensors.

Table 1. The SPS Component Selection

			Component						
#	Criteria	Weight	Transmission Beam/Frame	Frame/Beam Joint	Bulkhead	Fitting	Skins/Stringers	MR Spindle	TR Horn
1.0	Structural Criticality	1.0	10	8	6	6	4	8	8
1.1	Site has potential for crack	1.0	5	5	3	1	3	3	3
1.2	Component is critical for maintaining safety	1.0	5	3	3	5	1	5	5
2.0	Complexity	1.0	6	2	6	8	4	8	10
2.1	Simplicity of geometry (Ability to model/test)	1.0	3	1	3	5	3	5	5
2.2	Simplicity of loading (Ability to model/test)	1.0	3	1	3	3	1	3	5
3.0	Sensor Feasibility	1.0	15	13	13	7	15	3	11
3.1	Capability to place sensor for detection in laboratory	1.0	5	3	3	3	5	1	5
3.2	Capability to place sensor for detection in service	1.0	5	5	5	3	5	1	3
3.3	Accessibility to data and transfer	1.0	5	5	5	1	5	1	3
4.0	Component Testability	2.0	4	2	2	4	4	4	10
4.1	Ground test is planned	1.0	1	1	1	1	1	3	5
4.2	Ease in building test set-up	1.0	3	1	1	3	3	1	5
5.0	Benefit	1.0	16	12	6	14	10	18	14
5.1	Difficult to inspect component	1.0	3	3	1	5	3	5	5
5.2	Monitoring will reduce inspection time	1.0	3	1	1	5	3	5	3
5.3	Monitoring will reduce repair cost	1.0	5	3	1	3	3	3	3
5.4	Cost of repair	1.0	5	5	3	1	1	5	3
		Totals	55	39	35	43	41	45	**63**
		Mean	45.9						
		Standard Deviation	9.8						
		Mean+1	55.6						

Criteria Rating: Low = 1, Medium = 3, High = 5
Objective: Rate components relative to each other per criteria
Selection: Components that are ≥ 1 sigma

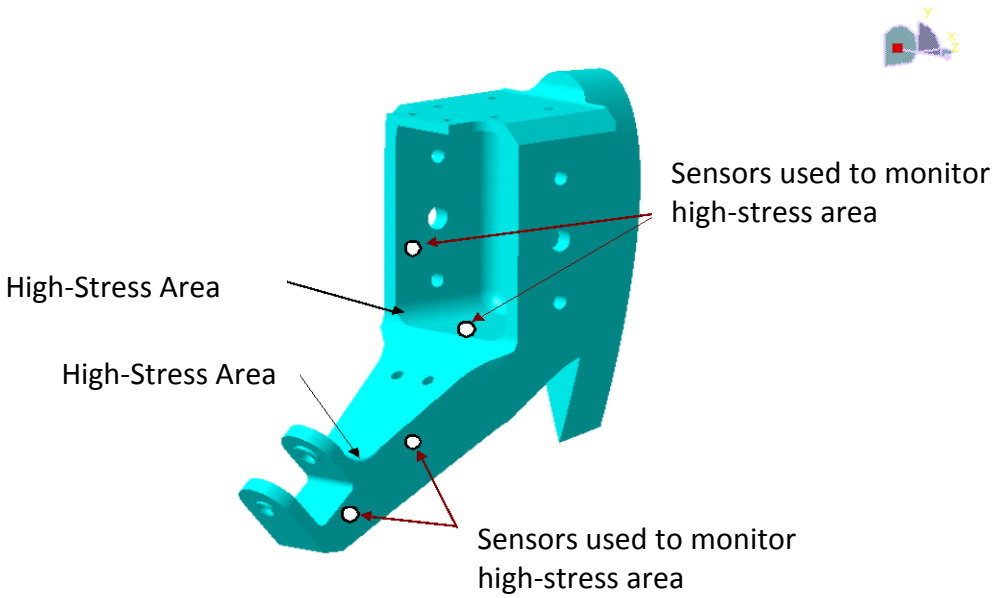

Figure 12. Sensor Locations on the TR Horn

A right-hand clevis fitting on a gearbox middle housing, which was already design, fabricated, and scheduled for the qualification testing, was used because it represented a flight-critical dynamic component. This fitting is shown in figure 13. The clevis fitting was a suitable application to demonstrate and validate the SPS design process for a flight-critical component to the SAC project and sustainment engineering personnel. The remainder of the SPS design development activities were targeted at this specific application.

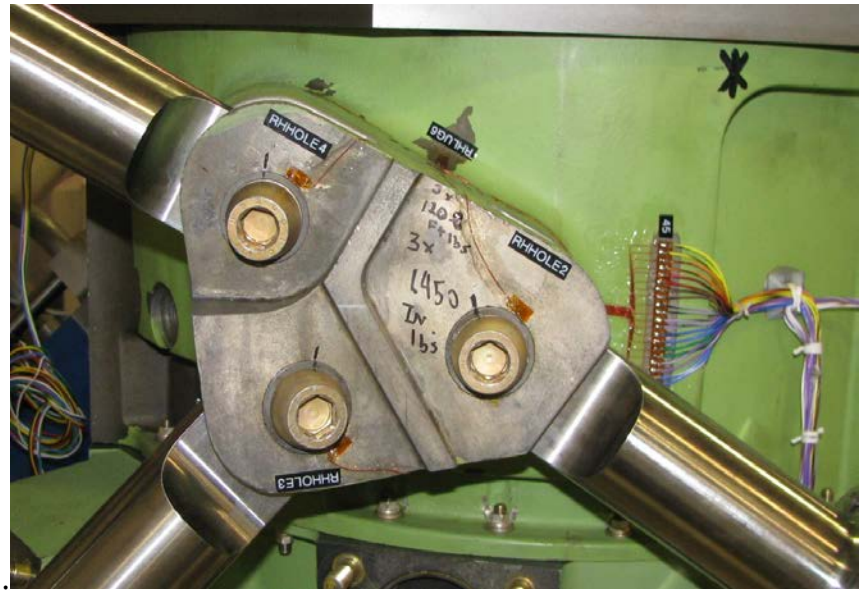

Figure 13. Gearbox Middle-Housing Clevis Fitting

2.2 THE SPS DESIGN—SYSTEM DESIGN AND OPTIMIZATION FOR ROTORCRAFT.

The SPS consists of three basic components, as shown in figure 14:

1. Smart Patch sensors/sensor network
2. Diagnostic hardware, including transmitters and receivers
3. Software to monitor the health condition of structures

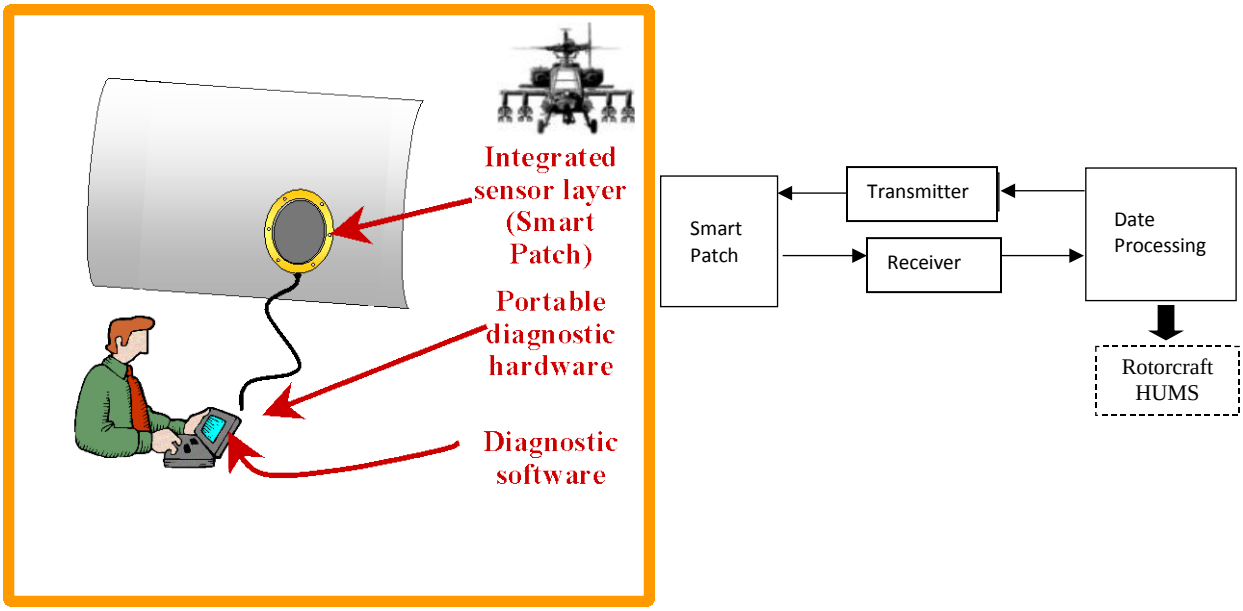

Figure 14. The SPS

The Smart Patch is a network of PZT transducers. Each PZT transducer can be used as an actuator or a sensor. An actuator-sensor pair forms a scan path. A scan is performed in two steps:

1. A signal is sent from the transmitter to the actuator.
2. The return signal is read from the sensor through the receiver.

Any specific area of the structure may have multiple paths going through it. This built-in redundancy increases the reliability of the system. An example of a Smart Patch is shown in figure 15. There are nine sensors/actuators on this patch.

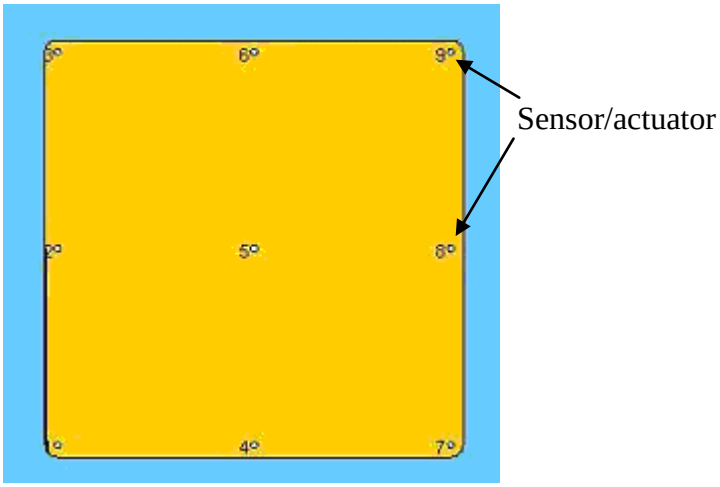

Figure 15. Example of Smart Patch

The function of the Smart Patch as a part of the SPS is as follows:

- Transmitter—The transmitter sends the exciting signal to the actuator. The SPS contains function generation and data acquisition electronic circuits. It is connected to the Smart Patch via cables. It can send out different high-voltage waveform signals to the PZT sensor to generate acoustic stress waves.

- Receiver—The receiver receives the signal read by the sensor. The data acquisition function of the SPS can assimilate sensor responses into a readable format for the data processing unit to perform analyses.

- Data Processing—The data-processing unit performs data storage and data analysis tasks. When the SPS is first installed, a set of baseline data is collected while the component is in good health. The analysis phase of data processing compares the newly collected data against the baseline data. The output of the data analysis is a report of the condition (health) of the component.

2.2.1 Smart Patch Design.

This part of the research focused on the design of the Smart Patch for use with rotorcraft structures. The Smart Patch design for rotorcraft components is based on the Acellent's SMART Layer® technology. The Smart Patch consists of a sensor layer made of a thin dielectric film with an embedded network of distributed piezoelectric sensors and actuators and electrical circuitry. This sensor layer can be mounted on critical areas of the rotorcraft prone to damage. The Smart Patch is thin (1 to 2 mil) with an almost negligible weight, similar to the current SMART Layer.

Figure 16 shows the Smart Patch design. The Smart Patch consists of three parts:

- Transducers, such as piezoelectric
- Dielectric substrate to house the transducers
- Flexible circuit that integrates the dielectric film to connect the transducers together

Typical piezoelectric transducers used in the Smart Patch include:

- PZT.
- Piezoelectric single crystal.

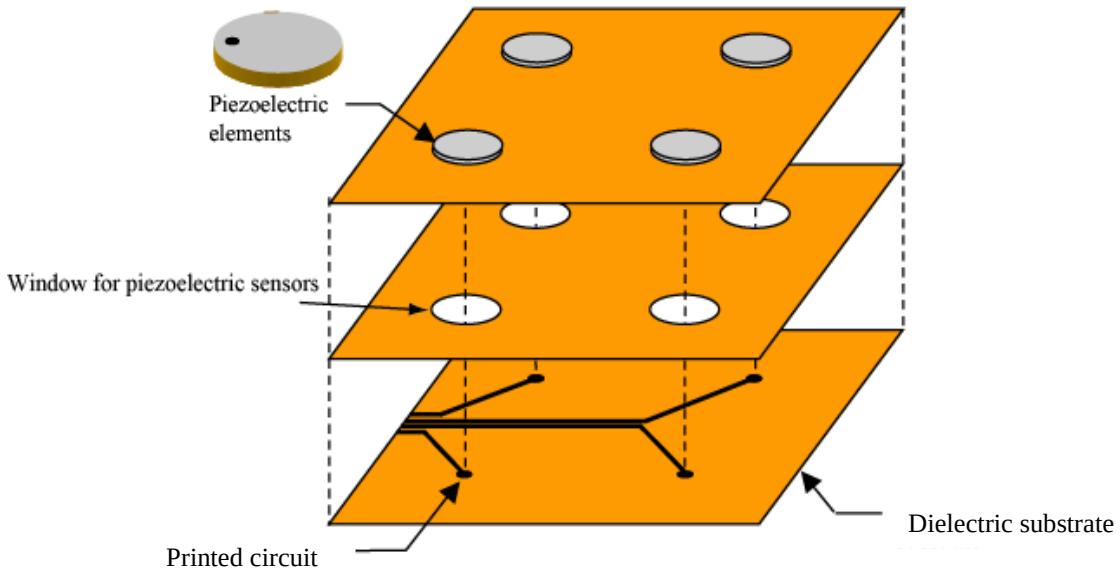

Figure 16. Smart Patch Components

The properties of PZT sensor and the piezoelectric single crystal are given in figure 17. The transducers can be used as follows:

- PZT sensor is used if the area where the transducers are to be mounted experiences strain of <0.15%.

- Piezoelectric crystal is used if the area where the transducers are to be mounted experiences strain >0.15%-1%.

Typical sizes of transducers selected include the following:

- Disc-shaped

  - 10-mil-thick 0.25″ diameter
  - 30-mil-thick 0.25″ diameter

  - 20-mil-thick 0.1″ diameter
- Rectangular
  - 10-mil-thick

The three important issues for Smart Patch design are sensor location, layer configuration, and internal and external connections. The procedures for these issues are briefly summarized as follows:

1. Sensor optimization and layout—Sensor location determination is dependent on the sensor density required to monitor damages and the geometrical limitation of the host structure. The sensor density can be calculated from the critical damage size to be detected and the travel distance of the stress wave. Structure users usually know the critical damage size. The travel distance of the stress wave depends on the material properties, the thickness of the structure, and the frequency of the stress wave. The sensor optimization and design criteria are used to design the optimal spacing for the sensors in the Smart Patch.

2. Layer configuration—Cross-sectional configuration of Smart Patch includes the types of substrate and sensor materials, shielding, and protective coating. The determination should be balanced between the performance of the layer at the operating environment and cost.

3. Connections—Connections include the circuits between the sensors and terminals, the connectors, and the cable from the connector to the diagnostic hardware. A strain-relief connector on the layer is necessary to avoid any electric disconnection. Depending on the host structure, the connector can be fastened to the structure or bonded on the structure.

To address these issues, work was conducted in two areas:

1. Sensor optimization and layout
2. Identification of rotorcraft components

Merging the information obtained from both these areas provides the information required for the Smart Patch design.

PZT Material:	
Relative Dielectric Constant	
K^T	1250
Dielectric Dissipation Factor (Dielectric Loss (%)*	
tan δ	0.4
Curie Point (°C)**	
T_c	325
Electromechanical Coupling Factor (%)	
k_p	0.59
k_{33}	0.72
k_{31}	0.35
k_{15}	0.70
Piezoelectric Charge Constant (10^{-12} C/N or 10^{-12} m/V)	
d_{33}	290
$-d_{31}$	125
d_{15}	480
Piezoelectric Voltage Constant (10^{-3} Vm/N or 10^{-3} m^2/C)	
g_{33}	26.5
$-g_{31}$	11
g_{15}	38
Young's Modulus (10^{10} N/m^2)	
Y^E_{11}	8
Y^E_{33}	6.8
Frequency Constants (Hz m or m/s)	
N_L (longitudinal)	1524
N_t (thickness)	2005
N_p (planar)	2130
Density (g/cm^3)	
ρ	7.6
Q_m	500

Property	TRS-X2B
Composition	PMN-30%PT
Dielectric, K_3^T	5500-7500
Loss (tanδ)	<0.01
T_{RT} (1 kHz, °C)	85
T_C(1 kHz, °C)	152
E_C (kV/cm)	3.2
d_{33} (pC/N)	1700-2200
d_{31} (pC/N)	-1000
d_{15} (pC/N)	2500-4000*
k_{33}	0.90
k_{31}	0.51
k_t	>0.55
N_{33} (Hz-m)	599
N_{31} (Hz-m)	721
N_t (Hz-m)	2002
Density (g/cm^3)	8.0

Figure 17. Properties of the Piezoelectric Materials Used in the Smart Patch

2.2.2 Sensor Optimization and Layout.

The focus of this task was to develop sensor optimization and layout criteria for rotorcraft components. This was done using information obtained through previous projects involving the sensors and structures used in aircraft and rotorcraft as a basis.

One objective was to determine how the detectable crack size varies with structure thickness when using sensors placed on the opposite face of the structure. In thin structures, the piezoelectric actuators excite Lamb modes that saturate the entire thickness and are sensitive to structural changes on the top and bottom surface of the structure. For thicker structures, if the actuator and sensor are too close to each other, the wave propagation angle required to detect a crack on the opposite face may be too steep (figure 18). For these situations, the actuator and sensor must be moved farther apart to allow enough distance for the propagating stress waves to fully saturate the thickness.

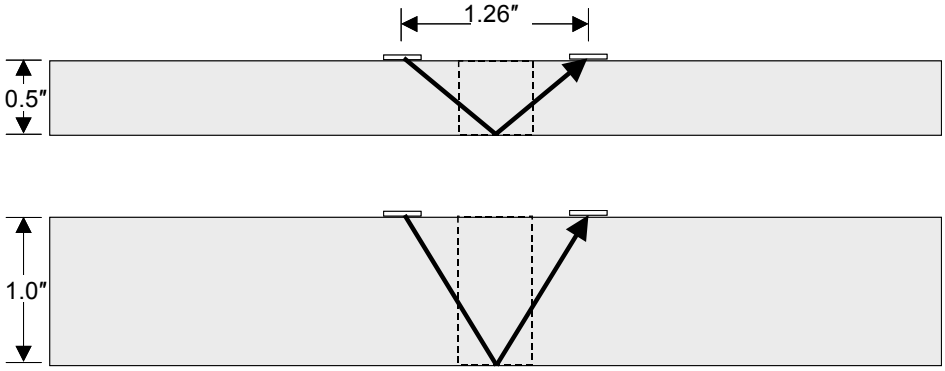

Figure 18. Required Signal Path to Detect Notch on Opposite Side of 0.5″ and 1.0″ Plates

To determine the relationship between actuator-sensor distance, structure thickness, and detectable size of crack on opposite face for different materials, simulation software to model the wave propagation in the structure can be used.

When run through the damage detection algorithms, these simulation results provide information to create a chart that relates structure thickness, actuator-sensor spacing, and detectable crack size (on opposite surface). This chart aids in the design of the sensor locations for the Smart Patch.

A flowchart was developed to assist in the design of the actuator or sensor layout for different components (figure 19).

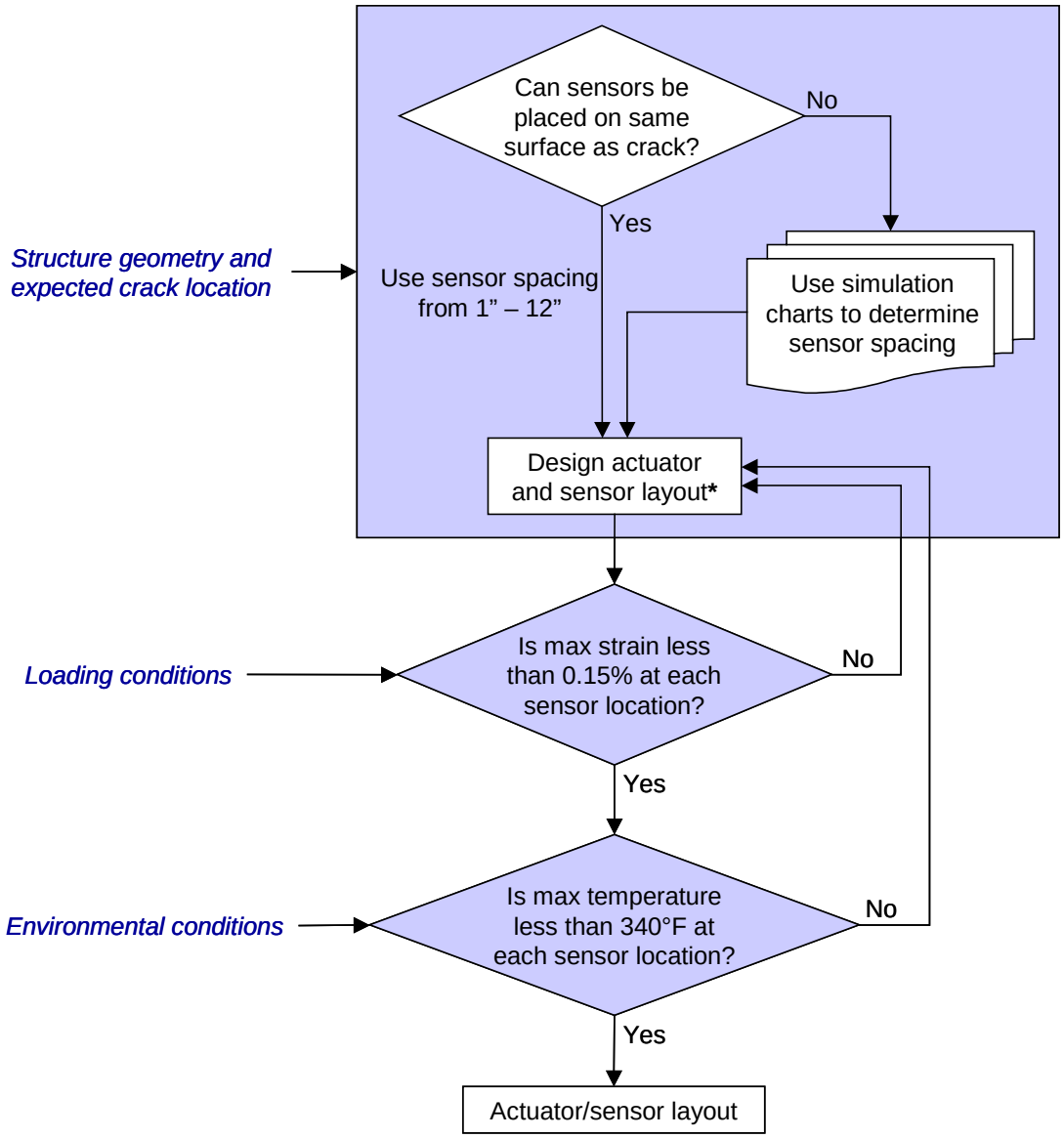

Figure 19. Determining Sensor Layout

To design the sensor layout, three sets of information are required: (1) the structure geometry and expected crack location, (2) the loading conditions, and (3) the environmental conditions. For applications where the sensors can be placed on the same side or surface of the structure as the expected location of the crack, the sensor spacing can be between 1″ and 12″. However, in cases where sensors must be placed on the opposite surface of the structure, the required sensor spacing depends on the structure thickness. For these cases, simulation software can be used to determine the relationship between actuator-sensor distance, structure thickness, and detectable size of crack on the opposite face (figure 20).

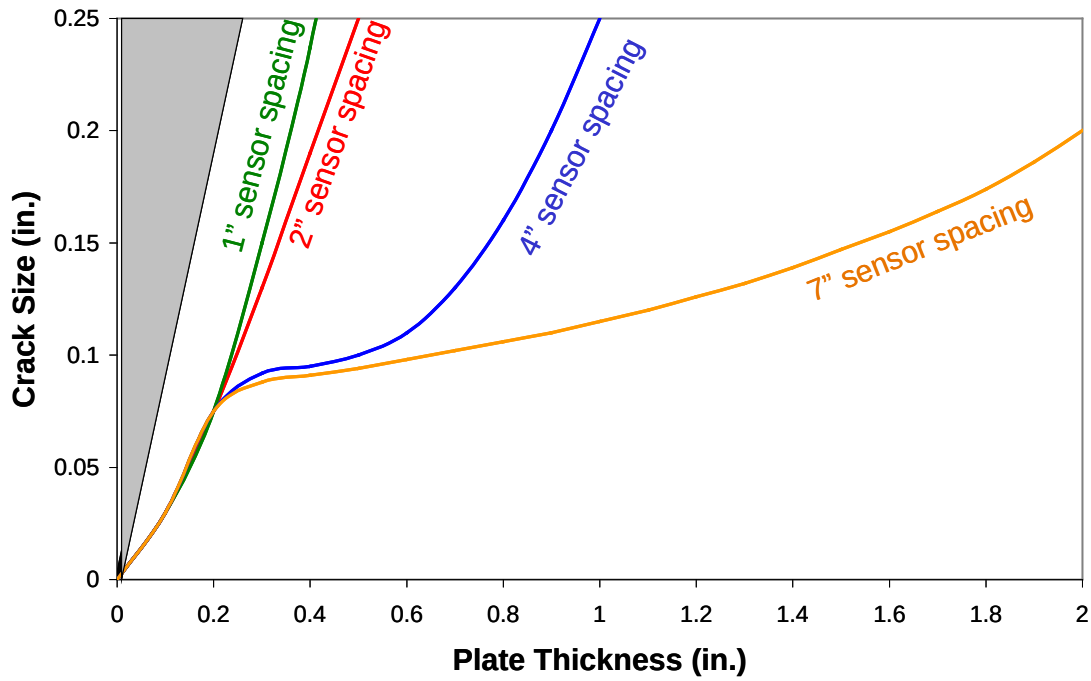

Figure 20. Relationship Between Sensor Spacing, Structure Thickness, and Detectable Crack Size on the Opposite Face

With knowledge of the appropriate spacing, the actuator or sensor layout can be determined. Sensors must be placed such that a direct path between sensors passes through the expected crack location with the following constraints.

- Each sensor requires a surface area of 0.3″ by 0.3″ for bonding.
- The out-of-plane clearance (the gap between adjacent parts) at each sensor location must be greater than 0.1″.
- Radius of curvature structure at each sensor location must be greater than 2.5″.

In addition to the structure geometry, the loading and environmental conditions must be known for each sensor location. The PZT sensors must not be placed in areas with a maximum strain greater than 0.15% or a maximum temperature greater than 340°F. These constraints are imposed by the physical limitations of the sensors.

These design procedures were used to develop SPS designs for both the TR horn (figures 11 and 12) and the clevis fitting (figure 13) for the gearbox middle housing. As mentioned in the previous section, the gearbox middle housing was chosen as the component for additional validation tests. The design of the SPS for the clevis fitting of the gearbox middle housing is shown in figure 21.

The crack was expected to initiate and grow along one of the fillet radii. Therefore, actuators or sensors were installed along the fillet radii and the monitoring was focused in these areas, as

shown in figure 21. The red dots indicate the actuator locations and the yellow dots indicate the sensor locations.

The sensor layouts are typically designed so that the actuator-sensor paths go through the crack region. This allows for detection of cracks by analyzing the changes occurring in the initial part (first arrival) of the sensor signals.

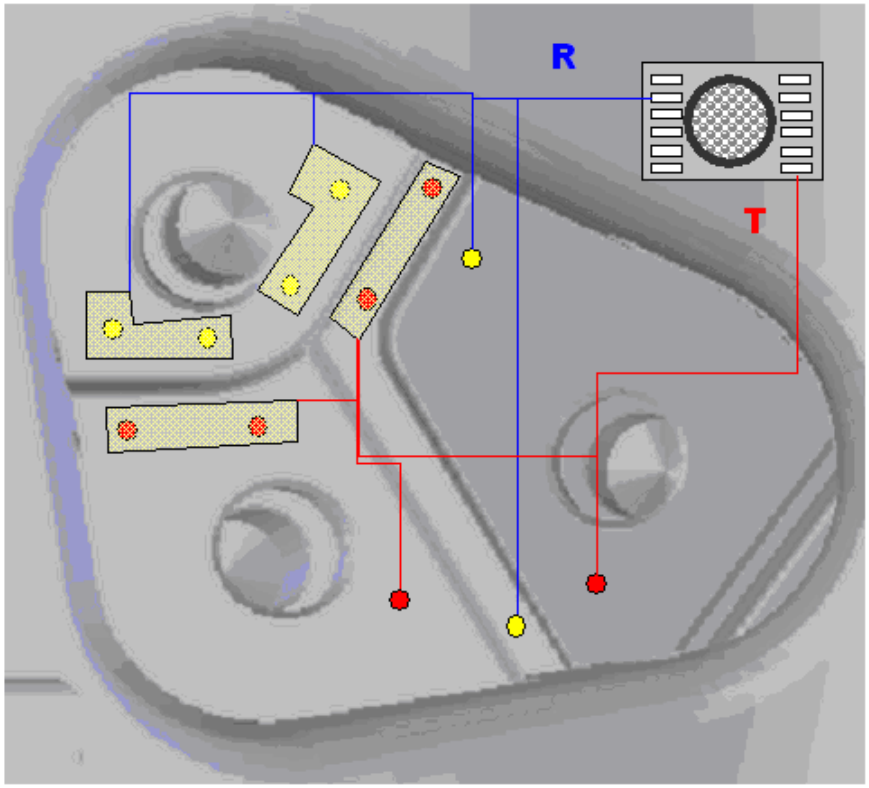

Figure 21. The SPS Design for Gearbox Middle Clevis Fitting

2.2.3 Damage Detection Software Development.

The objective of the software for the SPS design was to identify the location and size of fatigue damage in rotorcraft structures, while eliminating false calls caused by environmental changes or degraded sensors. The goal of the software development was to provide:

- High accuracy.
- Low false acceptance and false rejection damage detection rate.
- A quantitative condition indicator correlated to damage extent and trended to critical threshold.
- Correct diagnosis of the damage size and location along with a measure of uncertainty.

- Easy-to-use applications.
- An automatic system setup.
- Automated calibration procedures.
- High reliability.
- Compensation for environmental changes.
- Self-diagnostics for sensors.

Although this software has many applications in both the laboratory and the field, the primary use is for health monitoring of in-service rotorcraft structures that are susceptible to fatigue damage. These include critical structures where the presence of damage could lead to a reduction in performance or operational safety.

This section covers the design of the SPS software. The software was specifically written to work with Acellent's hardware, which contains all the required data acquisition, waveform generation, and processing capabilities. The software uses a Microsoft® Windows® operating system.

The SPS software controls the input waveform used to send to actuators and assimilates the sensor responses in a format that is easily read and interpreted. The software was designed to facilitate the data-collection process associated with active sensing with an array of piezoelectric sensors, to perform sensor self-diagnostics, to analyze sensor signal data, and to interpret the data in terms of damage size and location. A high-level view of the SPS code is shown in figure 22. The SPS code first asks the user for workspace files to open, if any exist. Typically, the workspace contains information regarding sensor layout, data acquisition settings, path definition, and data collection inputs that are associated with a set of test data. If the workspace does not exist, the user will need to fill them in before any measurements can be made.

The SPS software provides the end-user with a graphical user interface to set up the input files for active sensing of any type of structure. The input parameters are subdivided into three separate files (SNS, STP and DFN), each file being given a different filename extension. Sensor measurements are stored in a data file that is given a DAT as a filename extension. All data are stored in a binary format. The program also gives the user the option to store all input and output files under a workspace, which is given the filename extension of .ace. The workspace (.ace) module relates all input files created by the sensor layout, data acquisition, and path definition modules to the data files defined by the user as one workspace.

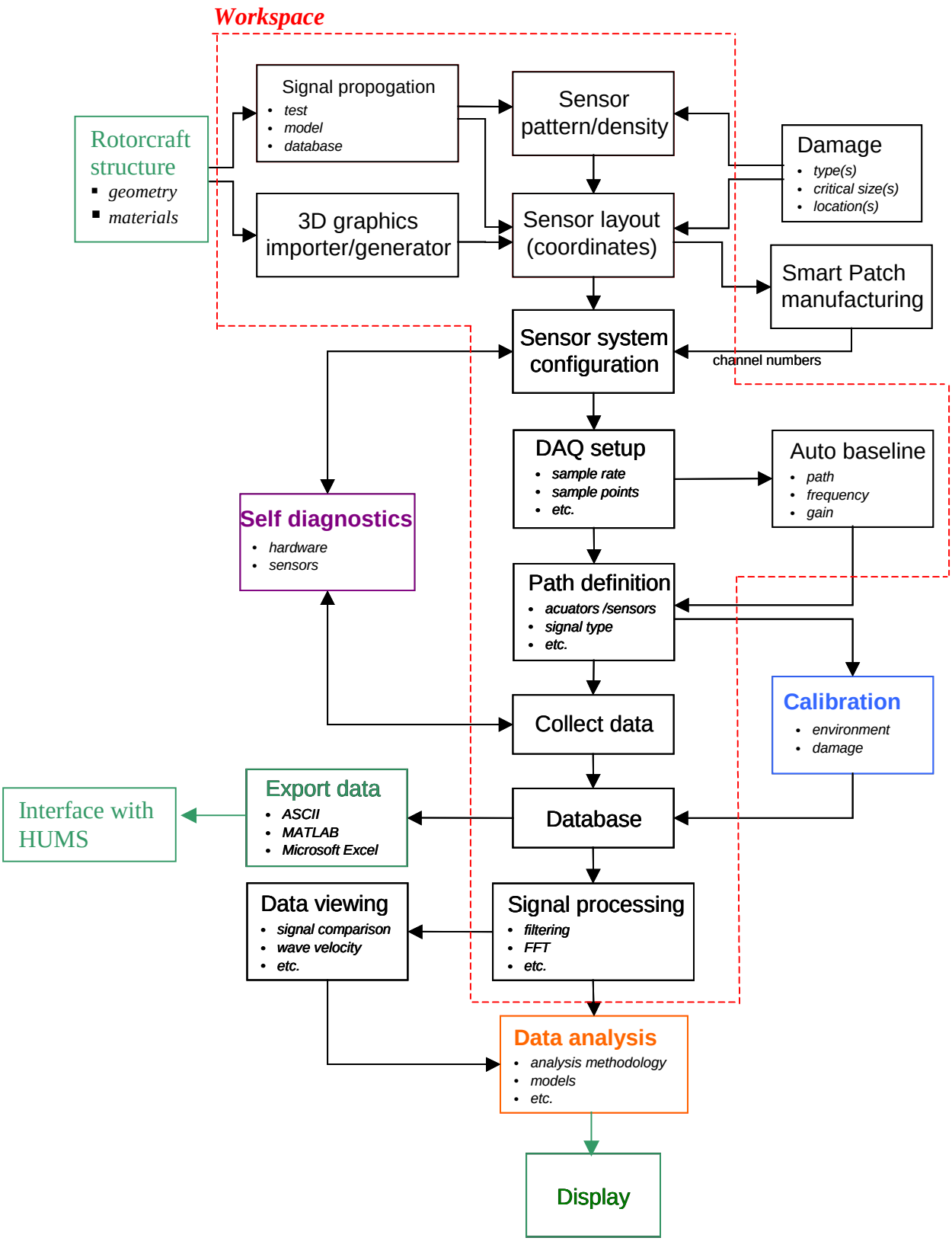

Figure 22. Software Overview

The SPS uses hardware drivers in an executable called Automated Simultaneous Constraint Optimized Parameter Extraction (ASCOPE) to acquire data from the sensors. Using user-defined setup/definition parameters, the SPS software creates an input file and then calls ASCOPE. ASCOPE reads the input file, controls the hardware to generate signals and collect data, and stores the recorded sensor data in an output file.

The SPS software then copies the data from the output file into a user-named binary data file that contains the workspace setup/definition parameters and stores the file in the data folder. The setup/definition parameters are stored in a structure array called setup.

The sensor data are stored in the same format as in the output file. It is stored in 2N single-precision vectors (one column arrays), a0, a1, ..., aN-1, s0, s1, ..., sN-1, where N is the number of measurement paths. The number of data points in each vector is user-defined and depends on the chosen sampling rate and desired capture time.

2.2.3.1 Data Management.

The data management software is used to link damage detection algorithms with a rotorcraft HUMS system. The hardware used in the damage detection system consists of the following major components:

- A computer that will run the software
- A transmitter that will send the actuation signal to a piezoelectric element
- A receiver that will receive the sensor signal from a piezoelectric element
- A channel switch to switch the signal between channels
- A piezoelectric sensor network that will monitor the health of the structure

As shown in figure 23, the system works by pairing tranducers. In each pair, one transducer is designated as the actuator and the other as the sensor. An exciting signal is sent from the transmitter through the channel switcher to the actuator. The actuator activates a mechanical stress wave that propagates to the sensor. The channel switch then switches to the sensor and reads the electrical signal back to the receiver.

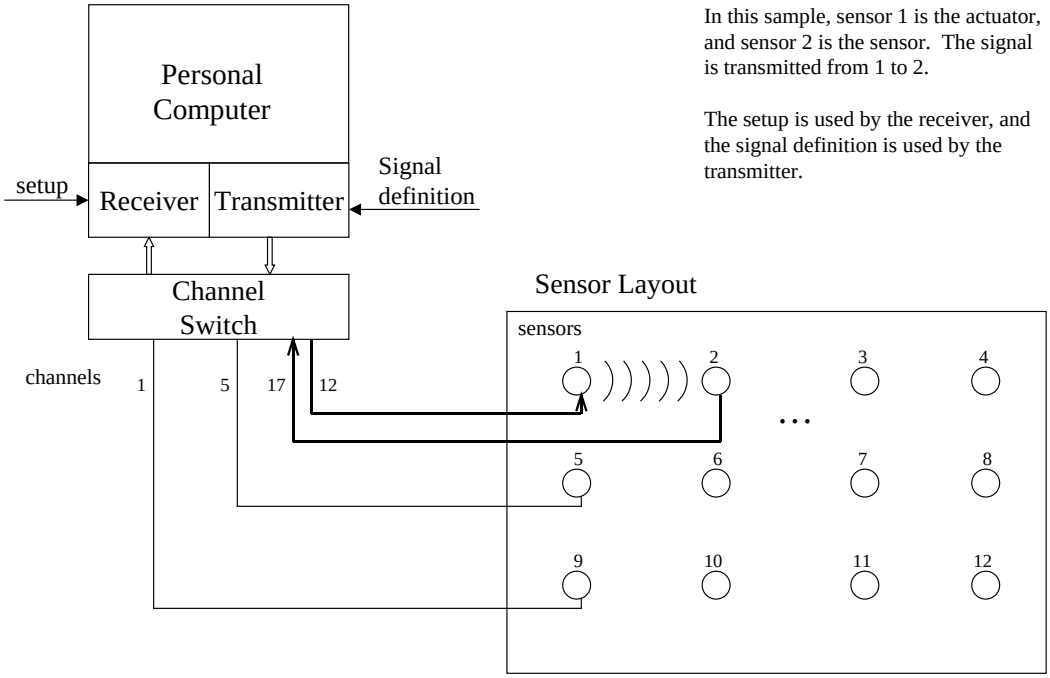

Figure 23. The SPS System Diagram

By repeating the process above through all pairs in the sensor network, the structure is scanned and a set of data that represents the health of the structure is collected. The set of data is analyzed using the software to detect damages.

The system uses a configurable transmitter and receiver for scanning the structure. The configuration data for the transmitter is called signal definition and the configuration data for the receiver are called setup.

The PZT sensors are permanently mounted on the structure. The locations of the sensors and the channel assignments of the sensors can then be stored as sensor definition.

2.2.3.2 Conceptual Software Architecture.

The architecture of the active software (figure 24) is designed to allow flexible yet reliable implementation of the damage monitoring software. The software is structured as three major building blocks:

1. A user interface block
2. A platform block
3. An application block

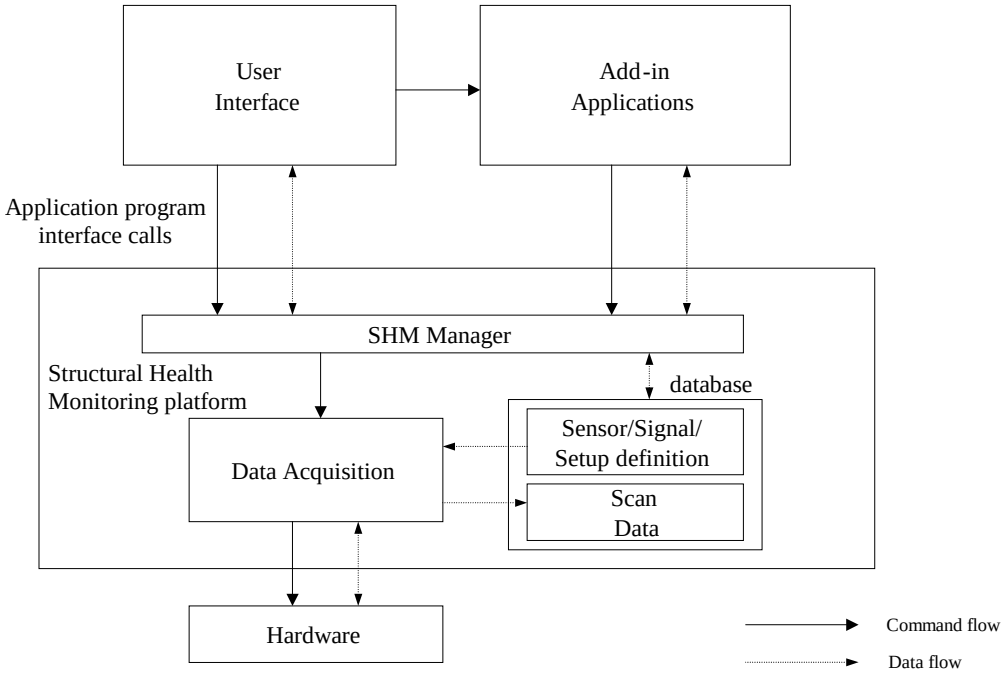

Figure 24. The SPS Architecture

The function of each block is described below.

- User interface block—It manages the interaction of the software with the end user.

- Platform block—It manages all the hardware-related functions. To manage the functions, it maintains the state of the current configuration. The configuration parameters include the sensor definition of the sensor network, the signal definition of the transmitter, and the setup of the receiver. Based on the configuration, it commands the device driver to scan the structure and store the scan result in the database. This is the basic data acquisition function. In addition, it also provides a set of system maintenance functions, including self-diagnose, automatic optimization of signal gain, automatic signal definition generation, and direct imaging to display the scan result.

- Applications block—Multiple applications can be built on top of the platform. The applications perform data analysis and report damage based on the collected data. A variety of algorithms can be implemented at the application level. It is also possible to combine several algorithms into a single application.

2.2.3.3 Data Management System.

The data management system is a central part of SPS. It manages large amounts of data for fatigue and damage detection. The objectives of the data management system development are to:

- Handle large amounts of data.
- Be easy to use.
- Have flexibility to make changes.
- Have the ability to archive and restore data.
- Be cost effective.

Sequential processing is the nature of data processing in SPS. There is no random accessing of data. Therefore, an expensive database system is not needed. Based on the objectives above, it was decided to use a file system for data management. An advantage of using a file system is that the standard file archiving and restoring utilities can be used for long-term data storage.

The SPS data management system groups files into workspaces. Each workspace represents a single project. The workspace file has the file extension *.ace. The workspace file keeps track of all the files in the workspace.

The procedure for the software flow process and its interface with the data management software is shown in figure 22.

Each workspace includes data used in the following functional blocks:

- Sensor system configuration: Data used in this function consist of sensor layout geometry and data channel assigned to each sensor. The configuration data are stored in files with extension *.sns.

- Data acquisition (DAQ) setup: The DAQ will set up the data acquisition configuration parameters, such as sampling rate and number of sampling points. The parameters are stored in files with extension *.stp.

- Path definition: This function defines the signal paths and signal parameters, such as signal pattern and voltage, used to scan the structure. The information is stored in files with extension *.dfn.

- Database: This is the collection of user data obtained from scanning the structure using the *Collect data* function. Each pass generates a single file. The structure can be scanned multiple times, therefore generating multiple files. The sum of all the user files forms the database. Each user data file has the file extension *.dat.

Each type of data is stored in a separate directory. For example, all the sensor layouts are stored in one directory and DAQ setup in another directory. The advantage of using this structure is that common configurations can be leveraged in separate workspaces without redefining them.

The Smart Patch sensor layout requires the user to enter inputs pertaining to the sensor position and corresponding channel. The required inputs are given in table 2.

Table 2. Required Inputs to the Sensor Layout Module

Inputs
Number of sensors
Number of layers
Units for sensor coordinates (in. or cm)
Sensor coordinates
Channel number
Layer number
Sensor Layout ID

After the sensor layout is defined, the layout is saved in a file (figure 25). The user interface allows the user to specify a file to save the layout.

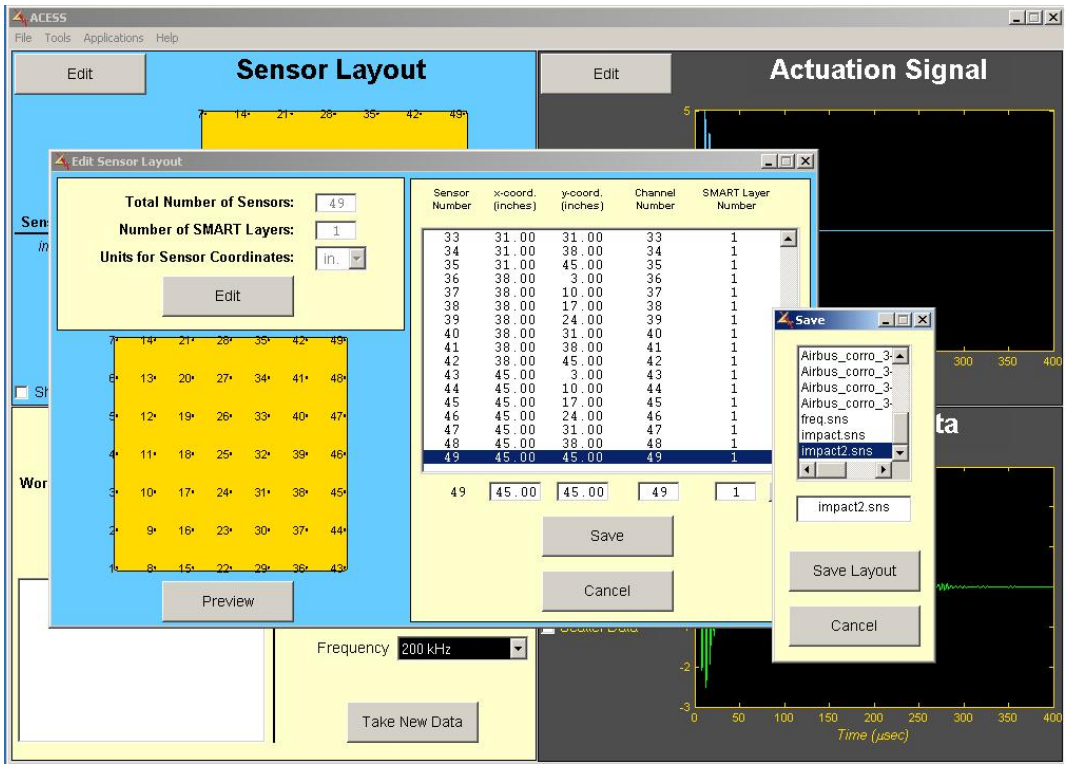

Figure 25. Sensor Layout Windows

When the user chooses a DAQ setup from the possible values provided in the menu, the selection can be saved in a file (figure 26) and for the signal path definition (figure 27).

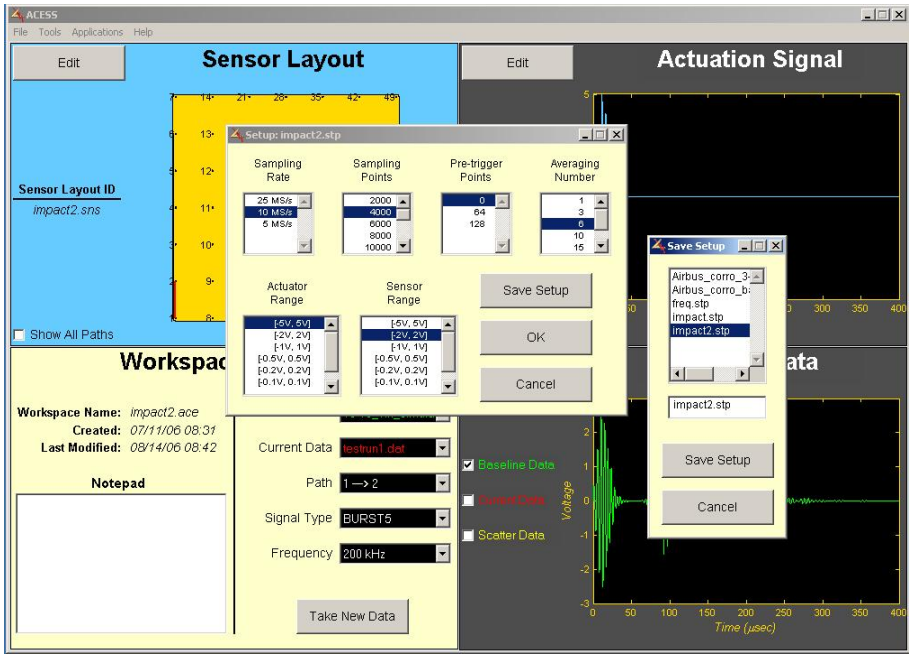

Figure 26. Windows for DAQ Setup

The user may edit the signal path definition table (figure 27). When it is completed, the table can be saved in a file.

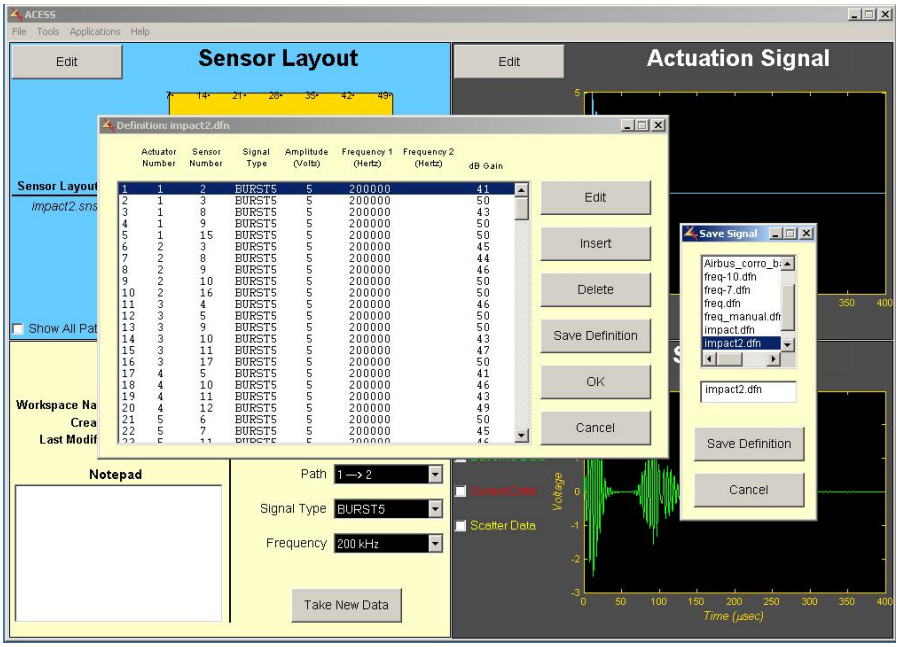

Figure 27. Windows for Signal Path Definition

Every time new data are collected, the scanned data is stored in a file for later analysis (figure 28).

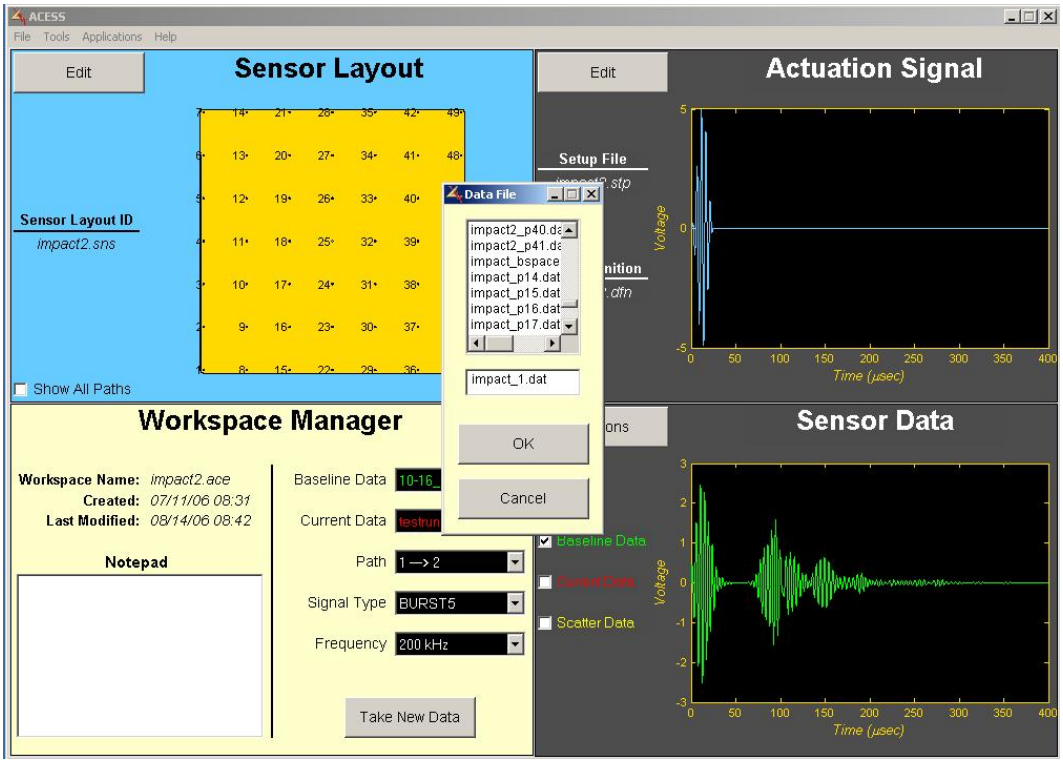

Figure 28. Window for Data Collection

2.2.3.4 Importation of Computer-Aided Design Structural Mesh.

The software interface has the ability to import a computer-aided design (CAD) model with *.stl or *.slp format. Acellent successfully imported a CAD structural mesh into the Smart Patch interface and displayed the three-dimensional (3D) geometry (figure 29). A light source has been fixed in the upper left side of the window and the structure can be rotated to view from any angle.

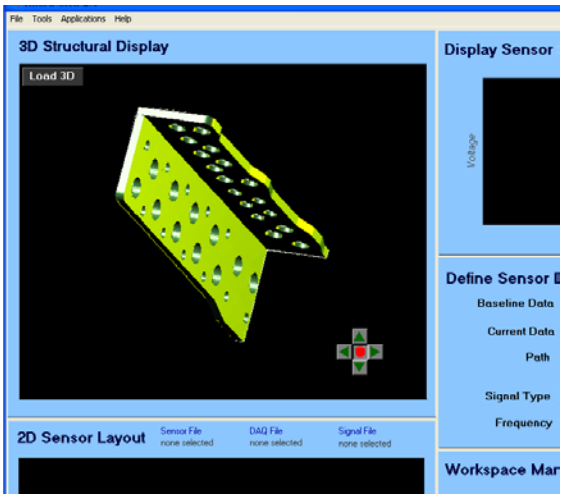

Figure 29. Interface Displaying 3D Geometry

Acellent currently uses MATLAB® to program the placement of the sensors on the 3D structure and to map the image of detected damage onto the surface. A plan for converting the code from MATLAB to Microsoft® Visual C++ programming language is being developed.

Sensor self-diagnostics is an important tool. If one or more sensors are degraded, damaged, or missing, the SPS may not function properly and will usually give false indications of structural damage. Measuring the impedance of each channel can find an open or short circuit. This can indicate a missing sensor or damaged connection or wiring. But a degraded or damaged sensor may go undetected using the impedance method. To resolve this, a reasoning process was designed using the active sensor signals to detect degraded or damaged sensors that the impedance method may miss.

2.2.3.5 Self Diagnostics.

If one or more sensors are degraded, damaged, or missing, the SPS may not function properly and can give false indications of structural damage. Measuring the impedance of each channel can allow an open or short circuit to be found, which can indicate a missing sensor or damaged connection/wiring. But a degraded or damaged transducer may go undetected using the impedance method. To resolve this, a reasoning process was designed using the active sensor signals to detect degraded or damaged transducers that the impedance method may miss. The self-diagnostics software developed earlier by Acellent was used here and adapted for rotorcraft application.

For the impedance method, the following are included in the input file:

- The measurement parameters
- The sensor number and the corresponding channel number

The output file is an ASCII (American Standard Code for Information Interchange) file with two columns of numbers. The first column is the transducer number and the second is the fault code. There are four values for the fault code ranging from 0 to 3, and they are defined as follows:

- 0: Normal
- 1: PZT transducer open circuit or broken
- 2: PZT transducer circuit shortage
- 3: Cables not connected or connected incorrectly

SPS software reads the fault codes and generates a graphical diagnostic display.

If all transducers pass the impedance test (i.e., there is no open or short circuit), but there are no sensor signals recorded (i.e., signals do not exist or are very weak) for all actuator-sensor paths associated with a given PZT transducer, then this indicates a disbonded sensor.

If all transducers pass the impedance test and all actuator-sensor paths record a signal, then a more detailed reasoning process is used to check for degraded transducers. This reasoning process involves comparing signals on paths going directly through a suspect sensor. If there are signal changes between the current data and baseline data for all actuator-sensor paths associated with a given PZT transducer, but there are no signal changes on paths going directly through the transducer, then this is an indication of a degraded sensor (partially damaged or disbonded). For example, as shown in figure 30, if paths 1 to 2 and 2 to 3 show signal changes, but path 1 to 3 does not show any changes, then this indicates transducer no. 2 is partially damaged or disbonded.

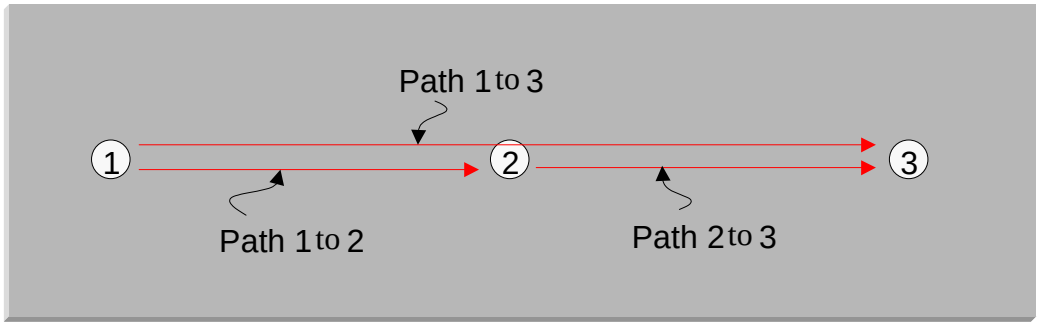

Figure 30. Self-Diagnostic Reasoning Process Compares Signals on Paths Going Directly Through Affected Sensors

If a sensor is flagged as degraded, damaged, or missing, all signal data from the faulty sensor are removed from the analysis routines.

2.2.3.6 Signal Processing.

Bandpass filtering is applied to the recorded sensors' signals. The center frequency for the filter is the defined driving frequency of the actuator. The filter coefficients are generated by a Hamming-window-based finite-impulse-response filter called fir1. It is used in designing filters

for standard low-pass, high-pass, bandpass, and bandstop configurations. By default, the filter is normalized so that the magnitude response of the filter at the center frequency of the passband is 0 dB.

The coefficients are used as input into a zero-phase digital filter called filtfilt. This filter performs zero-phase digital filtering by processing the input data in both forward and reverse directions. After filtering in the forward direction, it reverses the filtered sequence and runs it back through the filter. The resulting sequence has precisely zero-phase distortion and double the filter order. Filtfilt minimizes start-up and ending transients by matching initial conditions, and works for both real and complex inputs. In addition to the forward-reverse filtering, it attempts to minimize startup transients by adjusting initial conditions to match the DC component of the signal and by prepending several filter lengths of a flipped, reflected copy of the input signal.

If the center frequency is 150 kHz or less, then a low-pass filter is used instead of bandpass filter.

The inputs into the module are the raw signal data, the sampling rate, and the center frequency. The output is the filtered signal data.

2.2.3.7 Environmental Compensation.

An environmental compensation technique that uses multiple sets of data (obtained from the structure under various environmental conditions) was designed and can be used to compensate for effects caused by environmental changes in the rotorcraft operational environment. The method used here was adapted for use on rotorcraft structures from previously developed environmental compensation programs.

With this technique, data are collected from the structure under various conditions (e.g., different temperatures) and at different times. The signals from each temperature (or load, strain, moisture content, or any other condition that causes changes in a sensor signal) can be used to dynamically create a baseline for each individual actuator-sensor path and/or region on the structure. When a sensor scan is performed to search for damage, the newly recorded signals are compared to the dynamically created baseline with the effects of the environment removed. The method can also be used to determine a “best-fit” to the temperature (or load, strain, moisture content, or any other condition that causes changes in a sensor signal). This can be used to report the temperature (or load, strain, moisture content, or any other condition that causes changes in a sensor signal) of the structure along the corresponding actuator-sensor path and/or region on the structure, as well as the baseline data to use for damage assessment.

The automated data-collection process used to create and build the baseline space is shown in figure 31. The parameters that make up the three dimensions are:

- Dimension 1—Time series for each sensor signal
- Dimension 2—Actuator-sensor path number
- Dimension 3—Environmental parameter, such as temperature

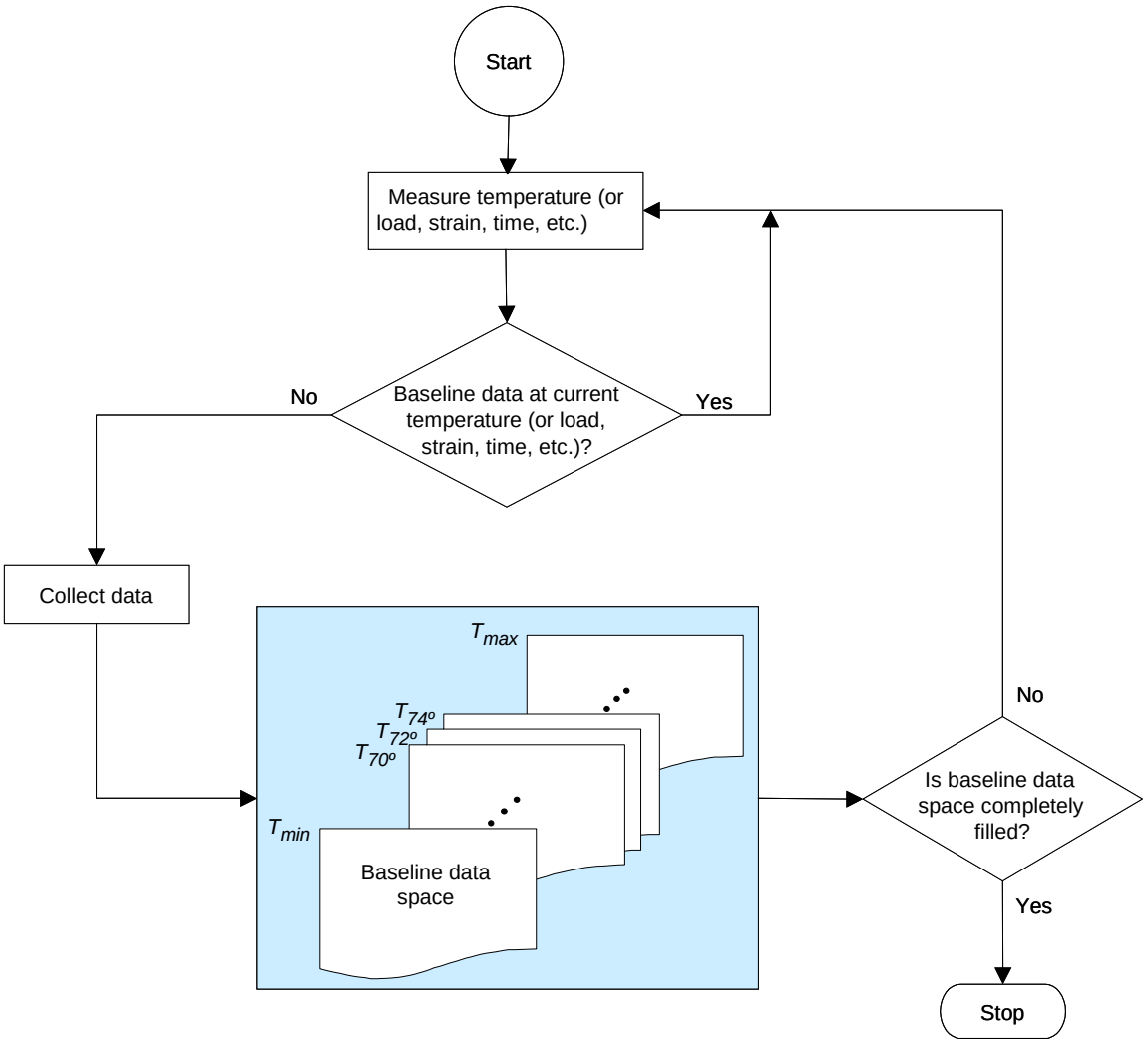

Figure 31. Data Collection Based on Predefined Trigger (Temperature, Load, Strain, Time, etc.)

Once the data collection process is started, the temperature of the structure is measured using a temperature sensor attached to the structure. (Note: The same process can be used with other parameters such as load, strain, moisture, time, etc.) If there are no baseline data at the current measured temperature, then a set of baseline data is collected and stored in the baseline space. If baseline data already exist at the current temperature, then the system will continue to measure the temperature and wait until it reaches a value at which there is not any previously recorded baseline data.

After the system has gone through the user-defined range of the temperatures and the baseline space has been completely filled with baseline data sets, then the process is stopped.

Prior to performing damage detection, the baseline space must be configured. The default setting uses all the data sets that were collected during the temperature measurements. But the user may want to add more data sets to increase the calibrated range or remove some data sets that may no

longer be valid. Adding or modifying the baseline space data files is accomplished using an interface. Once configured, the baseline space data files are stored in a file. The names of the data files are stored as a cell array of strings, where each string is a baseline data set filename.

The process for the temperature calibration technique uses multiple baselines (baseline space) at different temperatures, as shown in figure 32. After a sensor scan to search for damage is performed, the newly recorded signals (current data) for each path are compared to the corresponding baseline space data sets to determine a best-fit along the temperature axis. This gives the temperature of the structure along the corresponding actuator-sensor path, as well as the baseline data to use for damage assessment.

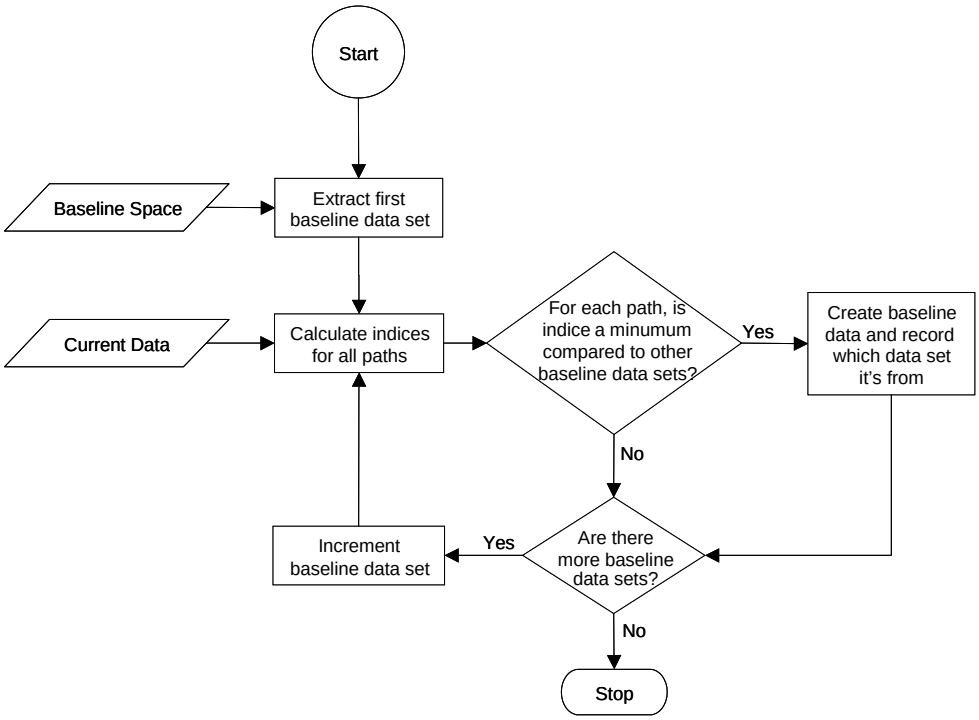

Figure 32. Temperature Calibration Process

The data files in the baseline space are selected one at a time and compared with the current data. The total signal energy (TSE) in the scatter signal for each path is calculated by taking the difference between the selected baseline space data and the current data. An index is then calculated for each path using the energy in the first arrival window of the scatter signal.

$$\text{Index} = \frac{\text{TSE of scatter data}}{(\text{TSE of current data}) + (\text{TSE) of baseline data})}$$

The next set of data in the baseline space is then selected and the indices for each path are calculated as above. The process continues until all sets of data in the baseline space have been compared with the current data and the corresponding indices have been calculated.

For each path, the best-fit data from the baseline space corresponds to the data with the minimum index value. The best-fit data for each path is used to construct the set of baseline data that is used for damage detection.

2.2.3.8 Data Analysis.

To analyze the data collected for damage detection, a methodology for fatigue crack detection in rotorcraft structures was designed. Depending on the actuation frequency, cracks at different locations with different lengths affect the signals in different ways. Specifically, when the crack size is relatively small, it can change a segment of one mode of the signal. The environment effects, especially temperature, often change a signal over the whole length. Therefore, accurate extraction of only the damage-sensitive signal segment is very important for increasing the signal-to-noise ratio and improving the reliability.

For damage detection, the first arrivals of the first symmetric and anti-symmetric modes of a signal are extracted. Then, for each mode, the first arrival and the wave packet immediately after the first arrival (the scattering wave packet) are used as the featured component. The algorithm that was developed for extracting the first arrival of different modes was designed using the following steps:

1. Select a set of signals that have the same frequency and same path length.

2. Locally shift the signals for phase alignment.

3. Add all the signals and compute the envelope of the sum. This enhances the first arrival of each mode and suppresses other components.

4. Choose the first wave packet in the sum that is greater than a threshold. This wave packet is the first arrival of one mode (usually the first symmetric Lamb wave mode − *S*0 mode). Then, choose the corresponding scattering wave packet.

5. Choose the second wave packet in the sum that is greater than a threshold. This wave packet is the first arrival of another mode (usually the first antisymmetric Lamb wave mode—*A*0 mode). Then, choose the corresponding scattering wave packet.

6. Compute the group velocity corresponding to the two modes.

7. Use the group velocity to determine the time instant of the first arrival of other paths. Then, choose the corresponding scattering wave packet.

After the featured components are extracted, the new signals are compared to the baseline. Then the following indices are used for damage detection:

$$I_{S0} = \sqrt{\frac{\left| e_c^{S0} - e_b^{S0} \right|}{e_c^{S0} + e_b^{S0}}} \tag{1}$$

where e_b^{S0} is the energy of the featured component of the baseline corresponding to the symmetric mode and e_c^{S0} is that of the current data, respectively. Similar notations are used of the anti-symmetric mode *A*0 in equation 2.

$$I_{A0} = \sqrt{\frac{\left| e_c^{A0} - e_b^{A0} \right|}{e_c^{A0} + e_b^{A0}}} \tag{2}$$

In damage detection, if either of I_{S0} and I_{A0} of at least two neighboring paths is greater than the corresponding threshold, then damage exists. To identify the damage location, a moving window $g(t)$ (e.g., a Gaussian with the same length as the actuation signal) is applied to the featured components of the current and baseline signals, denoted by $x_c(t)$, the featured component of the current signal, and $x_b(t)$, the featured component of the baseline signal. Then, the following local energy is defined by:

$$E_c = \int \{x_c(t) g(t)\}^2 dt \tag{3}$$

$$E_b = \int \{x_b(t) g(t)\}^2 dt \tag{4}$$

and the following local energy difference function:

$$I(t) = \frac{\left| E_c(t) - E_b(t) \right|}{E_c(t) + E_b(t)} \tag{5}$$

This function is defined for both the *S*0 and *A*0.

The Smart Patch software also has an imaging tool that uses the recorded sensor data to generate and display a graphical representation of structural anomalies, which gives the ability to quickly compare and evaluate data-analysis methodologies for different applications. To facilitate the comparison and evaluation, various controls (push buttons, slider bars, checkboxes, and radio buttons) are provided to allow the user to quickly change analysis methodologies and adjust parameters.

Direct path image function provides the capability of direct comparison of the current data with baseline data, and produces an image that gives a qualitative visual representation of damage. To access the direct path image, the user selects the current data file and the baseline data file from the Workspace Manager file (figure 33).

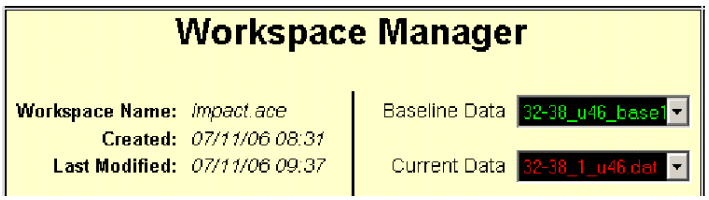

Figure 33. Baseline Data and the Current Data File Selections

Once the files of interest have been identified, the user accesses the menu bar and clicks Application→Direct Path Image, as shown in figure 34.

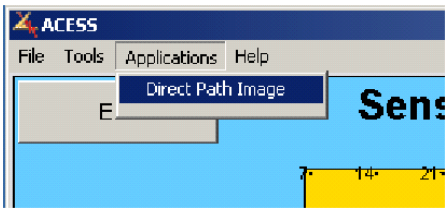

Figure 34. Selecting the Direct Path Image from the Applications Menu

The application opens an imaging window, as shown in figure 35. If image settings for the particular workspace have been previously defined and saved, those settings are used to set the controls. If not, default settings are used.

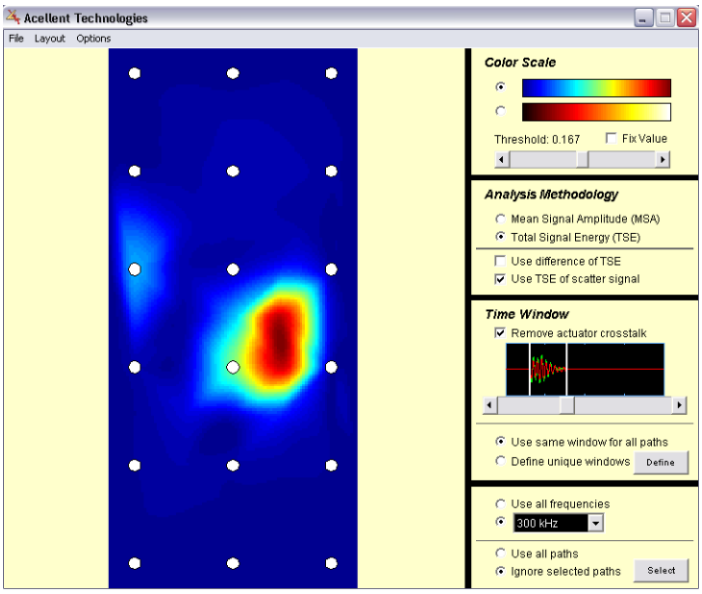

Figure 35. Imaging Window

The Direct Path Image function provides several controls to help refine the image. Using the user-selected parameters (paths, frequencies, time windows, and analysis methodologies), an image is generated. A description of each of the controls is provided below each image.

The user can choose from two color scales by clicking the radio button associated with the color scale of choice.

By using the threshold adjustment bar (figure 36), the user can adjust the mapping of the data values to the color scale. Adjusting the slider bar to the left decreases the threshold and makes the smaller values appear larger (i.e., it makes the image more sensitive to small values). Adjusting the slider bar to the right increases the threshold and makes larger values appear small (i.e., this makes the image less sensitive to small values).

The system sensitivity is selected by dragging the threshold sliding bar. In addition to the sliding bar position, a threshold value is displayed on top of the sliding bar. When a desired threshold is set, it can be locked by checking the *Fix Value* box.

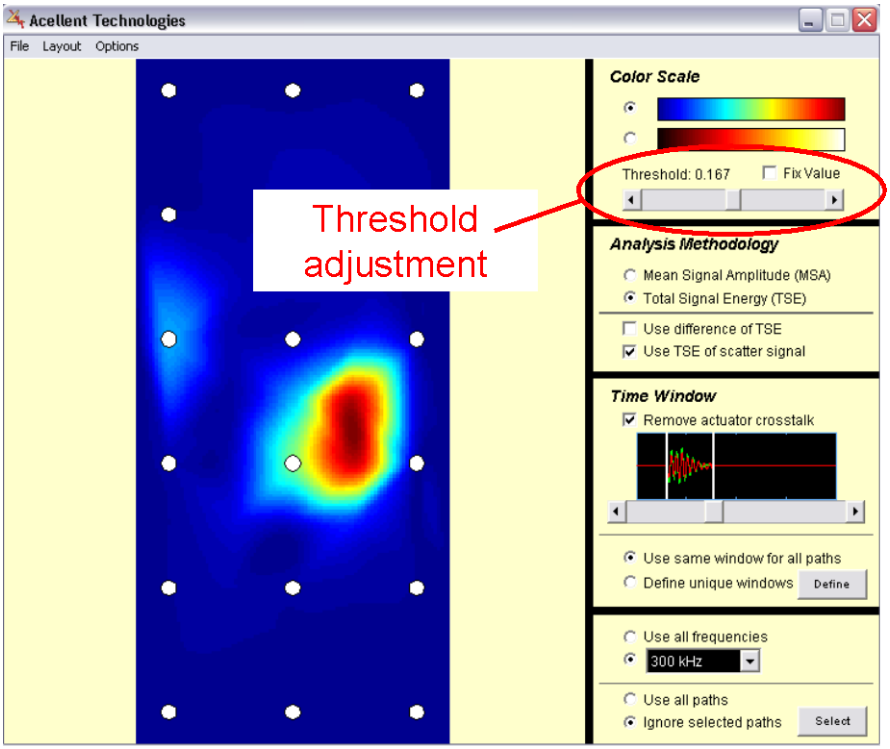

Figure 36. Controls to Adjust Threshold for Imaging

Two methodologies are provided to compare the current data against the baseline data, the mean signal amplitude (MSA) and the total signal energy (TSE). The methodology is selected by clicking the radio button that corresponds to the methodology (figure 37).

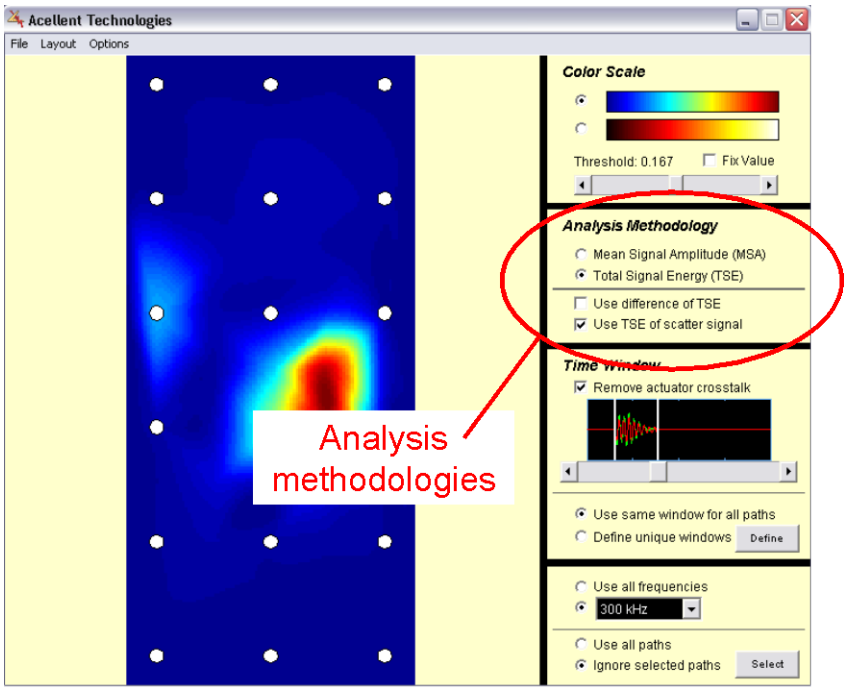

Figure 37. Controls to Select Analysis Methodologies

The MSA is calculated by finding the mean of the absolute value of the signal voltage within the specified time window. The TSE is calculated by finding the total energy in the signal within the specified time window.

For each methodology, the user can select one or both of the following options:

- The *Use difference of MSA (or TSE)* option calculates the MSA (or TSE) of the baseline data and current data first, then subtracts the MSA (or TSE) of baseline data from MSA (or TSE) of the current data.

- The *Use MSA (or TSE) of scatter signal* option calculates the MSA (or TSE) of the scatter signal, which is the difference between the current data and the baseline data.

If the difference of MSA (or TSE) is selected, then the index value for each path is calculated by:

$$\text{Index} = \frac{[\text{MSA (or TSE) of current data}] - [\text{MSA (or TSE) of baseline data}]}{[\text{MSA (or TSE) of current data}] + [\text{MSA (or TSE) of baseline data}]}$$

If the MSA (or TSE) of the scatter signal is selected, then the index value for each path is calculated by:

$$\text{Index} = \frac{\text{MSA (or TSE) of scatter data}}{[\text{MSA (or TSE) of current data}] + [\text{MSA (or TSE) of baseline data}]}$$

The time window controls (figure 38) limit the comparison of current data and baseline data to the time span as specified.

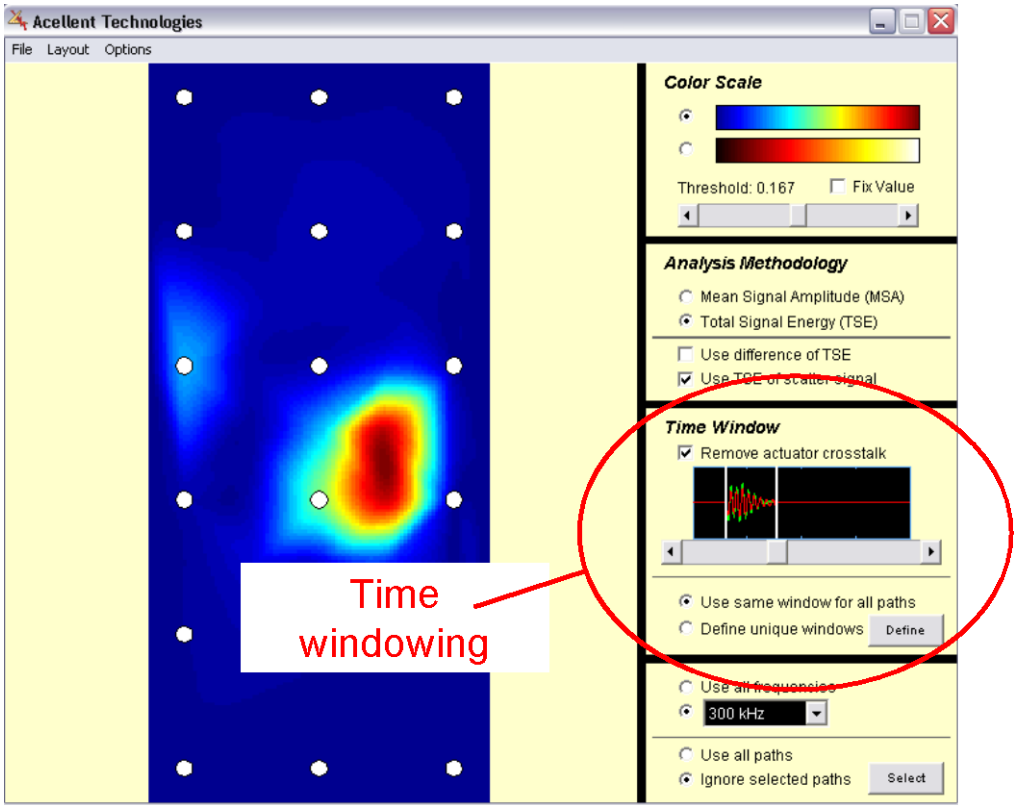

Figure 38. Controls to Select Time Windows for Imaging

The *Remove actuator crosstalk* checkbox allows the user to eliminate the leading crosstalk part of the signal from comparison.

The sliding bar at the bottom of the time window allows the user to eliminate the trailing part of the signal from comparison.

The *Use same window for all paths* checkbox, when checked, allows the user to apply the same time window for all data paths.

The *Define unique windows* checkbox allows the user to define a unique time window for each individual path. This feature is not implemented in this version. It is reserved for a future release.

If the *Use all frequencies* radio button is selected (figure 39), then the image is generated using all frequencies.

When generating an image, data from all defined actuation frequencies or from individual frequencies may be used.

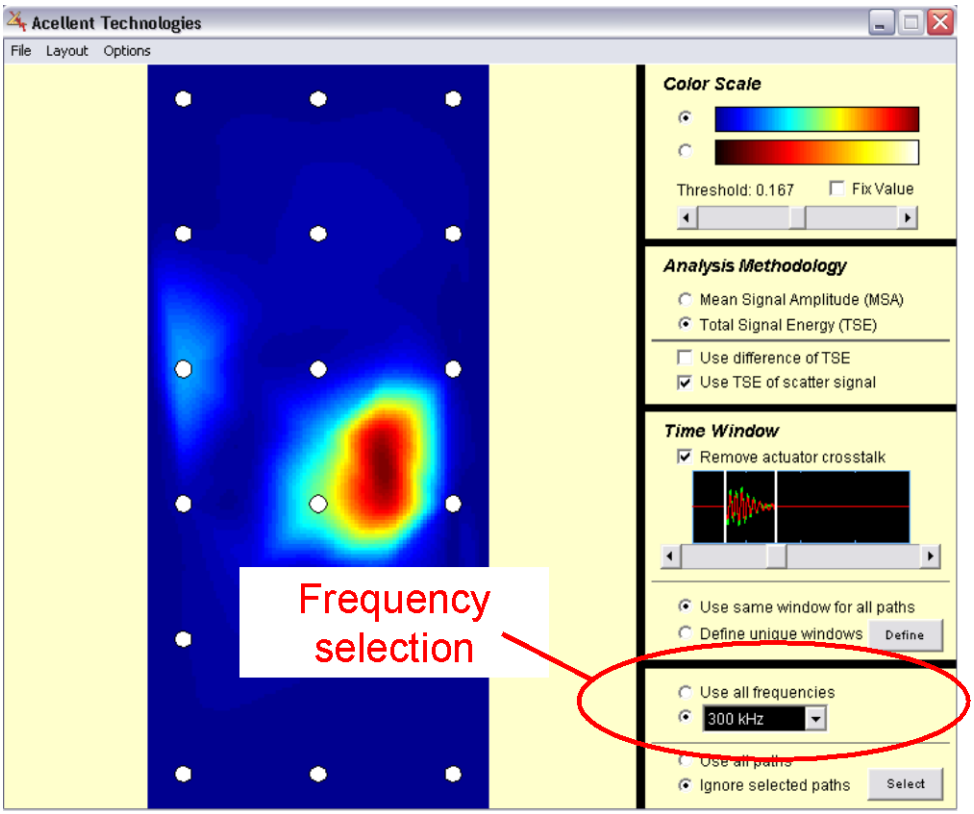

Figure 39. Controls to Select Frequencies for Imaging

If the second radio button is selected, then the user can select the individual frequency from the pull-down menu. Checking the frequency radio button and selecting a frequency limits the comparison to use only the paths with the specified frequency. The image is then generated using only the individual frequency.

When generating an image, data from all defined actuator-sensor paths may be used, or some user-selected paths can be ignored in the analysis.

If the *Use all paths* radio button is selected (figure 40), then the image is generated using all actuator-sensor paths.

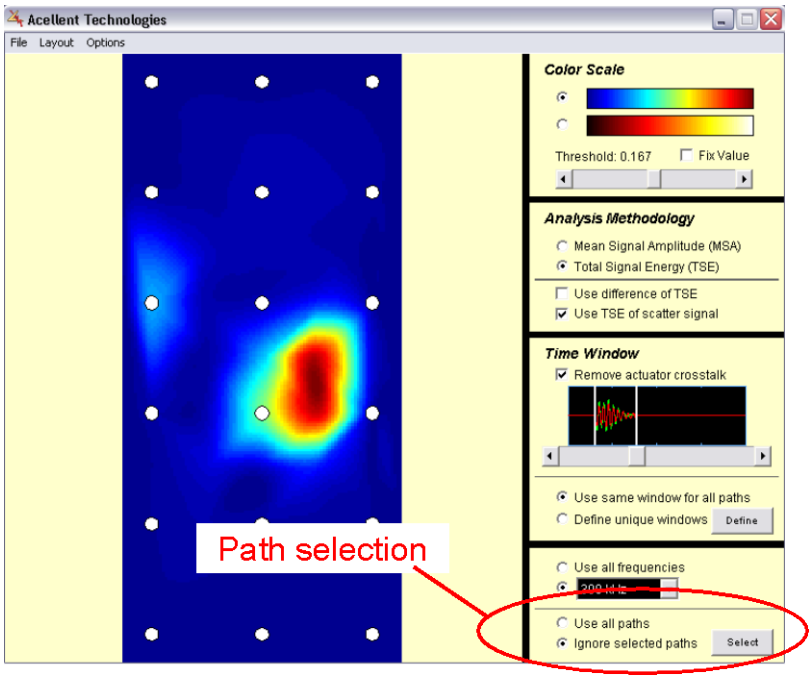

Figure 40. Controls to Select Paths for Imaging

If the *Ignore selected paths* radio button is selected, then the user can select the individual paths to ignore in the analysis by pushing the *Select* button. When the *Select* button is pressed, the interface shown in figure 41 is opened and is used to select and define the operating paths to be used in the analysis.

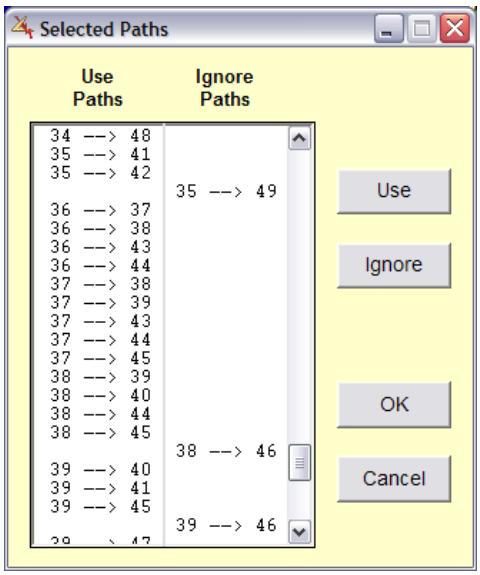

Figure 41. Interface for Selecting and Ignoring Paths

2.2.3.9 Damage Quantification.

A software tool was developed to output quantitative damage growth measures. This section describes how the tool works and gives the step-by-step procedure on its use.

An empirical-based quantification scheme was used that will gain accuracy as tests are conducted on rotorcraft structures. The flowchart in figure 42 shows the quantification process.

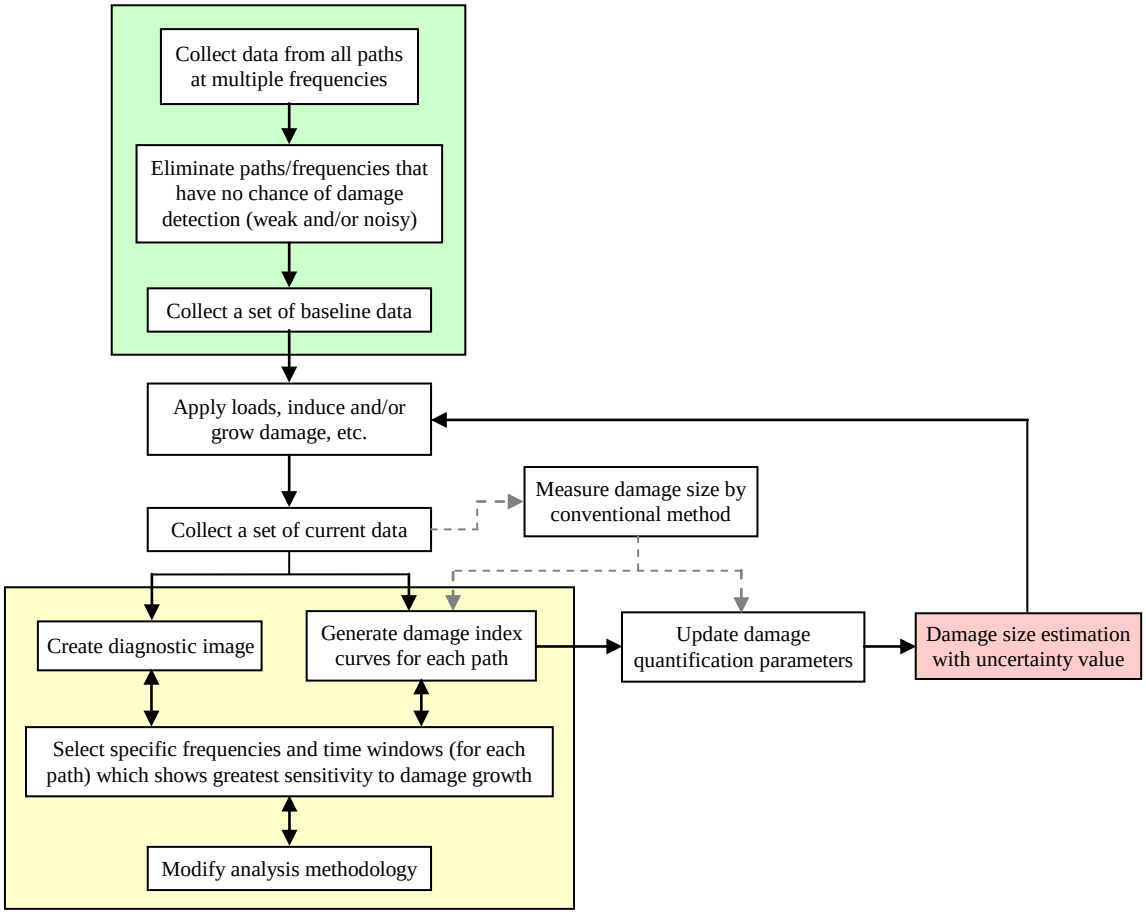

Figure 42. Flowchart for Empirical-Based Damage Quantification Scheme

The green box in figure 42 highlights the basic steps that are always taken for a new structure. First, data is collected from all paths at multiple frequencies. Depending on the number of paths and frequencies, it can take more than 10 minutes to acquire all the data. Also, the file sizes can be prohibitively large. To minimize the data acquisition time and reduce the size of the data files, the paths and frequencies that have little or no chance of being sensitive to damage (i.e., signals that are relatively weak, noisy, or both compared to the rest of the signals from the structure) must be eliminated. Then, a baseline data set can be collected using the remaining paths and frequencies that have the best chance of being sensitive to damage.

Next, fatigue loads or impacts are applied to the structure to initiate and grow damage (some other method may also be used to induce damage). As the damage grows, new data will be collected at various intervals and compared to the baseline data.

Specific frequencies and time windows (for each path) that show the greatest sensitivity to damage growth are then selected, and the analysis methodology is chosen to calculate damage indices for each path. The damage indices are used to create a diagnostic image highlighting the location of structural changes.

From the menu bar on the image window, the *Options* → *Generate report* option is selected. A new window (figure 43) opens that allows the user to input the data filenames, number of cycles (if fatigue testing), and damage size, as measured by a conventional method. This information is saved and only needs to be input once.

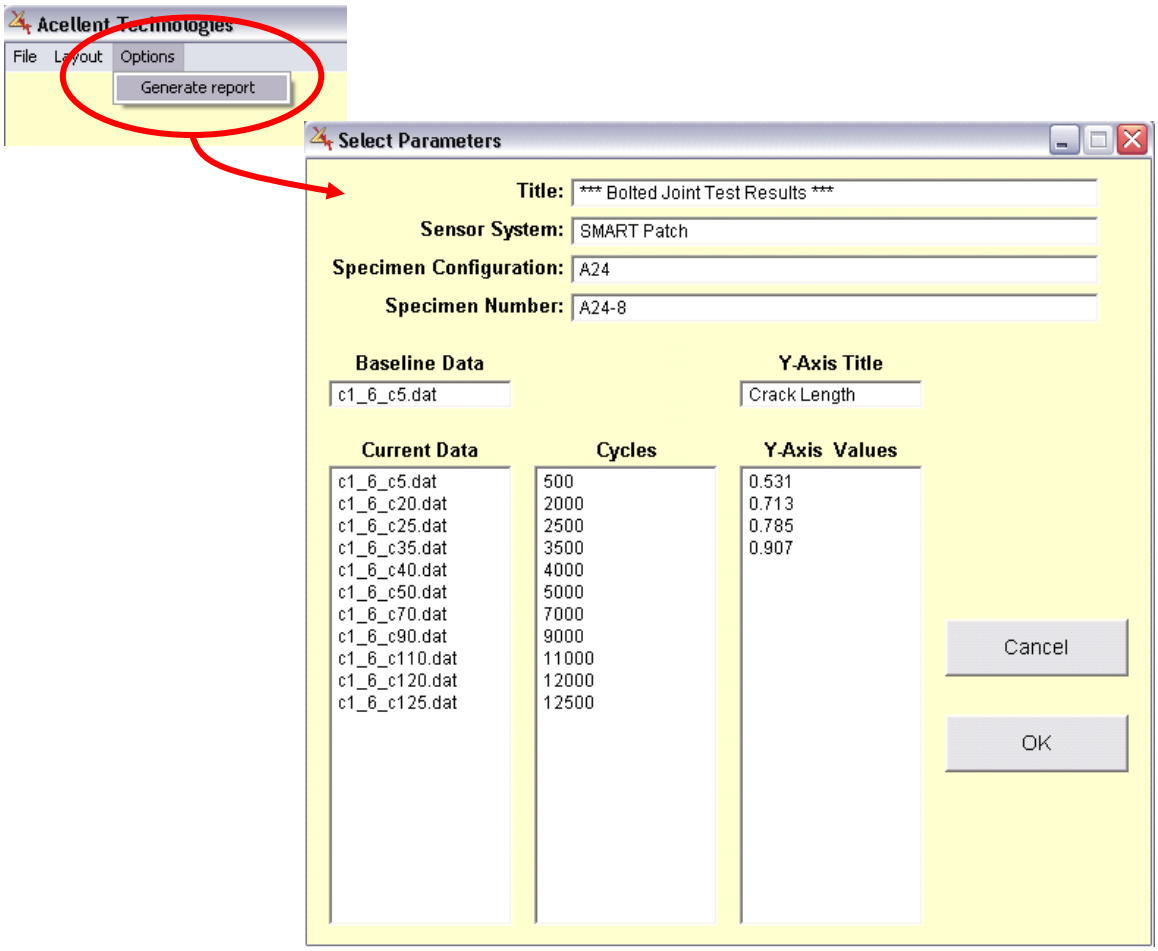

Figure 43. Window for Inputting Parameters

This information is used to generate damage index curves (for the selected frequencies, time windows, and analysis methodology) for paths passing through or near the damage (figure 44).

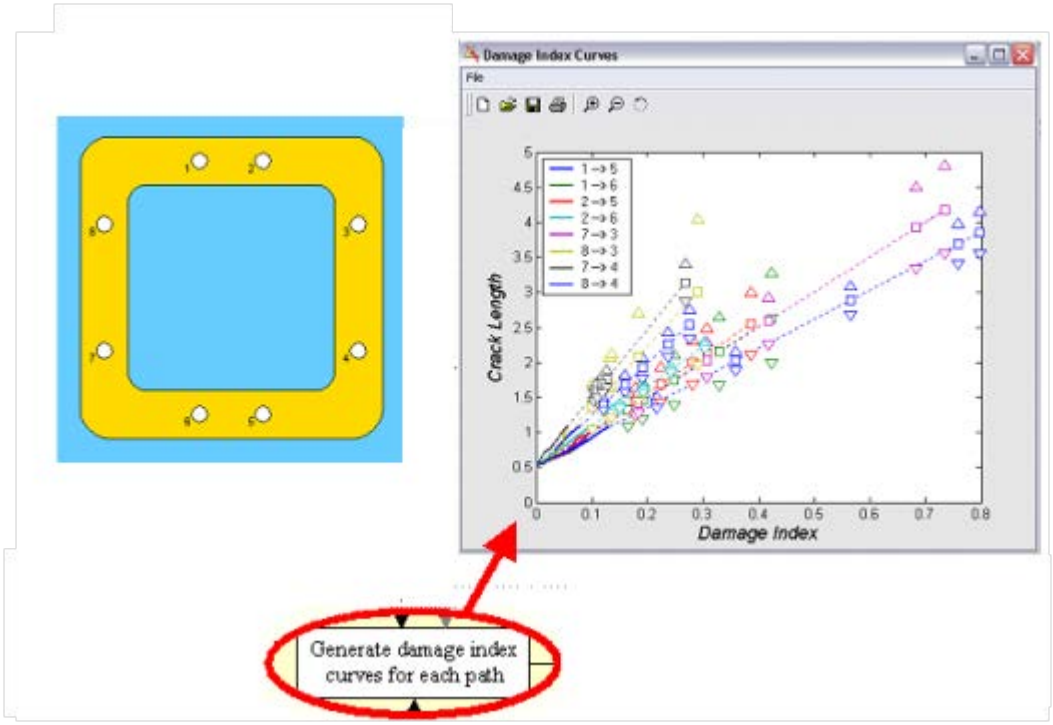

Figure 44. Damage Index Curves for Each Path

These curves are constructed using the damage indices along with the known values of the damage size, as measured by conventional methods. The objective is to have the damage index curves be correlated with damage size so that any calculated damage index can be directly related to damage size. Therefore, the frequencies, time windows, and analysis methodology may need to be adjusted after several measurements have been made.

For each path, a linear curve fit is applied to the data and error estimates are calculated. When sensor data are collected, the linear curves are used to extrapolate damage sizes using the measured damage indices. The more measurements that are used, the better the predictions of damage size will be.

The predicted damage size is then calculated using a weighted average from all the paths, giving more weight to the paths with smaller error estimates. The associated uncertainty value is also calculated using the weighted average and corresponds to a 95% confidence interval. The damage size estimates, along with the uncertainties, are presented in tabular form (figure 45).

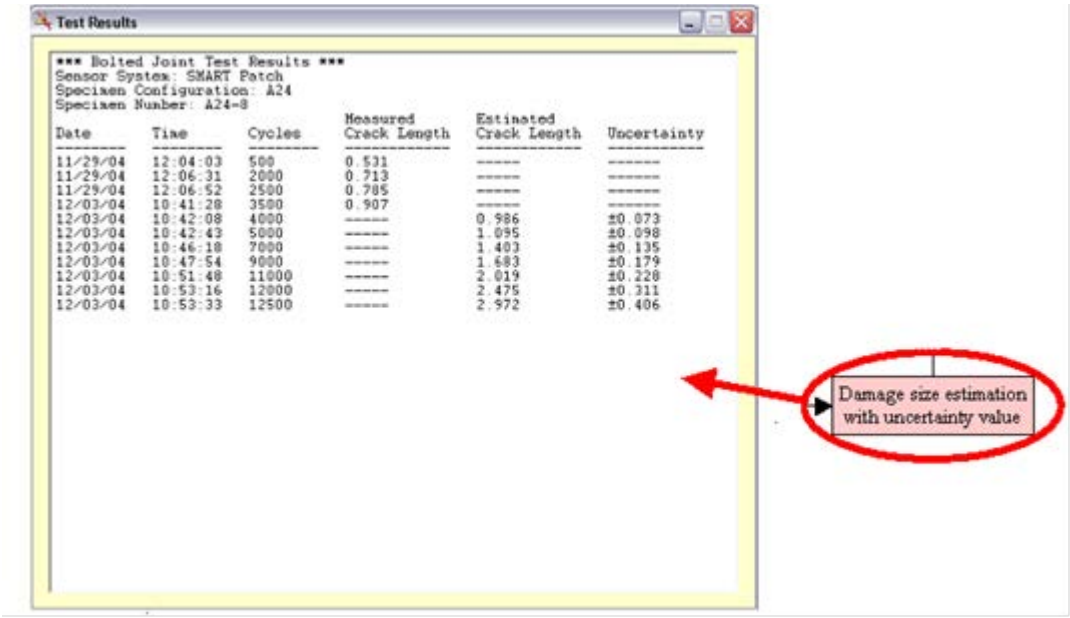

Figure 45. Damage Size Estimates and Uncertainty Values

The calibration procedures for both environmental compensation and damage sizing were coded as separate modules and were packaged together in the SPS software. The environmental calibration module uses a temperature sensor to measure the temperature of the structure. During calibration, the structure temperature is used as a trigger for the SPS to collect and store baseline data. During assessment of the structural integrity, the baseline data is used to distinguish damage from environmental effects.

The scheme used to calibrate for both environmental compensation and damage quantification is shown in figure 46.

The SPS software has the following features:

- An interface to input damage sizes as measured by conventional methods
- A module to automatically generate the damage index curves using the selected frequencies, time windows, and analysis methodology, and an unlimited number of data files
- An automated approach to calculate the slope of each damage index curve (and/or other quantification parameters) and extrapolate to estimate damage sizes
- An automated method to calculate the uncertainty in the damage size estimates
- A module to automatically generate the results in tabular form
- A module to import CAD structural meshes to display 3D geometries

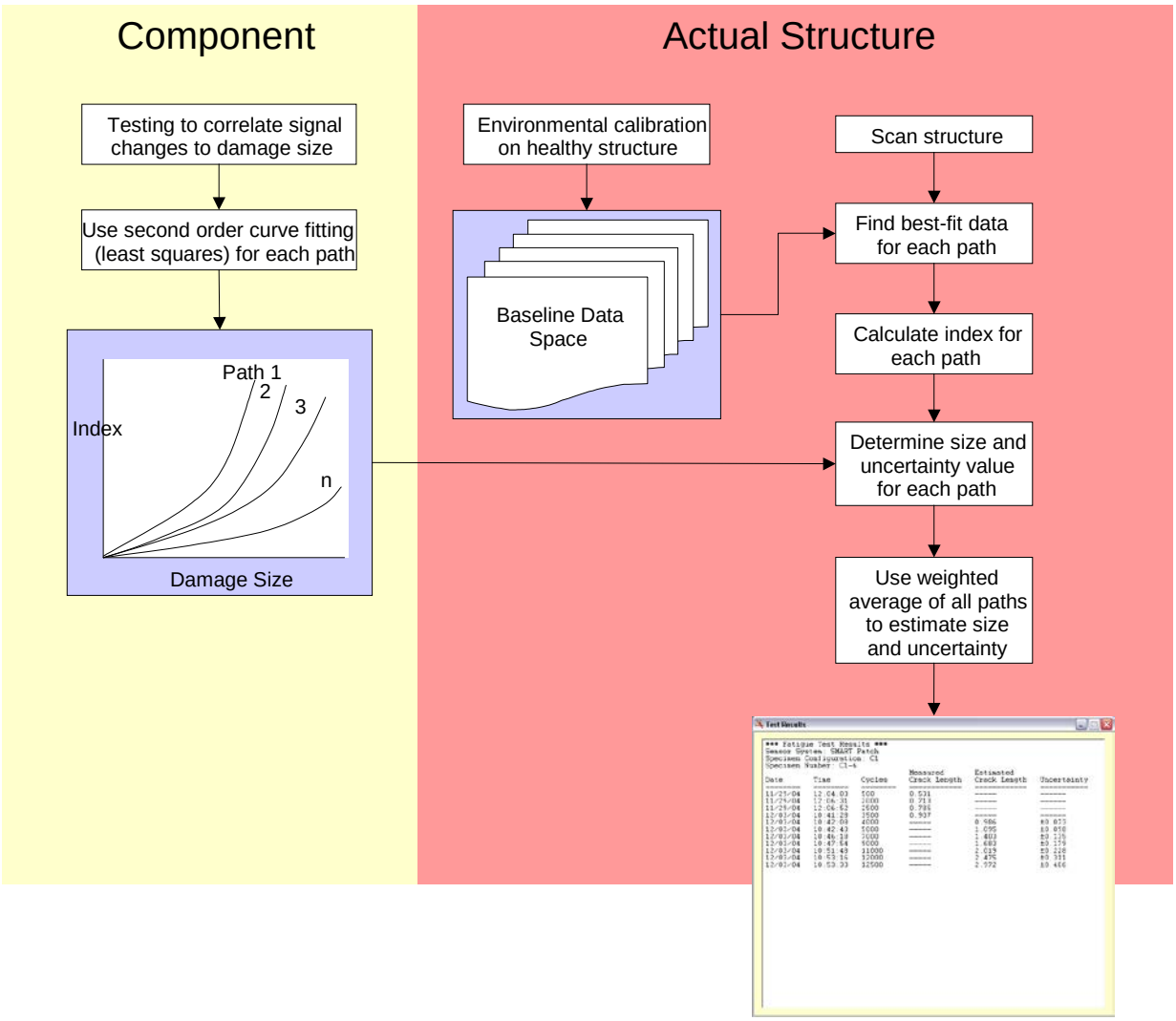

Figure 46. Calibration for Both Environmental Compensation and Damage Quantification

2.2.3.10 The HUMS Interface.

After the data have run through the damage detection algorithms and any detected damage has been quantified, the results are generated. Building on previous work integrating structural health monitoring (SHM) with integrated vehicle health management systems, the suggested interface protocol and command line messages for software integration with rotorcraft HUMS were defined and the event messages are shown in table 3.

Table 3. Event Messages for HUMS Interface

Field	Data Type	Units	Description
Inspection Time (GMT)	double	seconds	Time of inspection in seconds from midnight of January 1 of the current year.
Location - *x*	short	inch	Estimated location of damage in *x*-direction relative to reference point.
Location - *y*	short	inch	Estimated location of damage in *y*-direction relative to reference point.
Damage size	short	inch	Estimated damage diameter
Growth rate	short	inch/sec	Growth rate based on previous estimated damage size and time since last inspection

2.2.4 Reliability Issues—POD and False Aarm Rates, Sensor Reliability, and System Reliability.

Reliability issues regarding the use of the SPS for rotorcraft structural applications were investigated. The goal of the task was to ensure the reliability of the SPS for rotorcraft. Utilizing previous work conducted by Acellent to develop POD statistical data, this task developed methods to determine the POD and sensor self-diagnostics. Self-diagnostic methods to discriminate between sensor failure and structural damage were also adapted from those previously developed by team members. This information was then incorporated into the FHA.

Traditional NDE techniques are based on single-point measurements for detecting damage, and their associated POD is generally determined through experimental testing. This traditional test approach to determine the POD is difficult to adopt for an SHM sensor network because of:

- Sensor positions and network arrangements.
- Structural geometries and boundary conditions.
- Damage locations, orientation, and severity.

To minimize the amount of required testing, a hybrid approach was proposed that uses numerical simulation coupled with carefully designed experiments [8 and 9]. The numerical simulations are being developed under a parallel effort, with the goal of developing a practical method to build a sufficient database, from which a POD can be determined for any given sensor arrangement.

A major issue that needs to be accounted for in SHM is changes in environmental and boundary conditions. For traditional NDE, inspections typically occur in a controlled environment and may involve cleaning the structural surface first. In contrast, SHM is intended for on site use in the field without any structural teardown, so the conditions may vary widely. Model-assisted

POD methods coupled with the use of damage simulators are being developed to provide a sufficient amount of statistically independent data points while minimizing the amount of required empirical testing [9].

Sensor self-diagnostics is an important tool. If one or more sensors are degraded, damaged, or missing, the SPS may not function properly and will usually give false indications of structural damage. Measuring the impedance of each channel can be used to find an open or short circuit. This can indicate a missing sensor or damaged connection/wiring. But a degraded or damaged sensor may go undetected using the impedance method. To resolve this, a reasoning process using the active sensor signals was designed to detect degraded or damaged sensors that the impedance method may miss. The self-diagnostics methodology is described in more detail in the software development section 2.2.3.4.

3. TESTING AND VALIDATION FOR THE SPS SYSTEM.

The goal of this effort was to ensure that the SPS design and software development are directly applicable to rotorcraft used in the field and can be used for credit validation. System testing and validation was conducted on three levels as follows:

1. Coupon/laboratory level tests
2. Component level tests
3. Simulated flight tests

The objective of the validation testing was to determine if the SPS design and software developed in sections 2.1 and 2.2 can identify and quantify the cracks occurring in the structures during testing. The test results were validated using existing nondestructive inspection (NDI) techniques.

3.1 COUPON TESTS.

The goal of the coupon tests was to ensure:

- Sensor survivability.
- That clean, usable data could be obtained.

Since the Smart Patch for rotorcraft structures is based on Acellent's SMART Layer and uses a network of piezoelectric sensors embedded in a flexible dielectric film, tests conducted previously with the SMART Layer can be used towards achieving these goals.

Therefore, the coupon test plan was focused on the following two tasks:

- Collecting and summarizing relevant data from previously conducted tests
- Developing and conducting tests for missing elements

To ensure Smart Patch sensor survivability, data from previously conducted survivability tests were collected and are summarized in the coupon test report contained in appendix B.

This includes survivability data from:

- Fatigue tests.
- Temperature tests.
- Vibration tests.
- Moisture and salt fog tests.

Data usability is based on the strength of the sensor signal. For most aircraft structures, a signal-to-noise ratio greater than 20 dB is considered appropriate for the data to be usable for analysis and signal processing. Figure 47 shows an example of typical data that is usable for analysis.

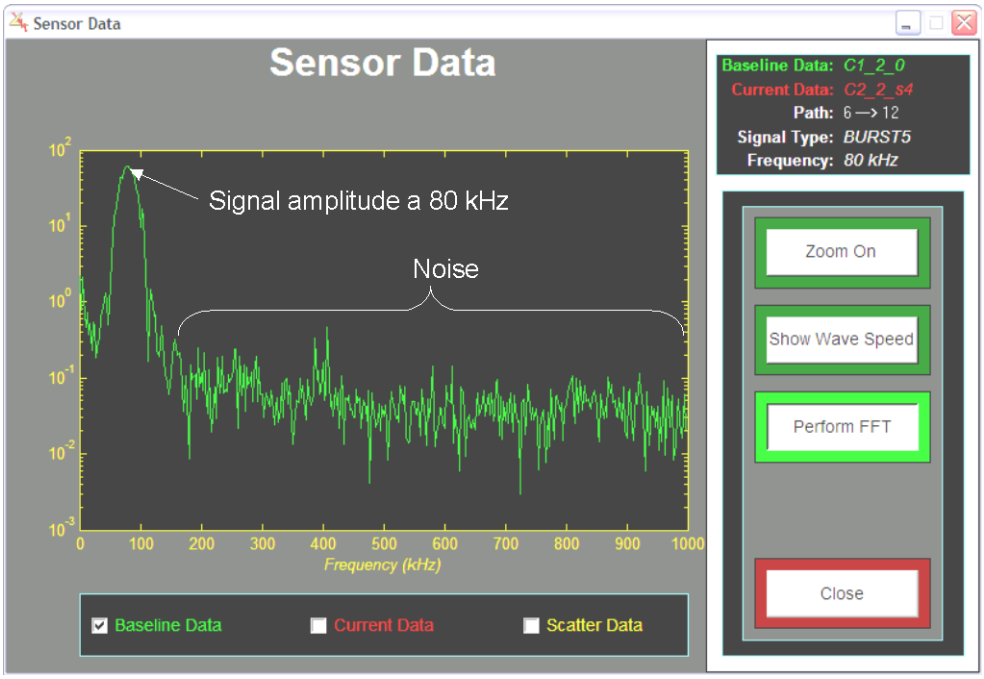

Figure 47. Example of Signal-to-Noise Ratio for Usable Data

Data usability is a factor of the intended structural application, in addition to structural geometry and the placement of sensors and actuators. For rotorcraft, structural applications can be classified as follows:

- Static Airframe structures such as:
  - Frame
  - Frame (upper deck)
  - Bulkhead
  - Beams/spars
  - Stringers

- Skins
- Attachments/lugs

- Dynamic structures such as:

  - MR and TR blade/spar
  - MR hub, cuff and yoke
  - Transmission
  - TR hub and horn
  - Control system

Previous tests were conducted on single lap joints, thick plates (up to 1.5″), and complex geometrics to determine if usable data could be obtained.

It was determined that coupon test data were missing for bolted and double lap joints. Therefore, during the course of this program, coupon level tests were conducted for signal transfer in bolted joints and fatigue testing in double lap joints to cover the areas missing from the above list.

Fatigue tests on the bolted joints' coupons were conducted in collaboration with the Structures Laboratory of Stanford University. A total of five test specimens were used. One specimen was used to determine the appropriate fatigue loads; there were no SMART Layers mounted on this specimen. Another specimen was used to determine if useful signals could be transferred through the structure layers. Five SMART Layers were mounted on each of the other three specimens, as shown in figure 48. For the remainder of this discussion, the three specimens used for fatigue testing will be referred to as specimen 1, specimen 2, and specimen 3**.**

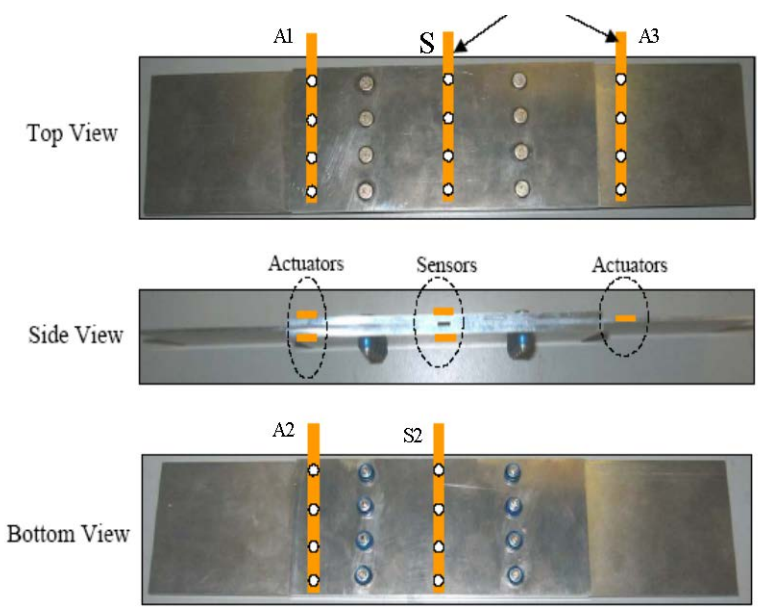

Figure 48. Test Specimens for Bolted Joint Test

Before each fatigue test, two sets of baseline data were collected over a range of frequencies (100 kHz to 400 kHz) at the designed minimum load and mean load, respectively. After starting

fatigue cycling, the signals were recorded at every 1000 or 2000 cycles until the sensor signals showed changes. The software was configured as shown in figure 49.

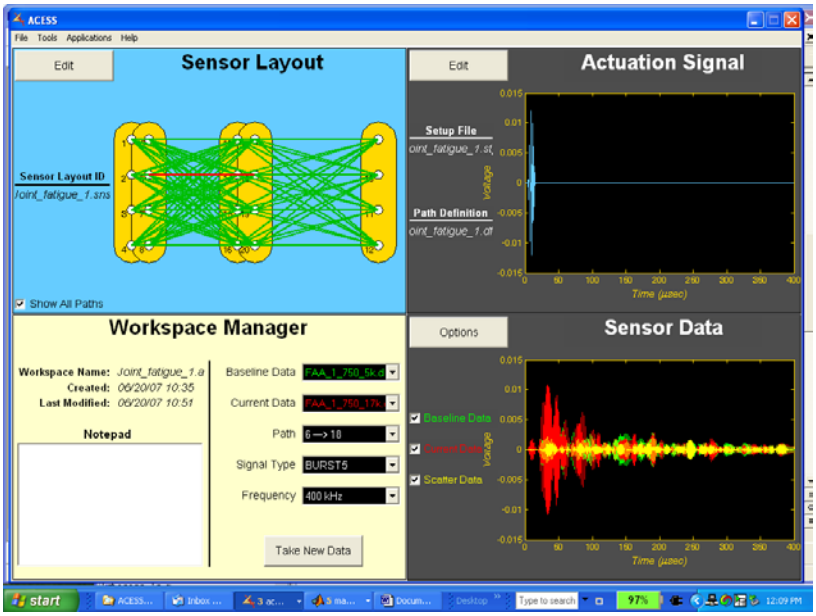

Figure 49. Workspace of Data Acquisition Software

As shown in figure 50, an MTS machine was used to perform the tests. Specimens 1 and 2 were subject to fatigue loading with a maximum load = 7500 lb, ratio of minimum load to maximum load = 0.1, and load frequency = 3 Hz.

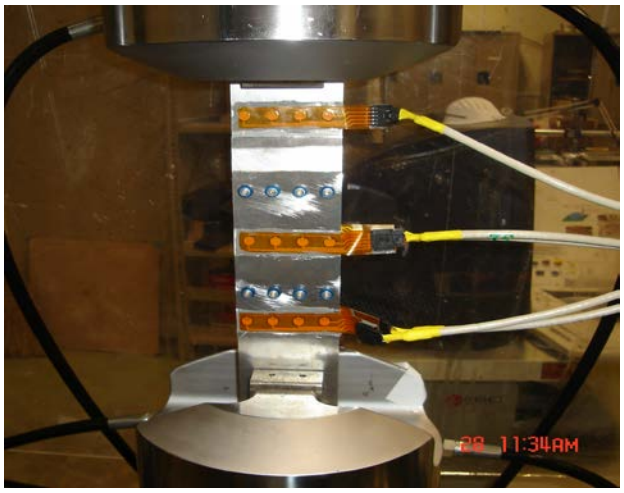

Figure 50. Test Setup

During specimen 1 tests, large signal changes were observed on the path shown in figure 51(a). Figure 51(b) shows the generated image highlighting the location of structural changes. After stopping the test at 17,000 cycles and disassembling the specimen, it was found that the bolt on that path was loosened.

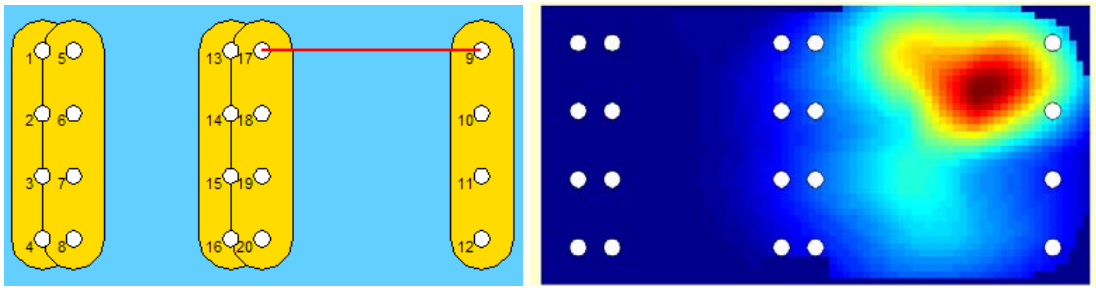

(a) (b)

Figure 51. Image Highlighting Location of Structural Changes in Specimen 1

Specimen 2 was tested at the same loads as specimen 1 and was cycled until failure at 52,000 cycles. During the tests, the SHM system indicated structural changes, as shown in figure 52.

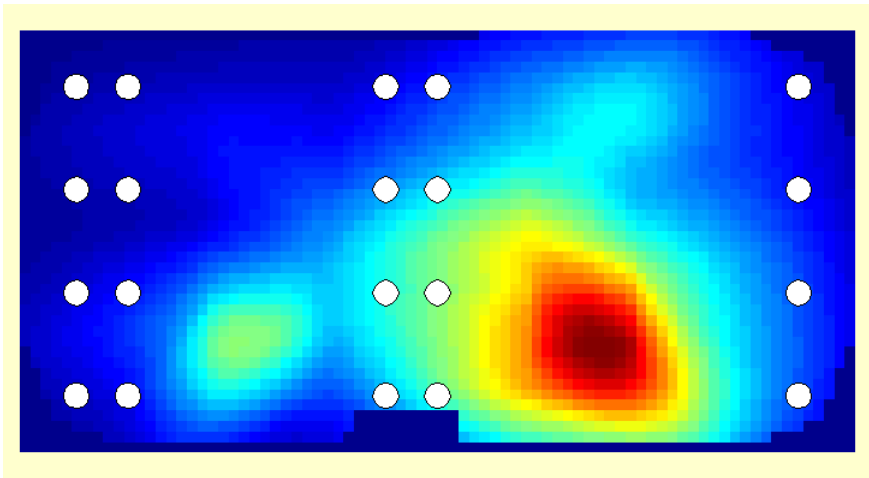

Figure 52. Image Highlighting Location of Structural Changes in Specimen 2

After failure, the specimen was disassembled and a fatigue crack was found to have initiated at the hole on the path between sensors 12 and 20. Figure 53 shows the damage index versus cycles up to failure for path 12 to 20. The chart clearly shows an increase in structural changes as the number of cycles increase. However, correlating the damage index with the actual crack size is difficult because the crack could not be verified until the specimen was disassembled.

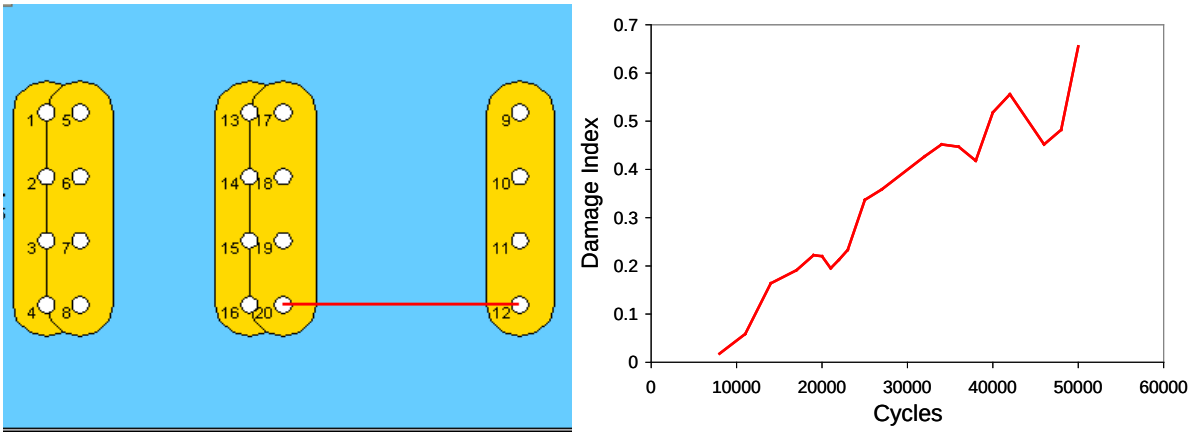

Figure 53. Damage Index vs. Cycles for Path 12 to 20 on Specimen 2

For specimen 3, the FAA suggested varying the cycling loads to form marker bands on the fatigue crack surface. It was intended to use these marker bands to help correlate the crack length to the number of cycles (and, thus, to the damage index).

Therefore, during the specimen 3 fatigue tests, the maximum load was alternated between 6550 and 8650 lb every 1000 cycles. The specimen failed at 25,000 cycles and was then disassembled. Fatigue cracks were found at the holes on sensor paths 5 to 9 and 6 to 10. A microscope was used to identify any marker bands on the crack surface, but none could be found. The resulting damage index versus cycles for paths 5 to 9 and 6 to 10 are shown in figure 54.

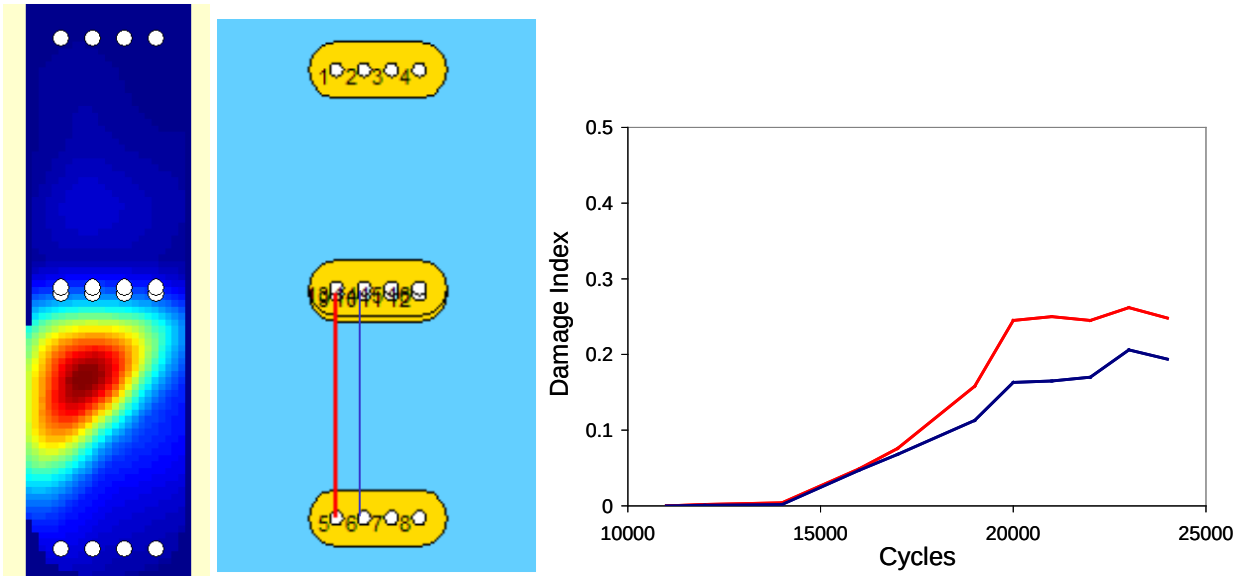

Figure 54. Detection Results for Specimen 3

In summary, bolted joint tests were conducted to determine if an SPS could detect cracks in the middle plate of a double lap joint using sensors bonded on the top and bottom plates. It was found that the sensor signals could be transferred between the structural layers, but the signals were noisier than those that travel in the same structural layer. Even with the higher noise, the SPS was shown to be able to detect cracks that were on a different structural layer than the sensors, as shown in figures 53 and 54. It was also found that bolt loosening could be detected, but currently cannot be distinguished from a crack. Also, correlating sensor signals to actual crack sizes is difficult because the cracks could not be verified until the specimens are disassembled. The coupon tests performed for this project and the relevant data from previously conducted coupon tests were sufficient to demonstrate sensor survivability and that usable data could be obtained reliably for the rotorcraft applications of interest.

3.2 COMPONENT TESTS.

As mentioned in section 2, Acellent and SAC explored several opportunities for component testing. In addition to the TR Horn, the other options included a gearbox lower housing, a gearbox middle housing, and an MR spindle. Of these other options, the main gearbox lower housing was also identified as a good potential application. A series of three fatigue tests was scheduled for this component, and Acellent targeted the second test in this series. However, during the first test, a crack developed in an unexpected region, resulting in a number of facility delays, which caused the component test schedule to slide.

It was then suggested that the triplex clevis fitting on the gearbox middle housing would be a good component for SPS validation and that the fatigue testing of this component could be scheduled to support the existing program schedule. Thus, it was decided to use this as the component test for validation of the SPS. With the assistance of the SAC design team, the Acellent SPS design team developed a suitable design for the SPS sensor layout for the clevis fitting.

The component testing was carried out on the right-hand triplex clevis on the gearbox middle housing as scheduled. Sensors were installed and engineers were trained on the SPS operation and how to collect data during the fatigue testing. A combination of 1- and 2-sensor layers was used for this test, as shown in figure 55. Each piezoelectric transducer was 1/8″ in diameter, and a total of six actuators and six sensors were installed to detect crack initiation and monitor its growth. The testing lasted about 4 weeks.

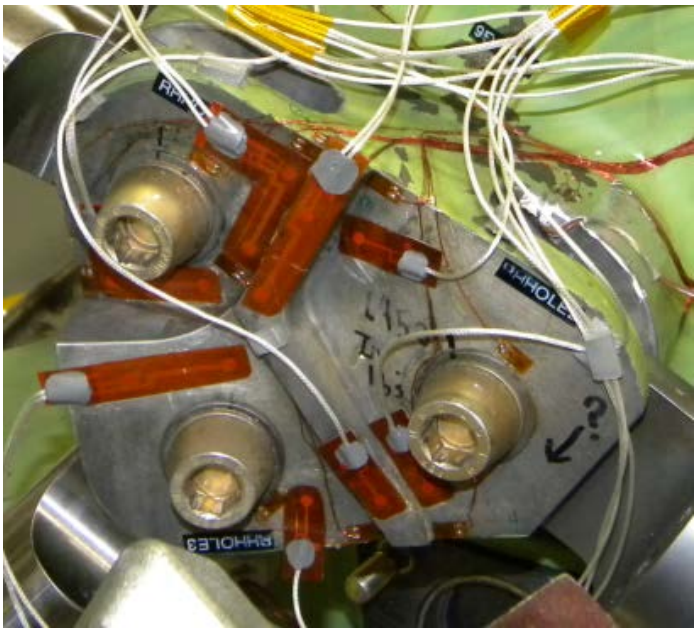

Figure 55. Smart Patch Layers Installed on the Right-Hand Triplex Clevis on Gearbox Housing

The results from the tests were analyzed. From past testing and analysis of the clevis, the crack was expected to initiate and grow along one of the fillet radii. Therefore, sensors were installed along the fillet radii and the monitoring was focused in these areas, as shown in figure 56. However, the crack initiated at the fastener hole on the right and grew away from the sensored areas.

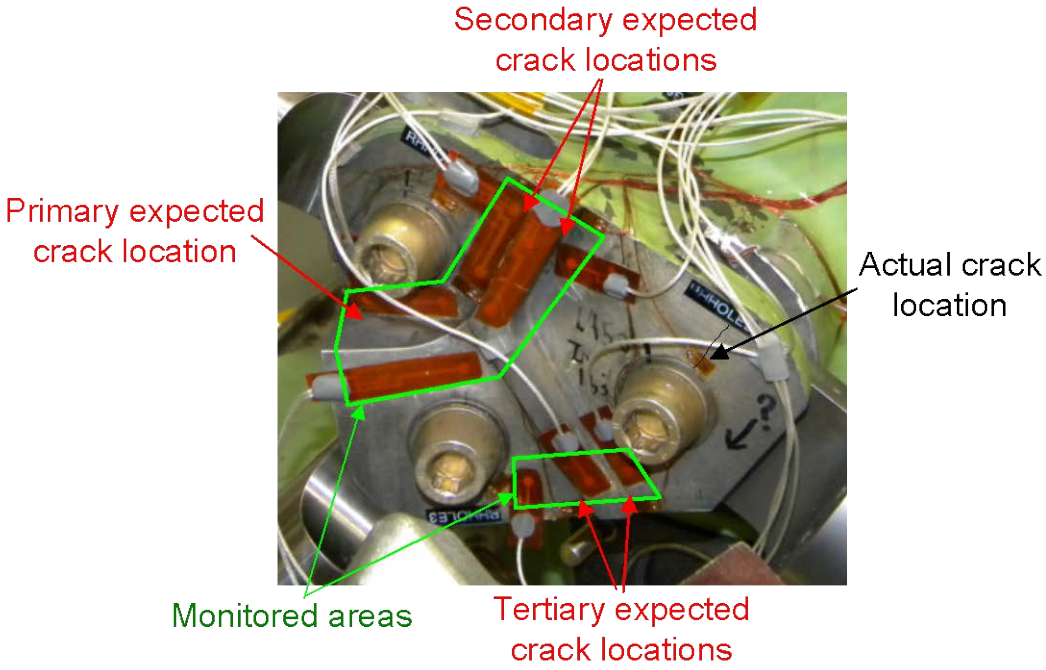

Figure 56. Expected Crack Locations and Monitored Areas

The sensor layouts are typically designed so that the actuator-sensor paths go through the crack region. This allows for detection of cracks by analyzing the changes occurring in the initial part (first arrival) of the sensor signals. The initial analysis using this technique did not show any indication of a crack because there was no crack in the vicinity of the actuator-sensor paths. But expanding the analysis to look for reflections in the later parts of the sensor signals did show indications of a crack. Using a reflection-based analysis, an image was generated highlighting the crack area, as shown in figure 57.

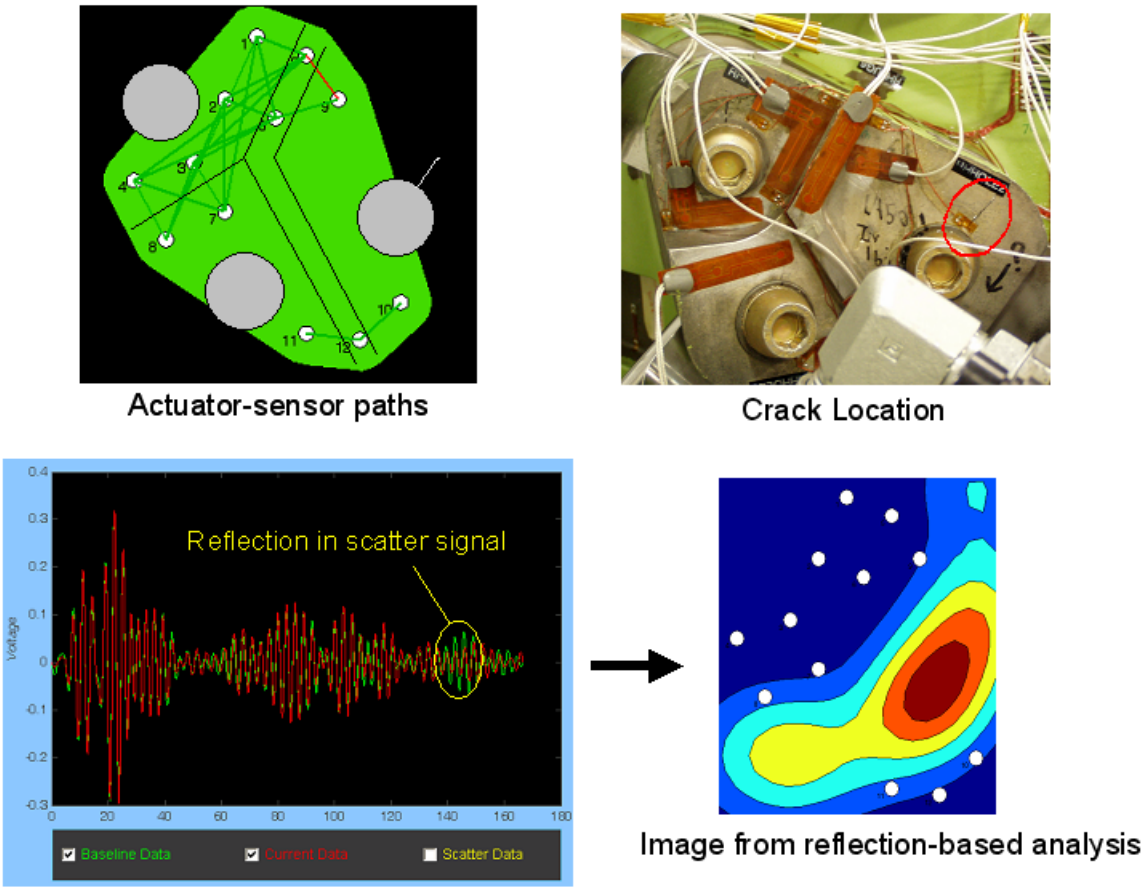

Figure 57. Reflection-Based Analysis Highlighting Crack Area

A detailed analysis of the reflection data was conducted. The damage index versus cycles plot below shows the reflection-based damage index can be used as a trendable parameter to track the crack growth. As shown in figure 58, the crack began to grow at about 1.6 million cycles.

In summary, component testing was conducted in collaboration with SAC on the clevis fitting for the gearbox middle housing. Post-test analysis found a crack, but not in the expected area. The crack initiated and grew away from the sensor paths. However, by using a reflection-based analysis, an image was generated that successfully highlighted the crack area. A detailed analysis of the reflection data was conducted and successfully demonstrated that data from the SPS would provide a trendable damage parameter that would track crack growth in a thick metal fitting.

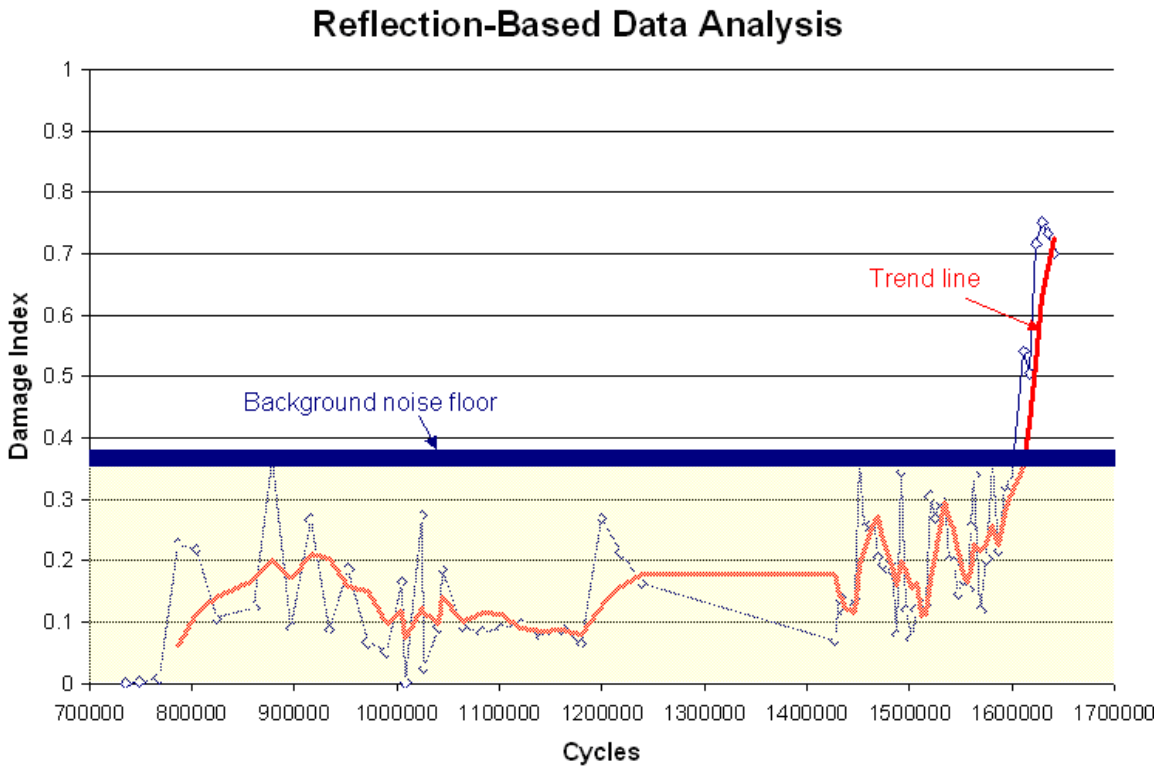

Figure 58. Damage Index vs. Cycles Plot Showing the Reflection-Based Damage Index

3.3 FLIGHT TESTS.

As a part of the effort to flight test the SPS, Acellent established two separate Cooperative Research and Development Agreements (CRADA) with the ARL. One CRADA integrated sensors on a Sikorsky EH-60L Black Hawk helicopter from the U.S. Army Aviation and Missile Research, Development, Evaluation Command (AMRDEC) Aeroflightdynamic Directorate (AFDD) located at the National Aeronautics and Space Administration Ames Research Center. The Black Hawk is the military variant of the SAC commercial rotorcraft. The EH-60L Black Hawk helicopter did not conduct dedicated flight events solely for sensor testing, but conducted its normal flight test program with the sensors installed and was used to obtain airworthiness substantiation for the sensors.

The other CRADA focused on demonstrating crack- and damage-detection capabilities of the SPS, using a URV with seeded faults in critical structural components.

For the Black Hawk, sensors were installed at the crack-prone area shown in figures 59 and 60. The sensors were installed on May 15, 2009 on both the inside and outside of the vehicle. The helicopter went through sandblast testing in brown-out conditions at Yuma Proving Ground in July 2009, and sensor data were collected periodically throughout.

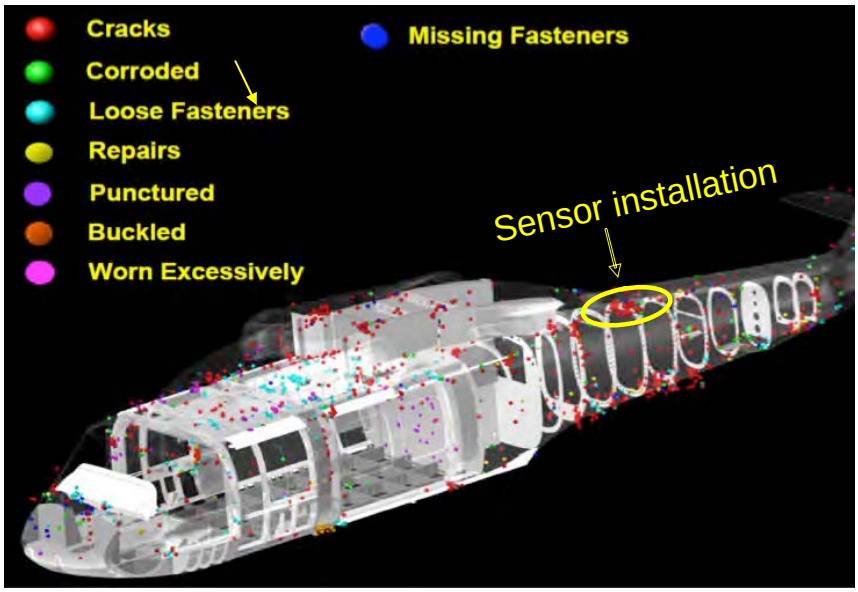

Figure 59. SMART Layers Installed at Crack-Prone Area on Tailboom

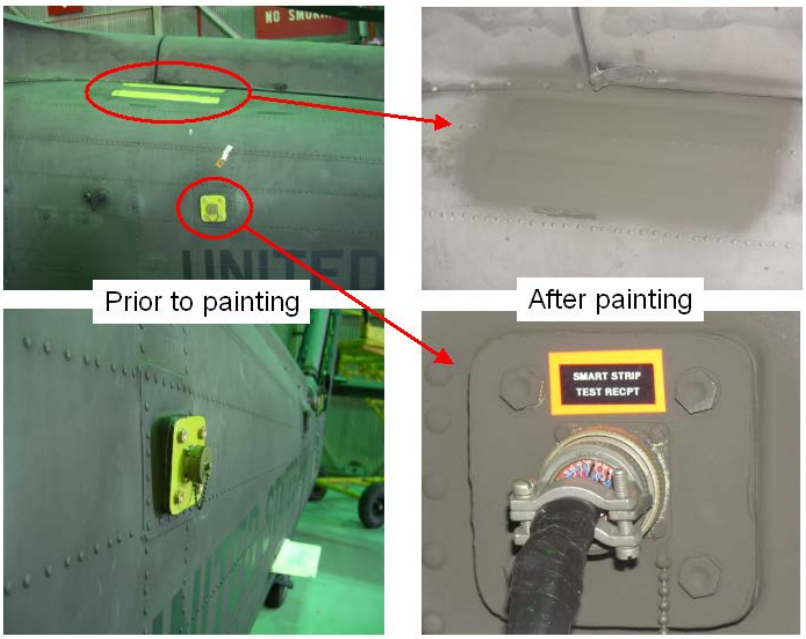

Figure 60. All SMART Layers Are Connected to a Single Connector

A number of data sets were collected from the Black Hawk flight tests. An example of a sensor signal comparison is shown in figure 61. The figure shows two sensor signals (one in green and one in red) that were taken on the ground between flights 14 months apart. As shown, the sensor signals were very stable and showed very little variation after being subjected to flight loads.

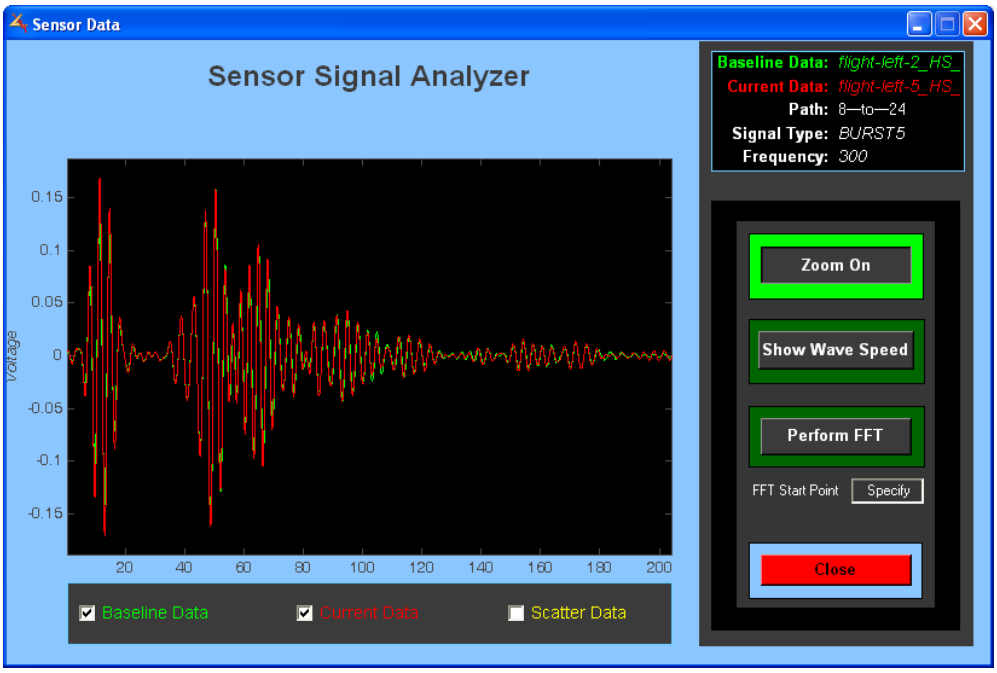

Figure 61. Sensor Data Collected From Black Hawk Flight Tests

Acellent continued to collect data from the Black Hawk between flights. The sensor signal raw data showed slight changes (increased wave speeds) because of the change in weather, but the built-in environmental calibration module was able to compensate for the changes.

At the conclusion of this research, the sensors have been installed for 16 months and all continue to function correctly. The system monitors 14 rivets on each side of the tailboom. Diagnostic images of the left and right side of the tailboom are shown in figure 62. On the left side, a small change is detected. Based on laboratory tests, changes due to a critical crack size would show up as yellow or red.

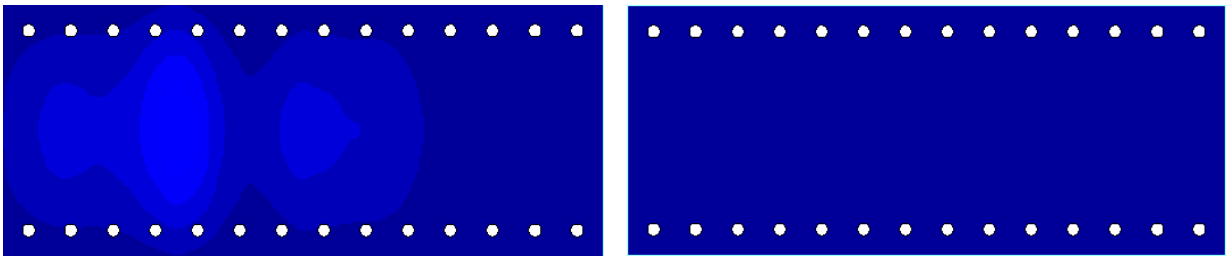

(a) Diagnostic image from left side of tailboom (b) Diagnostic image from right side of tailboom

Figure 62. Diagnostic Images From Tailboom

For the URV, through discussion with ARL, it was decided to use a Raptor-90 URV for the initial flight tests before using a larger and more expensive Yamaha RMAX helicopter. The following components of the Raptor-90 were initially identified for testing:

- Lower metal frame
- Metal tail boom
- Carbon fiber base plate
- Plastic skid brace
- Plastic main spur gear
- Plastic vertical fin
- Plastic horizontal fin

The intention was to modify or replace the above parts to induce known failures in the helicopter. The dimensions of the parts were identical to the original, but the plastic material was replaced with either metal or composite.

The component list was then condensed to include one airframe component (lower metal frame) and two dynamic components (tail rotor blade and shaft). The landing gear was also considered.

The ARL and Acellent selected the Raptor-90 airframe component (shown in figure 63) for flight tests. Components were manufactured in both aluminum and composite. Sensors were integrated onto the components for initial ground tests to induce seeded faults (damage). The seeded faults were induced by an explosive actuator attached to the panels (shown in figure 64). The purpose of the ground tests were to ensure the explosive actuator did not damage the Smart Patch sensors.

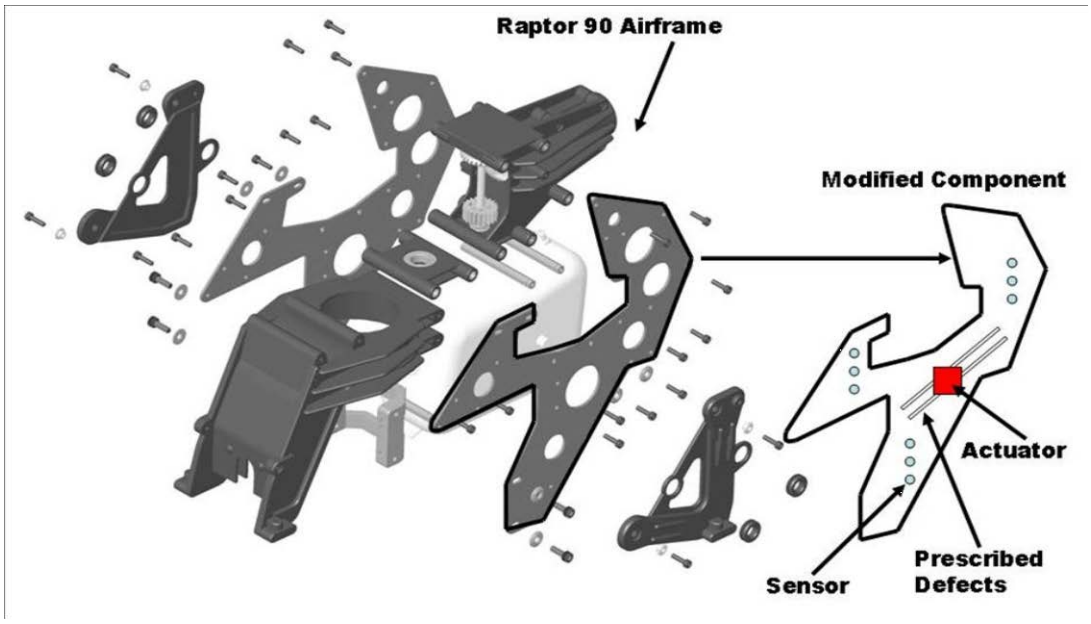

Figure 63. The Raptor-90 Airframe Component Chosen for Flight Tests

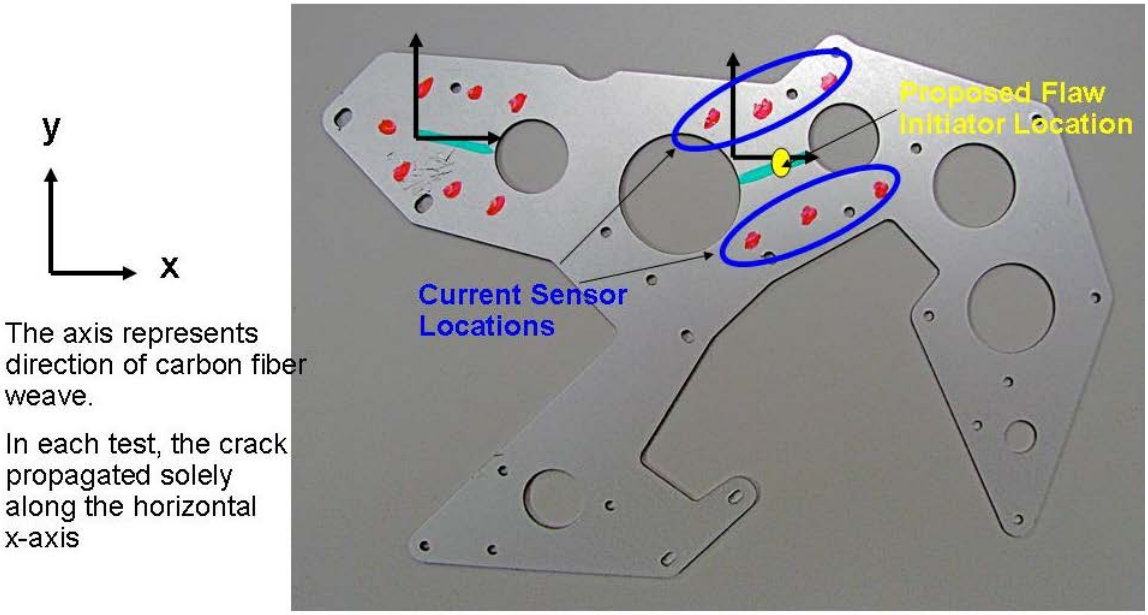

Figure 64. Seeded Faults on Sideframe

On July 20, 2010, ARL personnel and Acellent reviewed the URV (Raptor-90) flight test status and discussed methodologies to calculate maintenance credits and validate the certification framework to meet the FAA AC-29-2C, Section MG-15. The Raptor-90 airframe component chosen for the initial tests is shown in figure 65.

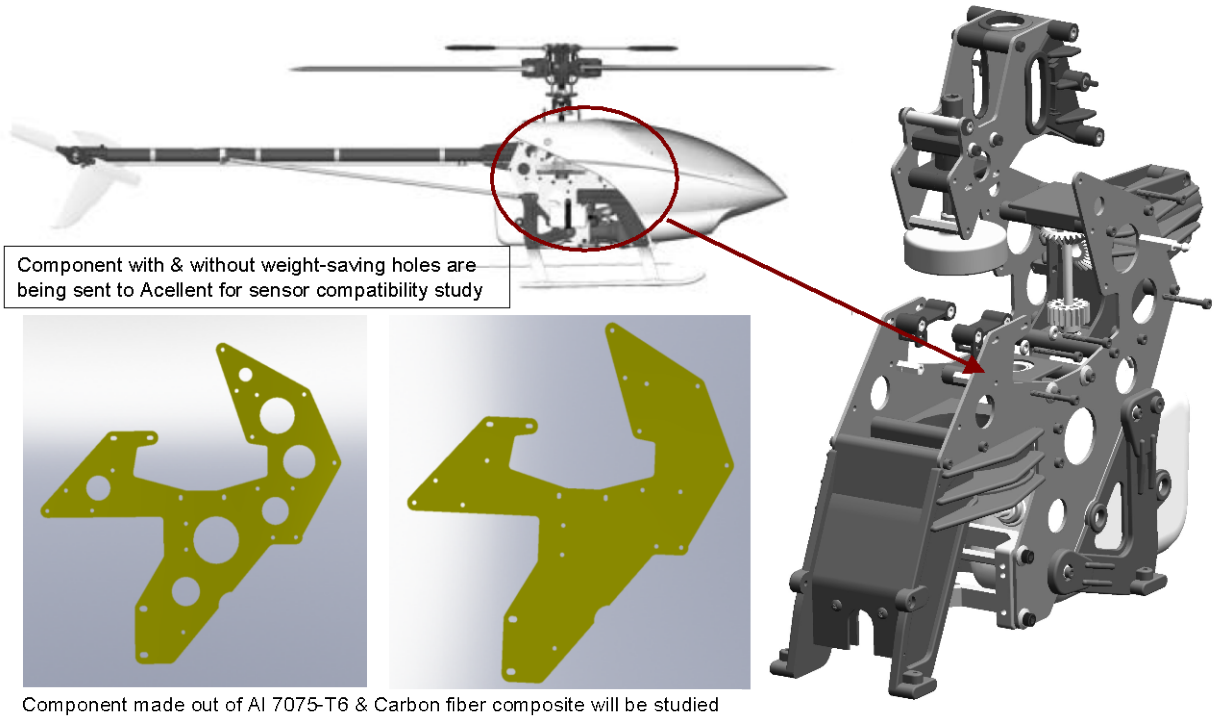

Figure 65. The Raptor-90 Airframe Component

As of this writing, there have been 58 flight hours logged on the Raptor-90. To accelerate the accumulation of flight hours, the ARL is developing a helicopter ground-test stand, as shown in figure 66. In addition to accumulating flight hours faster, the test stand will allow the introduction of structural flaws that would not be allowed on an actual flight test without a significant safety review. It will also provide the capability to test to failure, which is typically not possible during an actual flight test.

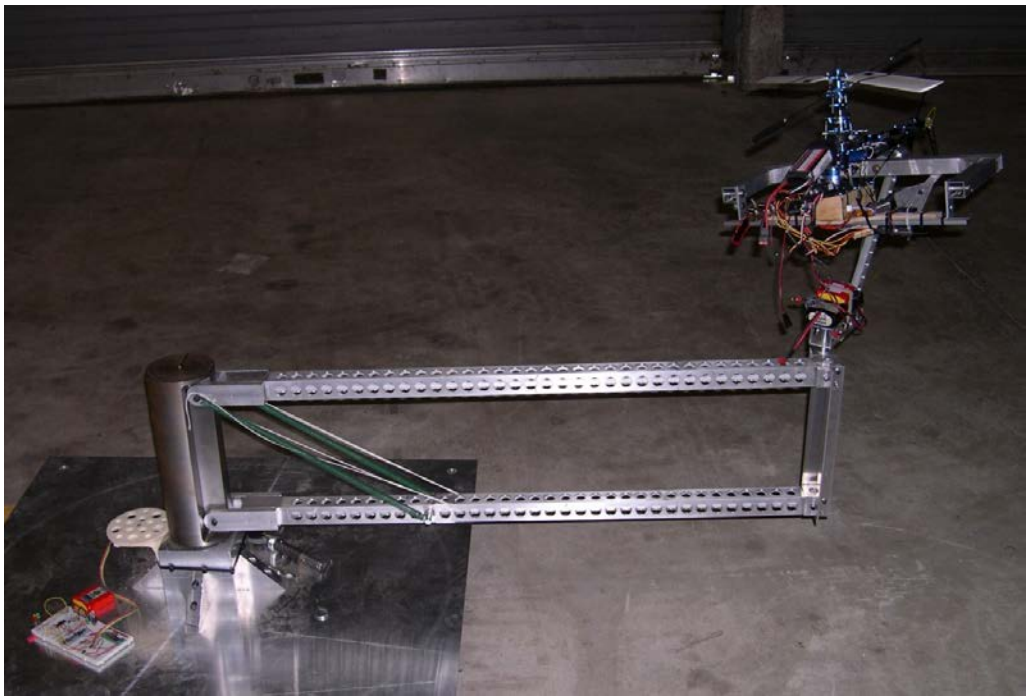

Figure 66. The Raptor-90 Flight Test Stand

Following the Raptor-90 flight tests, the larger and more expensive RMAX will be used. The tail boom of the RMAX is the targeted area to install sensors. Studies are currently being conducted to determine the best locations to add seeded faults to induce incremental damage growth during flight.

To prepare for the URV flight tests at the ARL, SMART sensor layers were mounted on the Raptor-90 composite airframe component, and small explosive devices were used to induce damage. Figure 67 shows the SMART Layers (in the upper-left picture) along with the diagnostic results. The ARL is conducting further testing to improve the method to induce damage.

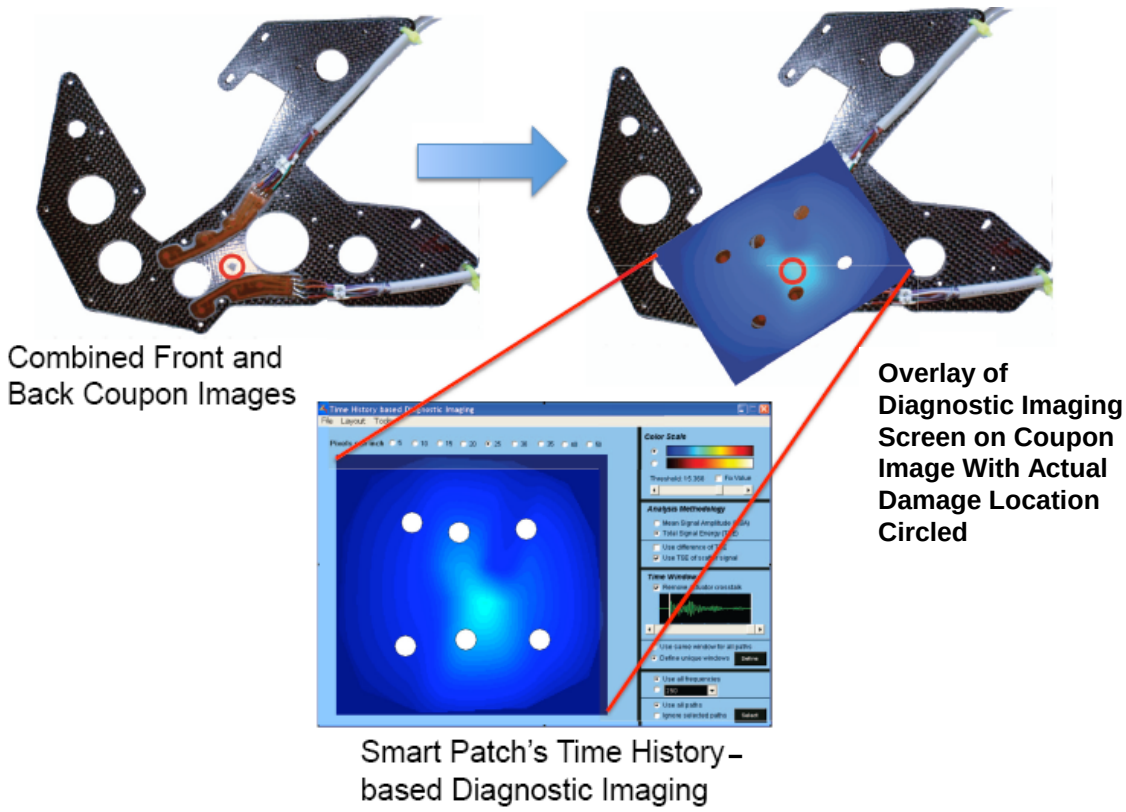

Figure 67. The SPS Sensor Layers Mounted on URV Component

It is expected that these flight tests performed under the CRADAs with the ARL are ongoing efforts that are scheduled to continue for several years. This flight test effort will verify the longterm functionality and reliability of the SPS under operational flight environments and loads. The data obtained will be required for any future efforts to certify the SPS for any rotorcraft application.

4. IMPLEMENTATION AND TECHNOLOGY TRANSFER PLAN.

The evolution leading to implementation of the SPS system, which spans the maturation, design, production, installation, utilization, and certification phases, are shown in figure 68. The certification phases, which involve both Acellent and the FAA, can be initiated through an application made by Acellent and an OEM or operator partner, and can be performed parallel to the evolution phases.

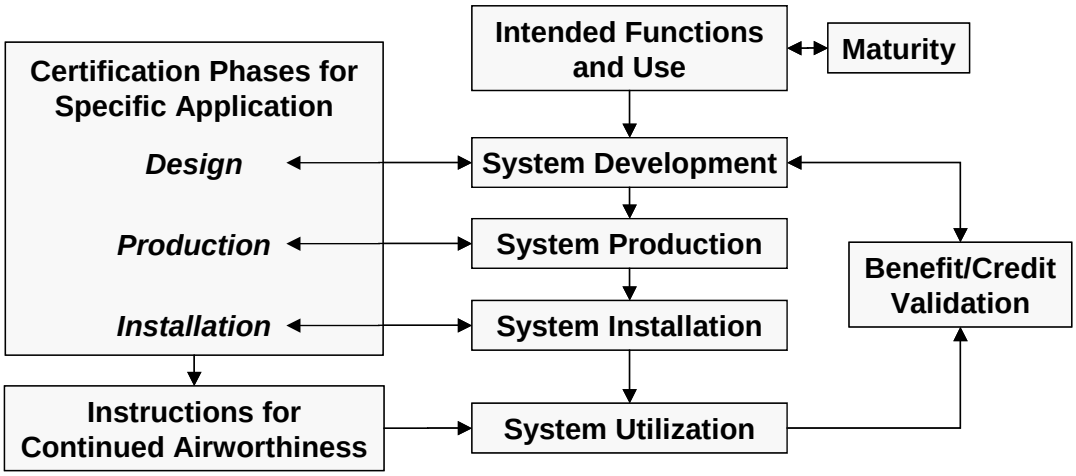

Figure 68. The SPS Certification Process for Benefit/Credit Validation

The following sections describe in more detail the evolution and certification phases outlined in figure 68.

4.1 INTENDED FUNCTIONS AND USE.

For each intended function, the SPS must comply with the applicable airworthiness regulations for the intended function of the SPS. The FAA regulation for "damage tolerance and fatigue evaluation of structure" given in Title 14 Code of Federal Regulations (14 CFR) Part 29.571 [10] states the following:

> "Based on the requirements of this section, inspections and retirement times or approved equivalent means must be established to avoid catastrophic failure. The inspections and retirement times or approved equivalent means must be inclined in the Airworthiness Limitations Section of the Instructions of Continued Airworthiness required by Section 29.1529 and Section A29.4 of Appendix A of this part."

4.2 MATURATION.

Technology Readiness Levels (TRL) 1 to 9 [11] are used to assess the maturity of evolving aerospace technologies and systematically incorporate them into aerospace systems when they reach a high TRL. The activities required to achieve a high TRL level (e.g., TRL 6 to 9) may overlap with system development activities. At the beginning of this program, the SPS had a TRL of 5. The work done in this project increased the TRL of the technology to 7. The TRL definitions from the Department of Defense are shown in table 4.

Table 4. Department of Defense TRL Definitions [11]

TRL	Definition	Description
1	Basic principles observed and reported	Lowest level of technology readiness. Scientific research begins to be translated into applied research and development. Example might include paper studies of a technology's basic properties.
2	Technology concept and/or application formulated	Invention begins. Once basic principles are observed, practical applications can be invented. The application is speculative and there is no proof or detailed analysis to support the assumption. Examples are still limited to paper studies.
3	Analytical and experimental critical function and/or characteristic proof of concept	Active research and development is initiated. This includes analytical studies and laboratory studies to physically validate analytical predictions of separate elements of the technology. Examples include components that are not yet integrated or representative.
4	Component and/or breadboard validation in laboratory environment	Basic technological components are integrated to establish that the pieces will work together. This is "low fidelity" compared to the eventual system. Examples include integration of ad hoc hardware in a laboratory.
5	Component and/or breadboard validation in relevant environment	Fidelity of breadboard technology increases significantly. The basic technological components are integrated with reasonably realistic supporting elements so that the technology can be tested in a simulated environment. Examples include high fidelity laboratory integration of components.
6	System/subsystem model or prototype demonstration in a relevant environment	Representative model or prototype system, which is well beyond the breadboard tested for TRL 5, is tested in a relevant environment. Represents a major step up in a technology's demonstrated readiness. Examples include testing a prototype in a high-fidelity laboratory environment or in simulated operational environment.
7	System prototype demonstration in an operational environment	Prototype near or at planned operational system. Represents a major step up from TRL 6, requiring the demonstration of an actual system prototype in an operational environment, such as in an aircraft, vehicle, or space. Examples include testing the prototype in a test bed aircraft.
8	Actual system completed and flight qualified through test and demonstration	Technology has been proven to work in its final form and under expected conditions. In almost all cases, this TRL represents the end of true system development. Examples include developmental test and evaluation of the system in its intended weapon system to determine if it meets design specifications.
9	Actual system flight proven through successful mission operations	Actual application of the technology in its final form and under mission conditions, such as those encountered in operational test and evaluation. In almost all cases, this is the end of the last bug fixing aspect of true system development. One example is using the system under operational mission conditions.

4.3 SYSTEM DEVELOPMENT.

The main development phases of the SPS for a specific application involve iterations through the following activities:

- Determination of detailed system requirements
- Determination of the criticality levels and associated integrity requirements
- System design
- System test and evaluation
- System integration
- Test and evaluation
- Flight test
- Development of installation
- Maintenance
- Operation instructions

The key activities are discussed in sections 4.3.1. and 4.3.2.

4.3.1 Determination of System Requirements.

The requirements must fulfill the system's intended functions and the designer, integrator and/or operator requirements. These requirements must comply with the FAA regulation "Function and Installation" in 14 CFR Part 29.1301 [12].

4.3.2 Determination of System Criticality.

The interpretation of the FAA regulation for equipment, systems, and installations in 14 CFR Part 29.1309 [13] and the compliance with this regulation are influenced by the derived requirements and the determined criticality. If the SPS is used for credit, the system critically is determined by an FHA that considers the severity of the end result that a HUMS application can have on the aircraft. When the declared intent is for credit, the end-to-end critically for such an application should be deteremined and used as input to establish the integrity level of the system or component. The system integrity is relied on for the system to function as required by the critically determined by the FHA. The FHA should consider that if the SPS is used for credit to extend a maintenance interval or to extend an inspection interval, and if the system malfunctions by providing bad data, a crack may be present and not detected by the SPS, which would have been detected during a regular, non-credit maintenance interval. Considering the case in which the SPS will only operate when the rotorcraft is on the ground, the associated components can be designed so that: (1) the occurrence of any failure condition that would prevent the continued safe flight and landing of the aircraft is extremely improbable, and (2) the occurrence of any other failure conditions that would reduce the capability of the aircraft or the ability of the crew

to cope with adverse operating conditions is improbable. In addition, to determine the system criticality, a number of criteria shall be considered, including whether:

- The site has potential for damage (crack, corrosion, etc.).
- The component is critical for maintaining safety.
- The component is difficult to inspect without significant structural teardown or vehicle downtime.

Also, the application's operational feasibility shall be considered, including:

- Capability to place sensors on component for monitoring in-service
- Accessibility for data transfer in-service

4.3.2.1 Factors Affecting System Criticality.

The system criticality is influenced by the following interacting factors:

- Intended function and the function use.
- Impact of the SPS on the aircraft structural criteria.
- System design. Different systems can be designed to achieve the same intended function and/or influence the same structural criterion. One design approach can limit the interaction between SPS items and aircraft systems; another approach can use aircraft resources, such as power and computing resources. Other design factors that influence criticality include calibration methods, onboard versus off-board system components, mitigation methods, etc.
- Impact of potential system failures on safety. The severity of safety risk can vary between system items. Hence, separate items can be developed at different assurance levels.

4.3.2.2 The Impact of the SPS on Structural Criteria.

The SPS criticality significantly depends on whether the system will influence the aircraft structural criteria. Therefore, sufficient analysis and safety assessment must be conducted to determine the degree of the SPS impact on structures.

The analysis and safety assessment should assess the impact of the SPS on the structures. It should also consider the structural regulations, subsequently determine the system criticality, and define the extent of tests and analysis required to demonstrate compliance with these regulations.

4.3.2.3 Methods Used to Determine Criticality Levels.

- Safety Assessment: During the design phase, an initial safety assessment starts by: (1) Analyzing an early system design to evaluate the impact of the system intended function on safety (2) Determining potential system faults (3) Assessing safety risks due to system failures by conducting hazard analysis (4) Proposing safety requirements and system criticality levels that may lead to design changes.

  During the various certification phases, the safety assessment is refined to identify, mitigate, prevent, and control all potential risks through proposed system features and processes influencing the design, production, installation, and utilization of the system. Risk prevention, mitigation, and control go beyond the system installation through maintenance and management activities. For example, a reliability-centered maintenance practice can be adopted to analyze potential failures within a system and determine the maintenance actions required to mitigate the risk of failures. The safety and hazard assessments implement analysis techniques, such as Fault Tree Analysis (FTA), Failure Mode and Effects Analysis (FMEA), and Failure Mode, Effects, and Criticality Analysis (FMECA).

- FHA: The purpose of the hazard analysis is to identify unacceptable risks and select a means of controlling or eliminating them. A hazard is defined by FAA as a "condition, event, or circumstance that could lead to or contribute to an unplanned or undesirable event" [14]. In most cases, a certain degree of safety risk can be accepted; a risk is quantified by combining the consequence severity of an associated accident and the probability of its occurrence. Risks with high severity and high probability must be mitigated to reduce the level of safety risk. The severity of consequence identified by the hazard analysis establishes the criticality and development assurance levels of the system and its software.

- FTA: This is a top-down, deductive analytical method in which primary events, such as component failures, human errors, and external events, are traced through Boolean logic to an undesired top event, such as an aircraft crash; then, ways to make the top event less probable are identified and the achieved safety goals verified. FTA is qualitative when the failure or event probabilities are unknown. When the failure or event probabilities are known, quantitative FTA is used to compute the probabilities of top events.

- FMEA: This is a bottom-up, inductive analytical method that may be performed at either the functional or piece-part level. For functional FMEA, failure modes are identified for each function of a system or equipment item, usually with the help of a functional block diagram. For piece-part FMEA, failure modes are identified for each part, such as a valve or connector. The effects of the failure mode are described and assigned a probability based on the failure rate and failure mode ratio of the function or part.

- FMECA: When combined with criticality analysis, FMEA is known as FMECA, which is used to chart the probability of failure modes against the severity of their consequences

and highlight failure modes with relatively high probability and severity. A piece-part FMECA requires far more effort, but can be preferred more than a functional FMECA because the reliance is more on quantitative data and less on engineering judgment. The criticality analysis may be quantitative or qualitative, depending on the availability of supporting part failure data. FMECA typically includes the steps and activities described in the following paragraphs:

- The first step involves system description and assumption declaration: the system is described into an indentured hierarchy including systems, subsystems, units, equipment, subassemblies, and/or parts. Functional descriptions are allocated for the systems and subsystems, covering all operational modes and mission phases. The declared assumptions can include mission profiles, mission durations, sources of data for failure modes and rates, fault detection coverage through built-in tests and criteria to be considered (mission abort, safety, or maintenance). Then, the systems and subsystems are depicted in functional block diagrams. Reliability block diagrams or fault trees are usually constructed at the same time. These diagrams are used to trace information flow and to identify critical paths and the higher-level effects of lower-level failures.

- For each part or each function, the failure modes are identified. Examples of functional failure modes include untimely operation, failure to operate when required, loss of output, and intermittent/erroneous/invalid output/response. Usually, each function or part is listed in matrix form with one row for each failure mode; a spreadsheet or a database is the most commonly used form for the matrix. A unique identifier is assigned to each item and to each failure mode of each item. Failure effects are determined and entered for each row of the matrix, considering the criteria identified in the declared assumptions. Failure effects are described for the various hierarchical levels (i.e., for the current subsystem/part, the next higher item, and, at the end, the entire system). Examples of system-level effects include system failure, degraded operation, and no immediate effect. Severity classification, such as Catastrophic, Critical, Marginal, and Negligible, is assigned within the matrix for each item failure mode based upon system level consequences.

- For each item and failure mode, the ability of the system to detect and report the failure is analyzed and described in the matrix; for example, the detection ability can be described as a positive/negative correct/incorrect status; the correct status indicates that the system correctly indicates safe conditions (correct positive) or malfunctions (correct negative); the incorrect status implies that the system erroneously indicates safe conditions in the events of malfunctions (incorrect negative) or false alarm malfunctions that do not exist (incorrect positive).

- The criticality of the failure modes are assessed qualitatively or quantitatively. For the qualitative assessment, failure probability levels are assigned and entered in the matrix; examples of these levels are Frequent (A), Probable (B), Occasional (C), Remote (D), and Improbable (E). The failure mode may then be charted on a

criticality matrix using the severity code as one axis and the probability level code as the other. For quantitative assessment, criticality numbers are calculated for each failure mode of each item, and for each item. The computations use such data as failure rates, failure mode ratios, mission phase durations, and conditional probabilities. The failure rates are usually based on predictions; the failure mode ratio may be taken from an existing database source. For functional level FMECA, engineering judgment may be required to assign failure mode ratio. A conditional probability indicates that the failure effect will result in the identified severity, given that the failure mode occurs.

- Often, the FMECA matrix may be sorted by severity and qualitative probability level or quantitative criticality number to identify critical items and critical failure modes for which design mitigation is desired. After performing FMECA, design recommendations are made to reduce the consequences of critical failures. Recommendations include selecting components with higher reliability, reducing the stress level at which a critical item operates, or adding redundancy or monitoring to the system. Finally, an FMECA report is compiled. Typically, the report contains system description, declared assumptions, conclusions, recommendations, and corrective actions to be tracked. The FMECA matrix is attached to the report and usually feeds into maintainability and logistic analyses.

4.4 SYSTEM INSTALLATION.

Installation includes all equipment needed for the end-to-end application of the SPS to structural components that are associated with acquiring, storing, processing, and displaying the SPS data, which include both airborne and ground-based data.

It is well understood in the field of SHM that networked, not individual, sensors, play a key role on the performance of the system. The ability of sensors and actuators in the network to communicate with each other establishes the intelligence of the system. The type, location, and number of sensors affect the sensitivity of the SPS. As more areas need to be monitored and the number of sensors and/or actuators increases, the workability of such a network into a structure can be very challenging or become impractical. The network sensors must be able to:

- Integrate easily with structure.
- Accommodate any structural configuration.
- Carry a minimal weight.
- Operate under variable and harsh environments.
- Have no effect on structural integrity.

Therefore, proper integration of the networked sensors with the host structure is an important part of the SPS, as described in section 2.1.

In addition to the methodology for mounting the networked sensors on the host structures, practical issues concerned with the integration of the sensor system for implementation on the rotorcraft need to be addressed. These include issues concerned with:

- Protective coatings: Most sensors cannot survive harsh operational environments. Research on military-grade coatings shall be based on:

  - Ease of use.
  - Coating thickness for effectiveness.
  - Ability to protect the sensors from operational environments.

- Installation processing: Issues of concern include surface preparation, installation procedures, adhesives to use, application of protective coatings, etc.

- Connections: A major challenge in the design of the sensor network is the design of the connections from the integrated sensor networks at different locations to the diagnostic hardware. The connections should be designed to be:

  - Easy to use and inexpensive.
  - Robust and able to withstand the harsh environments faced by the rotorcraft.
  - Low weight.

- Repairability: A method for removing and replacing damaged sensors mounted on the structure should be identified. In addition, redundancy should be built in so that neighboring sensors can monitor the area surrounding a damaged sensor.

4.5 CERTIFICATION FOR SPS.

Certification involves activities to verify and ensure adherence with functional requirements. Additionally, airworthiness and operating regulations must be followed and approval from the appropriate regulatory authority must be obtained. The output of successful certification activities is discussed in the following sections.

4.5.1 Design Approval.

Approval is granted after the applicant has demonstrated, and the regulator has verified, that the design meets requirements that include intended functions, software level, environmental test requirements, etc. Usually, approval is granted at the end of the development period during which the applicant must have agreed with the regulator regarding the means of compliance that will be met to address the regulations, such as the applicable CFR, which must be identified paragraph by paragraph. The compliance documentation should account for all data pertinent to defining the type design, including manufacturing specifications and to demonstrating compliance (including, but not limited to, test plans, test reports, test setup schematics, test instrumentation, drawings, analyses [e.g., stress analysis and safety analysis], material/process specifications, manuals, etc).

4.5.2 Production Approval.

Approval is granted after the applicant has demonstrated, and the regulator has verified, that the applicant has developed and is capable of maintaining a quality assurance system. This assures that only products and parts conforming to the approved design are released for service use. Applicants other than the design authority (DA) must seek permission from the DA to use their approved design data.

4.5.3 Installation Approval.

Approval is granted after the applicant has demonstrated, and the regulator has verified, that installation meets the airworthiness requirements and is applicable to the aircraft model requested. The installation instructions include standard practices, such as aircraft electrical wire selection. Specific instructions address more critical elements, including procedures for determining the placement, installation, and post-installation checkout of the system parts. This includes any required interface units. Post-installation checkout procedures could include: electrical load analysis, equipment mounting/wiring testing/verification, electro-magnetic interference/radio frequency interference test, etc.

4.5.4 Instructions for Continued Airworthiness.

The instructions include a plan to ensure continued airworthiness of those parts that could change with time or usage and the methods used to ensure continued airworthiness. 14 CFR 29.1529 [15] describes the FAA regulatory requirements.

4.6 BENEFIT/CREDIT VALIDATION.

The primary benefit of the SPS is that it decreases operational and maintenance costs and increases readiness. Directly, the SPS can provide any aviation platform with the ability to accurately assess structural health and project failure of critical aircraft components based on operational environments. This leads to decreased operational costs over the lifetime of the structure. Current maintenance practices are reactive to faults, not proactive, resulting in an excessive logistics support burden and high operating costs. The SPS can allows for in situ monitoring of structural flaws, thereby eliminating flight-hour-based inspections, which in turn will lead to reduced operation costs.

The SPS will provide the capability to:

- Obtain real-time information on the integrity of a structure during service.
- Provide an easy-to-use inspection tool for maintenance personnel to assess the integrity of damaged structures and take preventive action.
- Characterize and monitor damage growth.
- Avoid unplanned structural inspection/maintenance and catastrophic failures.
- Reduce the total structural inspection costs for rotorcraft structures.
- Provide maintenance credit by reducing the number of maintenance activities when the structural condition assessment shows no need for the scheduled work.

Credit validation includes providing evidence of the effectiveness of the developed algorithms, acceptance limits, trend-setting data, tests, and demonstration methods employed.

The system can monitor both airframe and dynamic components. An example of the calculated cost savings for one inspection region is provided below. Monitoring multiple regions would incur additional cost savings.

5. CONCLUSIONS.

A Smart Patch System (SPS) concept was developed for integration into a rotorcraft Health and Usage Monitoring System (HUMS) to support the development of usage credits for rotorcraft structures. A framework was developed outlining the process steps required for Federal Aviation Administration (FAA) certification of the SPS based on the guidelines provided in FAA Advisory Circular (AC) 29-2C, Section MG-15 for HUMS. The validation approach for the SPS addressed three basic aspects: installation, credit validation, and Instructions for Continued Airworthiness. With the support of Sikorsky Aircraft Corporation (SAC), a flight-critical dynamic component, the right-hand clevis fitting on a gearbox middle-housing was selected as a suitable application for demonstrating the SPS certification process. The SPS was designed using Acellent Technologies, Inc.'s SMART Layer® system as a basis. Software to accurately and reliably detect damage using the system per requirements provided by SAC was developed. In this project and parallel projects, a complete series of coupon, component, and flight tests were performed to verify the functionality, performance, and reliability of the SPS application. The coupon testing conducted as described in appendix B demonstrated the SPS sensor network survivability under extreme environmental conditions and that usable data could be obtained. The component tests, conducted in collaboration with SAC, demonstrated the versatility of the SPS design. During the test, the fatigue crack developed outside of the area predicted by the stress analysis and, thus, outside the area directly monitored by the SPS sensors. Using a reflection-based analysis, an image was generated that successfully highlighted the crack area. A detailed analysis of the reflection data was conducted and successfully demonstrated that the SPS

would provide a trendable damage parameter to track the crack growth in the clevis fitting. With a trendable damage parameter, the crack size could always be estimated through calibration. These tests demonstrated that the system could identify and quantify the size and location of cracks occurring in the structures and validated the applicability and usability of the system for monitoring crack growth in rotorcraft structures. At the time of this writing, the flight tests performed under Cooperative Research and Development Agreements (CRADA) with the U.S. Army have been underway for more than 1 year. When complete, they will verify the longterm functionality and reliability of the SPS under operational flight environments and loading conditions. A functional hazard assessment (FHA) of the system was performed and documented early in the program; however, it was found that the FHA had to be continually updated based on the results of the validation testing and implementation planning.

In summary, the objectives of this project were to:

- Develop, validate, and demonstrate SPS technologies, including advanced software, algorithms, and methodologies for structures and dynamic components to:
  - Detect fatigue cracks and damages before exceeding critical threshold or incipient failure.
  - Characterize fatigue cracks and damages.
- Develop preliminary certification compliance requirements and a framework for certification of an SPS that could be integrated into a HUMS for the fatigue crack monitoring of commercial rotorcraft structures per the guidelines provided in AC 29-2C, Section MG-15.

The work performed on this project directly showed the potential for the validation of the certification process of an SPS following the guidelines provided in the AC [1] and the requirements for system operation and validation obtained from the rotorcraft original equipment manufacturer (OEM). However, the SPS has not been validated to date. Future activities related to or resulting from the work performed on this project are as follows:

- Acellent is continuing to work with the major rotorcraft OEMs, such as SAC and Bell Helicopter Textron, for potential implementation of the SPS on their rotorcraft structures.
- Joint development agreements were initiated with the two HUMS equipment suppliers, Goodrich and Honeywell, to become a certified supplier of SPS components for integration into rotorcraft HUMS.

6. REFERENCES.

1. Federal Aviation Administration, "Airworthiness Approval of Rotorcraft Health and Usage Monitoring Systems (HUMS)," Advisory Circular 29-2C MG 15, January 2011.

2. Beard, S., Kumar, A., Qing, X. P., Zhang, D. C., and Patterson, J., A Smart Patch System for Monitoring of Bonded Pairs," *Proceeding of the 5th International Workshop on Structural Health Monitoring*, Stanford University, September, 2005.

3. Qing, X. P. Beard, S., Ikegami, R., Chang F.-K., and Boller, C., "Aerospace Applications of SMART Layer Technology," *Encyclopedia of Structural Health Monitoring*, Wiley, 2009.

4. Banerjee, S., Qing, X. P., Beard, S., and Chang, F.-K., "Rotorcraft's Hot Spot Monitoring Using Distributed Smart Patch System," *Proceeding of the 5th European Workshop on Structural Health Monitoring*, July, 2010.

5. Banerjee, S., Qing, X. P., Beard, S., and Chang, F.-K., "Prediction of Progressive Damage State at Hot Spot Using Statistical Estimation," *Journal of Intelligent Material Systems and Structures*, February, 2010.

6. Qing, X.P., Wilson, H., Baines, A.g., Bordick, N., Banerjee, S., Chung, H., Beard, S., and Pappakostas, M., "Hot-Spot Fatigue and Impact Damage Detection on a Helicopter Tailboom," *Proceeding of the 8th European Workshop on Structural Health Monitoring*, September, 2011.

7. Lee, S.J., Pollock, P., Janapati, V., Li, F., Chung, H., Kumar, A., Li, I., "Fatigue Crack Characterization for Rotorcraft Structures Under Varying Loads and Temperatures," *Proceedings of the American Helicopter Society's 69th Annual Forum*, May, 2013.

8. Beard, S., Liu, B., Qing, P., and Zhang, D., "Challenges in Implementation of SHM," *Proceedings of the 6th Int. Workshop on SHM: SHM 2007 Quantification, Validation, and Implementation*, Chang F-K (ed). DEStech Publications, Inc., pp. 65-84, 2007.

9. Mueller, I., Janapati, V. Banerjee, S., Lonkar, K., Roy, S., and Chang, F.-K., "On the Performance Quantification of Active Sensing SHM Systems Using Model-Assisted POD Methods," *Proceeding of the 8th European Workshop on Structural Health Monitoring*, September, 2011.

10. U.S. Federal Register, Title 14 Code of Federal Regulations Part 29.571, "Fatigue Tolerance Evaluation of Metallic Structures," May 9, 2010.

11. Department of Defense. "Technology Readiness Assessment Guidance," May 2011.

12. U.S. Federal Register, Title 14 Code of Federal Regulations Part 29.1301, “Function and Installation,” July 5, 2012.

13. U.S. Federal Register, Title 14 Code of Federal Regulations Part 29.1309, “Equipment, Systems, and Installations,” July 5, 2012.

14. U.S. Department of Transportation, FAA, “Risk Management Handbook,” 2009.

15. U.S. Federal Register, Title 14 Code of Federal Regulations Part 29.1529, “Instructions for Continued Airworthiness,” May 9, 2012.

APPENDIX A—FUNCTIONAL HAZARD ASSESSMENT

A.1 BASIC APPROACH FOR SMART PATCH SYSTEM CERTIFICATION.

The basic approach for certification of the Smart Patch System (SPS) for applications on rotorcraft structures was based on the certification of a Health and Usage Monitoring System (HUMS) according to AC 29-2C, MG-15 [A-1]. The basic aspects are as follows:

1. Installation—Includes all equipment needed for the end-to-end application of the SPS to rotorcraft airframe structural components that is associated with acquiring, storing, processing, and displaying the SPS data, which includes both airborne and ground-based data.

2. Credit Validation—Includes evidence of effectiveness for the developed algorithms, acceptance limits, trend setting data, tests, and the demonstration methods employed.

3. Instructions for Continued Airworthiness (ICA)—Includes a plan to ensure continued airworthiness of those parts that could change with time or usage and includes the methods used to ensure continued airworthiness.

The end-to-end SPS has the potential be an integral part of the rotorcraft HUMS that will provide in-service information regarding the health of new and existing rotorcraft airframe structures. Built-in sensor networks on the airframe components will provide data regarding the condition and damage state of the structure. Data-acquisition hardware and algorithms that provide diagnostic information in the form of location and size of damage sensor data will be processed. Diagnostics information will be generated and used to facilitate informed decision processes with respect to inspection and repair (e.g., repair versus no repair or replacement). Rotorcraft asset management can then be performed based on HUMS data that represent the actual health or usage of the structure, thereby minimizing in-service failures and maintenance costs, while maximizing reliability and readiness.

The basic approach for certification of the SPS for application to a variety of rotorcraft airframe components is shown in figure A-1. The approach addresses the three basic aspects for HUMS certification. These aspects are not totally independent and have varying interactions with each other. The declared intent for the end-to-end SPS application will be to obtain maintenance credit in that it will add to, replace, or intervene in existing rotorcraft maintenance practices or flight operations. The end-to-end criticality is determined by performing a Functional Hazard Assessment (FHA). The FHA is a top-down analysis that identifies the hazards to the rotorcraft and traces these hazards to the component level in the airframe structures affected by the SPS application. This document presents the FHA of the end-to-end SPS application to rotorcraft airframe structure, specifically the gearbox middle housing. Section A.2 identifies the failure modes of the middle housing, and the associated hazards to the rotorcraft. Section A.3 of the FHA is an overview of the SPS design, followed by the fault tree analysis. Sections A.4-A.8 identify and discuss the contributing areas to overall SPS failure, including inaccurate data, missing data, and incorrect algorithms. The contributing factors will be identified and mitigating

factors will be incorporated. Finally, section A.9 reviews SPS software considerations to determine certification level.

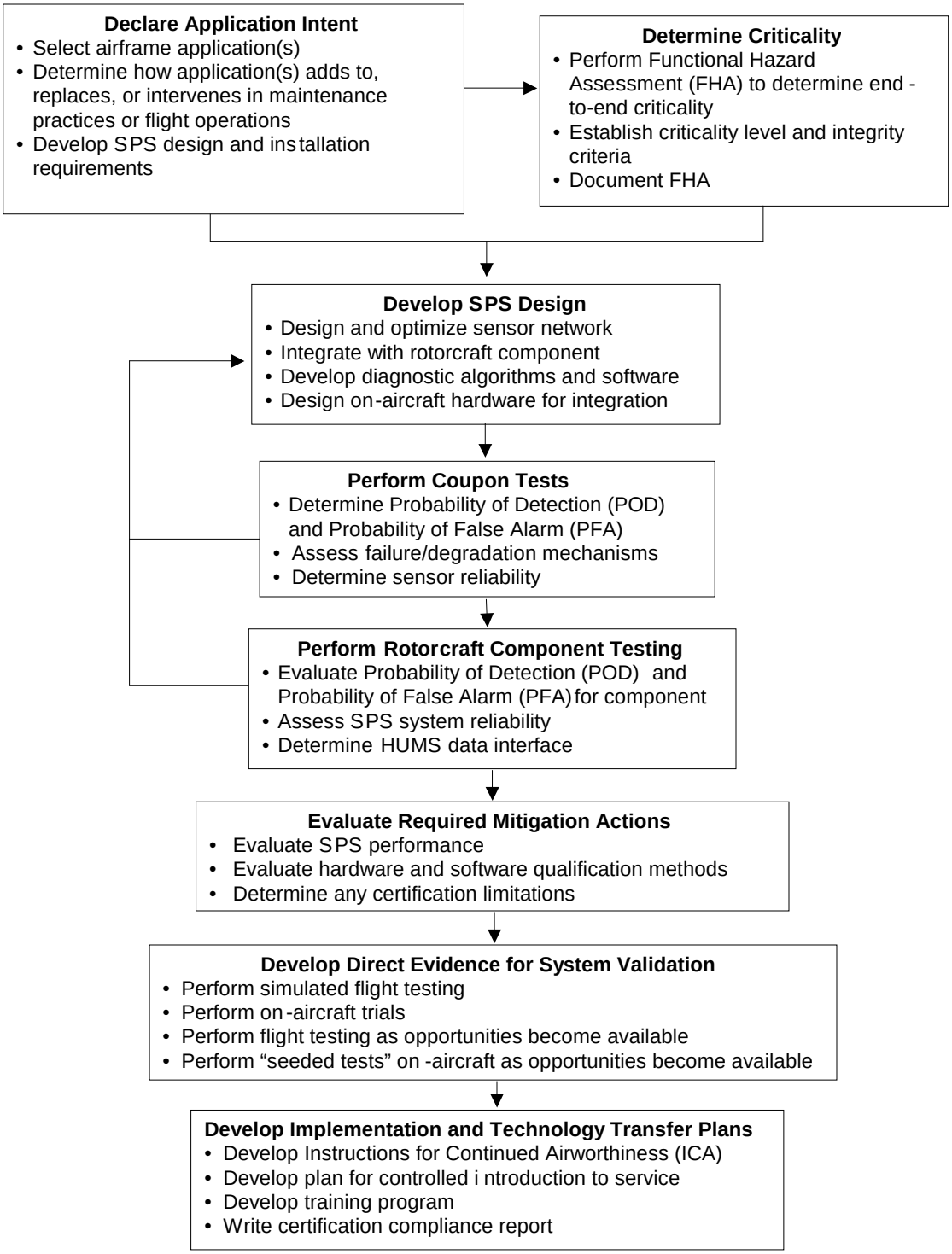

Figure A-1. The SPS Certification Approach

A.2 GEARBOX MIDDLE HOUSING.

The FHA is a top-down, function-based approach that is used to document and identify hazards to aircraft function that is structured around the functions of the aircraft. This translates to safety, as a loss of a given function results in reduced capability to safely complete the intended mission. This analysis identifies hazardous conditions that are based on aircraft function and then identifies the systems in which a possible failure could occur, resulting in a given hazardous condition. The hazards are grouped according to the guidelines described in AC 29-2C [A-1], which categorizes the hazards in the following manner: catastrophic, hazardous/severe major, major, minor, and no-effect. The five criticality categories are as follows:

- Catastrophic: Failure conditions that would prevent continued safe flight and landing.

- Hazardous/Severe Major: Failure conditions that would reduce the capability of the aircraft or the ability of the crew to cope with adverse operating conditions to the extent that there would be (a) a large reduction in safety margins or functional capabilities, (b) physical distress or higher workload such that the flight crew could not be relied on to perform their tasks accurately or completely, or (c) adverse effects on occupants, including serious or potentially fatal injuries to a small number of those occupants.

- Major: Failure conditions that would reduce the capability of the aircraft or the ability of the crew to cope with adverse operating conditions to the extent that there would be a significant reduction in safety margins or functional capabilities, a significant increase in crew workload or in conditions impairing crew efficiency, or discomfort to occupants, possibly including injuries.

- Minor: Failure conditions that would not significantly reduce aircraft safety and that would involve crew actions that are well within their capabilities. Minor failure conditions may include, for example, a slight reduction in safety margins or functional capabilities; a slight increase in crew workload, such as routine flight plan changes; or some inconvenience to occupants.

- No-Effect (Non-hazardous class): Failure conditions that do not affect the operational capability or safety of the aircraft or of the crew workload.

The main gearbox middle housing was selected as a representative component, as it is a non-redundant, life-limited component. If the gearbox housing fails, the pilot could lose control of the aircraft, which may lead to a catastrophic loss of aircraft, passengers, and crew. Table A-1 summarizes the identified failure modes and effects for the gearbox middle housing.

Table A-1. Gearbox Middle Housing Failure Modes and Effects

ID #	Function	Failure Mode	Interim Effects	End Effect	Detection Method	Failure Class	Compensating Provisions of Mitigating Actions
1A	React rotor/bearing loads to airframe	Crack in more than one mounting point	Mounting attachment cracks and propagates through to loss of one mounting attachment point. Crack goes undetected and 2nd attachement point cracks.	High vibration and/or possible separation of gearbox from aircraft.	Fixed inspection interval.	I/Catastrophic	Degraded mode testing and redundant load path
1B	React rotor/bearing loads to airframe	Crack in one attachment point	Attachment point cracks and crack may propagate thru to loss of one attachment point.	High vibration. Rotor loads reacted by other attachment points with one attachment point missing.	Fixed inspection interval. Possible increased vibration	II/Hazardous-Severe Major	Limited attachment point redundancy.
2A	Provide oil-tight chamber for lubrication	Oil passage clogs	Oil flow through cored oil passage is blocked or restricted.	Gearbox overheating. Wear of affected bearings/meshes is accelerated. Excessive wear may lead to chip generation.	Possible chip light or oil temperature light/gauge reading.	III/Major	Potential chip generation may be detected by chip detector. Conservative high reliability design component sizing, geometry, and material selection assure positive margin of safety at necessary loads. Likelihood of failure mode is improbable.
2B	Provide oil-tight chamber for lubrication	Crack through pressurized lubrication passage	Housing crack in or through pressurized oil passage.	Loss of gearbox cooling and lubrication. Possible external oil leak may result in fire hazard.	Oil pressure and temperature gauge reading.	II/Hazardous-Severe Major	Flight manual actions. Conservative high reliability design component sizing, geometry, and material selection assures positive margin of safety at necessary loads. Likelihood of failure mode is improbable.
3A	Provide structural support for bearing within housing	Structural crack other than mounting point	Possible loss of support and lubrication at affected bearings or gear meshes.	Possible loss of drive and some loss of lubrication and cooling. Land as soon as possible.	Possible vibration and oil pressure/temperature light illumination, visual inspection, and possible chip light from secondary damage.	II/Hazardous-Severe Major	Conservative high reliability design component sizing, geometry, and material selection assures positive margin of safety at necessary loads. Likelihood of failure mode is improbable.

The failure modes in table A-1 have a low probability of occurrence and an even lower probability of occurrence without detection. The low probability of occurrence is a result of compensating provisions (e.g., redundant fasteners, chip detectors) and directly affects the required SPS software classification as discussed in section A.9.

A.3 THE SPS SYSTEM OVERVIEW.

The SPS system diagram is shown in figure A-2. The interface to the rotorcraft HUMS does not currently exist, but preliminary protocol and command line messages have been defined.

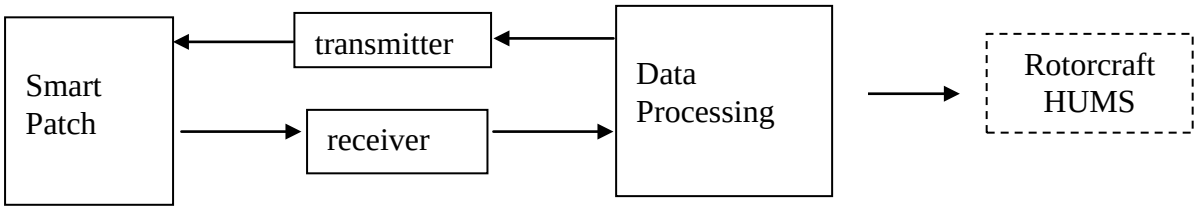

Figure A-2. An SPS System Block Diagram

A.4 DESCRIPTION OF THE SPS.

A.4.1 SMART PATCH.

The Smart Patch is a network of lead zirconate titanate (PZT) transducers. Each PZT can be used as an actuator or a sensor. An actuator-sensor pair forms a scan path. A scan is performed in two steps:

1. A signal is sent from the transmitter to the actuator.
2. The return signal is read from the sensor through the receiver.

A space on the structure may have multiple paths going through it. This built-in redundancy increases the reliability of the system.

An example of a Smart Patch is shown in figure A-3. There are nine sensors/actuators on this patch.

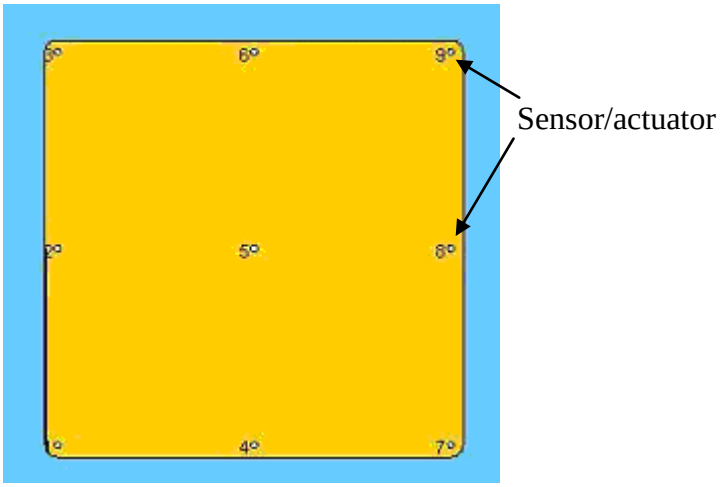

Figure A-3. Example of Smart Patch

The Smart Patch has demonstrated survivability at cryogenic temperatures as low as -321°F and short-term exposure (4 hours) to temperatures as high as 400ºF [A-2]. The temperature range for continuous operation with no degradation is -65ºF to 250ºF when bonded with Hysol® EA 9396™ or EA 9394™ adhesive.

A.4.2 TRANSMITTER.

The transmitter is used to send the exciting signal to the actuator. The SPS contains function generation and data acquisition electronic circuits. It is connected to the Smart Patch via cables. It can send out different high-voltage waveform signals to the PZT sensors to generate acoustic stress waves.

A.4.3 RECEIVER.

The receiver is used to receive the signal read by the sensor. The data acquisition function of the SPS can assimilate the sensor responses due to the excitation into a readable format for the data processing unit to analyze.

A.4.4 DATA PROCESSING.

The data-processing unit performs data-storage and data analysis tasks. When the SPS is first installed, a set of baseline data is collected while the component is in good health. The analysis phase of data processing compares the newly collected data against the baseline data. The output of the data analysis is a report of the condition (health) of the component.

A.5 FAULT TREE ANALYSIS.

The Fault Tree Analysis (FTA) for the SPS system involves specifying a top event to analyze followed by identifying all of the associated elements in the system that could cause that top

event to occur. The top event here is defined as "fail to detect the rotorcraft component failure." The top-down fault tree using logic OR gates representing the combination of events is shown in figure A-4. The FTA is consistent with the identified failure modes and effects analysis for the SPS and its components shown in tables A-2 through A-5.

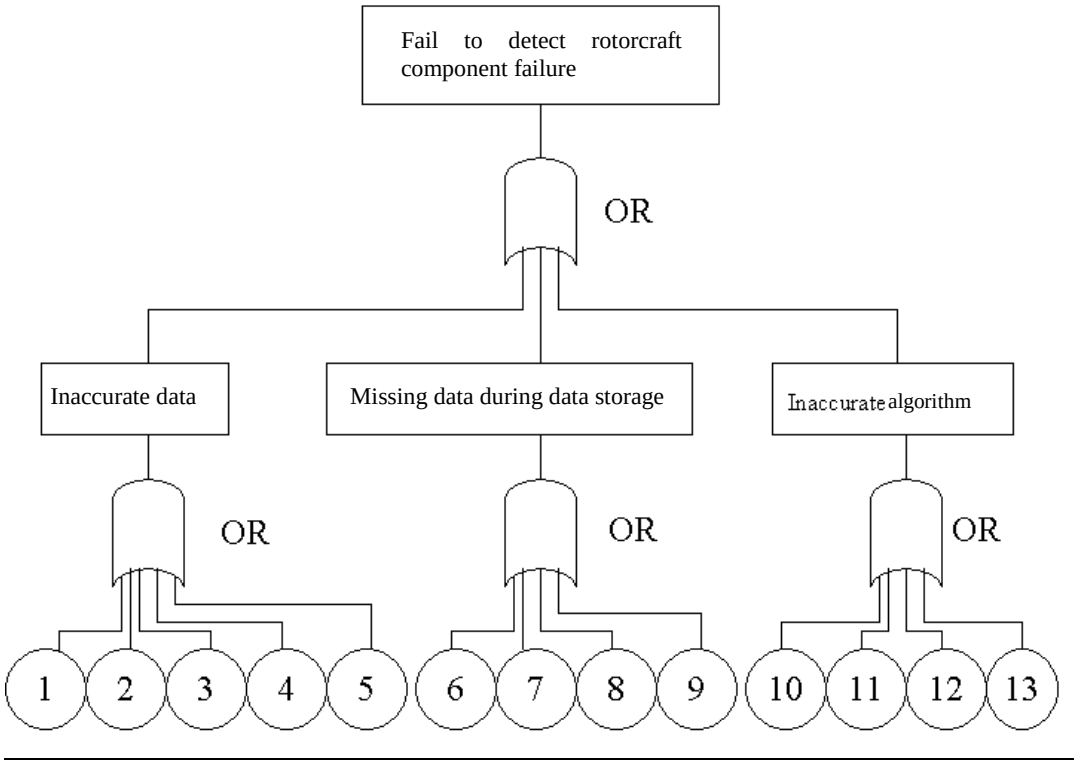

Figure A-4. Fault Tree for SPS

The numbers 1 through 13 correspond to the following faults:

1. Actuator or sensor wired to incorrect channel
2. Actuator or sensor wiring failure
3. Actuator or sensor degradation
4. Transmitter failure—incorrect signal
5. Receiver failure—incorrect signal
6. Transmitter failure—no signal
7. Wiring failure—no signal
8. Receiver failure—no signal
9. System failure
10. Software requirements incorrect
11. Software design incorrect
12. Coding errors
13. Testing

Table A-2. The SPS Failure Modes and Effects

No.	Component	Function	Failure Mode	Failure Cause	Failure Effect on SPS System	Failure Detection Method	Criticality Level	Mitigation
SPS System								
SPS1	Actuator or sensor connection with hardware	Wiring for data transfer between sensors/actuators and hardware	Incorrect data	Actuator/sensor wired to incorrect channel in hardware	Incorrect data	Wiring QA procedure to check that each sensor and actuator is connected to the correct channel	Major	Each sensor or actuator will be assigned a unique channel number. A first detection of incorrect channel assignment is to check if a channel number is assigned more than once. Once an incorrect wiring is detected, the wire will be redone. After all wirings are corrected, the wiring QA procedure will be executed one more time to verify the wiring for all the actuators and sensors in the Smart Patch.
SPS2	System	Data acquisition, storage, and processing	Missing data	Power failure, hardware failure, operating system freeze, and file system full	System will stop responding to user	Troubleshooting for detection of failure methods	Minor	Manuals for troubleshooting of system failure will be created. Once the problem is fixed, the system should be tested for data acquisition.
SPS3	Data storage	Data acquired from the system is stored on the hard drive for processing	Missing data	Loss due to hard drive failure	Loss of stored data		Minor	Data backup system will be established on a predefined schedule.

Table A-3. Smart Patch Sensor Layer Failure Modes and Effects

No.	Component	Function	Failure Mode	Failure Cause	Failure Effect on SPS System	Failure Detection Method	Criticality Level	Mitigation
Smart Patch								
S1	Piezo element	Sends and receives strain waves	Generation of voltage when strained		Electromagnetic interference	Pre-installation testing	Minor	Connector cover may short all piezos to mitigate this effect.
			Cracking and/or depolarization	Exceeding failure strain from flight loads	Piezo loses function, reduced system capability	Functional check prior to data collection using self-diagnostics	Minor	
				Mishandling			Minor	
				Impact from external object (debris, installation/removal of landing gear leg)			Minor	
			Disbonding from structure		Reduced sensitivity, reduced system capability	Visual inspection of sensor layer or measure sensor impedances	Minor	
S2	DuPont™ Kapton substrate	Provides support for sensors and sensor wiring	Degradation	Environmental exposure (hydraulic fluid, JP4, JP8, grease, moisture, high wind)	Loss of layer integrity, loss of system	Visual inspection of sensor layer	Major	Use protective coating.
S3	Wiring printed on Kapton	Carries electrical signals from connector to sensors	Wire breakage	Overstrain	Reduced system capability	Functional check prior to data collection using self-diagnostics	Minor	
				Impact from external object (debris, installation/removal of landing gear leg)	Reduced system capability		Minor	
S4	Adhesive bond between Kapton and structure	Attaches sensor layer to structure	Disbond	Impact from external object (debris, installation/removal of landing gear leg)	Detachment of Kapton from structure, loss of system	Visual inspection of sensor layer	Minor	Installation procedures with qualified adhesives will be used
			Degradation, weak bond	Environmental exposure (hydraulic fluid, JP4, JP8, grease, moisture, high wind, high/low temperatures)	Detachment of sensor layer from structure, loss of structure		Minor	Installation procedures with qualified adhesives will be used. Inspect for bond condition at each data collection.

Table A-3. Smart Patch Sensor Layer Failure Modes and Effects (Continued)

No.	Component	Function	Failure Mode	Failure Cause	Failure Effect on SPS System	Failure Detection Method	Criticality Level	Mitigation
Smart Patch								
S5	Copper shielding layer	Reduces crosstalk between actuators and sensors and reduces EMI from environment	Material degradation due to corrosion	Environmental exposure (hydraulic fluid, JP4, JP8, grease, moisture, high wind)	Increased crosstalk between actuator and sensors and increased environmental EMI, reduced system capability		Minor	Use protective coating.
			Shorting to wiring	Impact from external object (debris, installation/removal of landing gear leg)			Minor	
S6	Electrical connector	Provides location for connecting to external data acquisition equipment	Pins bending	Misuse (improper connector installation)	Loss of capability to collect data	Visual inspection of connector prior to data collection	Minor	Training procedures will be in place. Rebending pins should not be difficult. Alternate design could use receptacles on layer.
			Filling with debris	Environmental exposure (hydraulic fluid, JP4, JP8, grease, moisture, high wind)	Connector requires cleaning before use	Visual inspection of connector prior to data collection	Minor	An environmentally sealed connector cover will be required.
			Pins corroding	Environmental exposure (hydraulic fluid, JP4, JP8, grease, moisture, high wind)	Poor or no connection with data acquisition, loss of capability to collect data	Visual inspection of connector prior to data collection	Minor	An environmentally sealed connector cover will be required. Possible corrosion preventative on pins.
			Pins on back of connector shorting to structure	Contact between conductive structure and solder posts	Loss of signal for shorted circuits, reduced system capability	Functional check prior to data collection	Minor	Insulator required on pins.

Table A-4. Data Acquistion Hardware Failure Modes and Effects

No.	Component	Function	Failure Mode	Failure Cause	Failure Effect on SPS System	Failure Detection Method	Criticality Level	Mitigation
Hardware								
H1	Transmitter	Used to send excitation signal to the actuator	Sending incorrect exciting signal	Transmitter failure?		Visually verifying excitation signal	Minor	Methods for replacing transmitter will be in place. Software for comparison of a signal transmission pattern.
			Not sending signal at all	Transmitter failure?				
H2	Receiver	Used to receive the signal read by the sensor	Receiving incorrect sensor signals			Visualization of missing sensor signals and self-diagnostics. System will show damage all over.	Minor	Methods for replacing receiver will be in place. A test package consisting of a damage-free component that can be used for comparison purposes.
			Not receiving any signal at all					

Table A-5. The SPS Software Failure Modes and Effects

No.	Component	Function	Failure Mode	Failure Cause	Failure Effect on SPS System	Failure Detection Method	Criticality Level	Mitigation
	Software							
W1	Software requirements for crack detection	Requirements for software development		Incorrect requirements		Software development document	Minor	Software requirements/specifications will be documented in the System Requirement Document. The document will be used to track the software development process.
W2	Damage detection software design	Design for damage detection software		Incorrect design		Software design document	Major	Software design will be documented in the Software Design Document and will be reviewed against the software requirements.
W3	Coding	Coding of developed software for damage detection		Coding errors by engineers			Minor	Individual engineers will implement modules in the software design document and unit test the modules against the design. The complete implementation will then be integrated and tested for compliance with the design.
W4	Testing	To ensure that all software requirements are implemented correctly	Incorrect testing of software for functioning					A testing plan will be developed. The test plan will be executed by an independent test team. Any errors discovered during the testing phase will be fed back to the engineer team for fixing. The test will be repeated until no errors are found.

A.6 INACCURATE DATA.

Inaccurate data can result from the following causes:

- Actuator or sensor wired to incorrect channel
- Actuator or sensor wiring failure
- Actuator or sensor degradation
- Transmitter failure
- Receiver failure

Each cause and detection, and their mitigation, are discussed below.

A.6.1 ACTUATOR OR SENSOR WIRED TO INCORRECT CHANNEL.

Each actuator or sensor should be assigned a unique channel. A first detection of incorrect channel assignment is performed to determine if a channel number is assigned more than once.

After a Smart Patch is installed, a wiring quality assurance (QA) procedure is followed to verify each actuator or sensor is connected to the correct channel.

If incorrect wiring is detected, the wiring is redone. After all wirings are corrected, the wiring QA procedure is executed one more time to verify the wiring for all the actuators and sensors in the Smart Patch.

A.6.2 ACTUATOR OR SENSOR WIRING FAILURE.

A wire to an actuator or sensor can fail in two ways: either open or short circuits. The SPS has built-in capability to self-diagnose wiring failures. The capability is implemented in a hardware and software combination. The self-diagnosis software generates a report to pinpoint the failed wires and to report the type of failure as being open or short circuits.

Based on the self-diagnosis report, the failed wires can be quickly located and fixed. After fixing the wiring, the self-diagnostics shall be run one more time to verify that the wiring is functional.

Incorrect data could also be caused by intermittent failure of wiring or connectors. The common cause is a loose wire or connector that results in an open circuit. The error can be detected by visually verifying that the signal is missing.

After identifying the intermittent problem, the loose wire or connector should be fixed. A known signal should be sent and received in the loop to verify that the fault has been corrected.

A.6.3 ACTUATOR OR SENSOR DEGRADATION.

A weaker signal is characteristic of a degraded actuator or sensor. The weaker signal is also an indication of an increase in impedance. The SPS self-diagnostics can measure the impedance of

an actuator or a sensor. During the initial installation of an SPS, the self-diagnostics are run to diagnose the system and record the baseline impedance. During operation, the SPS self-diagnostics are run and the new impedance is compared with the baseline impedance. A degraded actuator or sensor is detected when its impedance changes more than the specified limit. Degraded actuators and sensors should be replaced.

In addition to using self-diagnostics to measure the sensor impedance, there is an additional mechanism to detect degraded sensors. The SPS software uses a cross-reference algorithm to verify the signal of each path and detect degraded sensors. The signals associated with degraded sensors will be automatically removed from the analysis phase.

A.6.4 TRANSMITTER FAILURE.

The transmitter can fail in two ways: by sending an incorrect excitation signal or by not sending an excitation signal at all. The excitation signal is looped to the SPS processing unit for display. An incorrect or missing excitation signal can be detected by visually verifying the excitation signal.

When a transmitter failure is detected, the transmitter should be replaced. After the replacement, a known transmitter pattern should be sent and the displayed transmitter signal should be compared with the known pattern for correctness.

A.6.5 RECEIVER FAILURE.

A receiver can also fail in two ways: by receiving an incorrect sensor signal or by not receiving any sensor signal at all. The received sensor signals are displayed, then analyzed by the SPS software.

In the case that a failed receiver does not receive any signal, it can be detected through visual inspection of the sensor signal in the display. Also, the SPS software can identify the sensors as nonfunctional because no sensor signal is detected.

In the case that a failed receiver gives faulty sensor signals, the result of the SPS software analysis phase can show damages all over the component. This indicates that the receiver is malfunctioning.

When a faulty receiver is detected, the receiver should be replaced. After the replacement, a known good component should be scanned using the SPS with the newly replaced receiver. The resulting sensor signal should be visually compared with the baseline of the good component. Then the SPS data processing should be run and the result should show no component damage.

A.7 MISSING DATA.

In the SPS, data are acquired and stored in files for processing. Missing data can result during either the data acquisition stage or the data storage stage.

A.7.1 MISSING DATA DURING DATA ACQUISITION.

All the causes of missing data during data acquisition are detectable by the self-diagnostic functions. After the problem is fixed and the system is in good working order, the component can be rescanned and data can be reacquired for damage detection. There is no permanent loss of data for data acquisition.

Missing data during data acquisition can be caused by:

- Transmitter failure
- Wiring failure
- Receiver failure
- System failure

Missing data caused by transmitter failure, wiring failure, and receiver failures have been discussed as subcases in sections A.6.2, A.6.4, and A.6.5. Missing data caused by system failure will be discussed below.

A.7.1.1 System Failure.

System failure can be caused by power failure, hardware failure, operating system freeze, and a full file system. In power failure, hardware failure, and operating system freeze, the system will stop responding to the user. In the case of a full file system, an error message will be given. Once the failure is detected, the problem should be fixed and the data reacquired.

A.7.1.2 Missing Data During Data Storage.

In the SPS, the acquired data are stored in files for processing. Stored data can be lost because of hard drive failure. To prevent loss of stored data, a data backup system is used. Data will be copied to the backup system periodically according to a predefined schedule.

A.8 INCORRECT ALGORITHMS.

The data processing unit is implemented in software. The software development process flows from software requirements to software design to coding to testing. Incorrect algorithms can result from (1) functionalities that were not translated into software requirements correctly, (2) software requirements that were not translated into software design correctly, and (3) software design that was not translated into correct coding. Once the software has been coded, the testing verifies that all the functionalities specified in the software requirements will function as expected.

A.8.1 SOFTWARE REQUIREMENTS INCORRECT.

The software requirements are documented in the System Requirements Document. It is reviewed and tracked throughout the software development process to ensure that all the specified requirements are implemented.

A.8.2 SOFTWARE DESIGN INCORRECT.

The software design is documented in the Software Design Document. It is reviewed against the software requirements.

A.8.3 CODING ERRORS.

Coding responsibilities are distributed among software engineers. Individual engineers will implement modules in the software design document and unit test the modules against the design. The complete implementation is then integrated and tested for compliance with the design.

A.8.4 TEST PLAN.

A test plan is developed, which includes test scenarios and test procedures. The test objective is to ensure that all software requirements are implemented correctly. The test plan is executed by an independent test team (no development engineers on the team). Any errors discovered during the testing phase are relayed to the engineering team that fixed the errors. The code fix is unit tested by the engineering team. After the code fix cycle, the integrated software is subjected to the testing cycle again for a full regression test.

A.9 SOFTWARE CLASSIFICATION.

Based on RTCA/DO-178B [A-3], the software level is based upon the contribution of software to potential failure conditions. The SPS is expected to be used for on-ground nondestructive inspection and is used to detect damage in components early to prevent failures. The integrity level of the software needs to match the criticality determined by the FHA for the worse end effect when used for credit. This is because the software could contribute to a potential failure condition if inaccurate data or analysis results in a crack not being identified by the SPS.

A simplistic approach of establishing criticality as a direct result of the worst possible identified failure mode will result in a requirement for Level A software for most dynamic components. This requirement is because most dynamic components provide a flight-critical function, which, if lost, would lead to a catastrophic failure, as defined in Title 14 Code of Federal Regulations (CFR) Advisory Circular (AC) 29.1309 [A-4]. For this reason, dynamic components are designed with compensating provisions (e.g., redundant fasteners, chip detectors) that result in extremely low probability of occurrence and even lower probability of occurrence without detection. The HUMS and prognostic health monitoring community have deemed that the cost of developing and maintaining Level A software is excessive and impractical and is not to be

required for most HUMS credits. Most existing HUMS are certified only to Level D or E software. The Sikorsky S-92, which has Level B software, may be the lone exception.

An approach that is compliant with AC 29-2C needs to be developed to establish credit criticality level and required software level through more in-depth understanding of risk. The following process could be performed to establish a correct software criticality that would allow HUMS credits while sustaining baseline risk. Analysis of the target component and credit would be conducted to establish a listing of "credible" failure modes of the component that account for compensating provisions and mitigating actions that would remain after the credit is implemented. This more sophisticated analysis would address "credible" failure modes, as defined by ADS-79B [A-5], as the focus, rather than failure modes that are "extremely remote" or "extremely improbable," as defined in reference A-4. This approach would apply engineering judgment, analysis, and testing to assess risk associated with the credit and define appropriate mitigating actions to maintain baseline risk in a manner similar to that used to establish baseline risk and define baseline maintenance requirements.

A.10 REFERENCES.

A-1. Federal Aviation Administration, "Certification of Transport Category Rotorcraft," Advisory Circular 29-2C, Section MG-15, September 30, 2008.

A-2. Qing, X.P., Beard, S., Kumar, A., Li, I., Lin, M. and Chang F.-K., "Stanford Multiactuator–Receiver Transduction (SMART) Layer Technology and Its Applications," *Encyclopedia of Structural Health Monitoring*, Wiley, 2009.

A-3. RTCA/DO-178B, "Software Considerations in Airborne Systems and Equipment Certification," September 1, 1992.

A-4. Title 14 Code of Federal Regulations Part 29.1309, "Equipment, Systems, and Installations," July 2012.

A-5. A-ADS-79 B Handbook, "Aeronautical Design Standard Handbook for Condition Based Maintenance Systems for U.S. Army Aircraft Systems," December 17, 2009.

APPENDIX B—COUPON TEST REPORT

B.1 COUPON TEST GOALS.

The goals of the coupon tests were to:

- Ensure sensor survivability.
- Ensure that clean/usable data can be obtained.

Since the Smart Patch System (SPS) for rotorcraft structures is based on Acellent's SMART® Layer and uses a network of piezoelectric sensors embedded in a flexible dielectric film, tests conducted previously with the SMART Layer can be used to achieve these goals.

The coupon test plan focused on two tasks:

- Collecting and summarizing relevant data from previously conducted tests
- Developing and conducting tests for missing elements

To ensure Smart Patch sensor survivability, data from previously conducted "survivability" tests were collected and are summarized in this appendix. This includes survivability data from:

- Fatigue tests.
- Temperature tests.
- Vibration tests.
- Moisture and salt fog tests.

Data usability is based on the strength of the sensor signal. For most aircraft structures, a signal-to-noise ratio greater than 20 dB is considered appropriate for the data to be usable for analysis and signal processing. Figure B-1 shows an example of typical data that are usable for analysis.

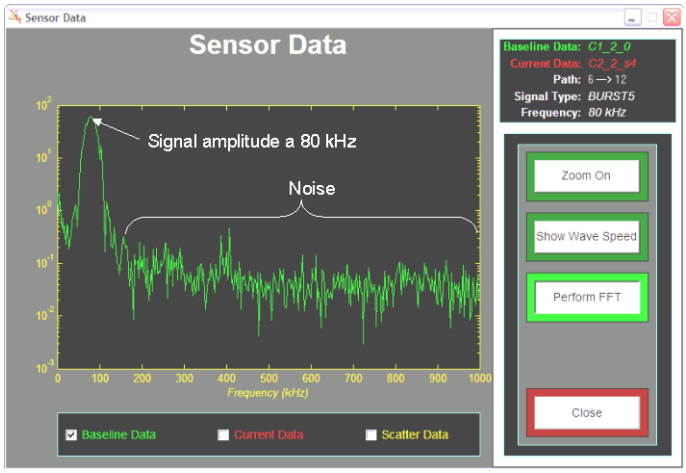

Figure B-1. Example of Signal-to-Noise Ratio for Usable Data

Data usability is also a factor of the intended application, placement of sensors and actuators, and structural geometry. For rotorcraft, structural applications can be classified as:

- Static Airframe structures
  - Frame
  - Frame (upper deck)
  - Bulkhead
  - Beams/spars
  - Stringers
  - Skins
  - Attachments/lugs
- Dynamic structures
  - Main rotor (MR) and tail rotor (TR) Blade/spar
  - MR hub, cuff, and yoke
  - Transmission
  - TR hub and horn
  - Control system

Previous tests were conducted on the following types of structures to determine whether or not usable data could be obtained:

- Single lap joints
- Thick plates (up to 1.5″)
- Complex geometries

It was determined that, for the listed structural applications, coupon test data were missing for bolted and double lap joints. Therefore, during the course of this program, coupon-level testing was conducted for "signal transfer in bolted joints" and "fatigue testing in double lap joints" to cover the areas missing from the above list. Test information and results are summarized below.

It is expected that these comprehensive tests will provide enough information to ensure sensor survivability and data usability for rotorcraft applications. The data from the tests are also summarized in table B-1.

Table B-1. Results of Survivability and Usability Sensor Tests

Test No.	Structure	Objective	Material	Geometry	Tests	Sensors Survived?	Data Usable?
1	Compact tension and dog-bone test specimens	Sensor survivability and damage detection	Aluminum (Al 2024-T3), titanium (Ti-6Al-4V), and steel (AISI 4340)	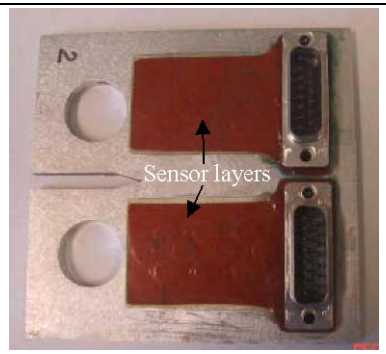	Fatigue cycling until failure	Yes	Yes
2	Pipeline sample	Detect and monitor the growth of a fatigue crack	Steel	12.75-inch outer diameter steel pipe with a 1.57-inch-thick wall	Fatigue cycling until crack in wall at 13,294,000 cycles	Yes	Yes

Table B-1. Results of Survivability and Usability Sensor Tests (Continued)

Test No.	Structure	Objective	Material	Geometry	Tests	Sensors Survived?	Data Usable?
3	Various	Temperature survivability testing	Metals	Not Applicable	Testing in oven and variable temperature conditions	Operational in the range of -321°F to 340 °F	Yes
4	Coupons	Slat fog and humidity tests for survival in harsh environments	AL test coupons	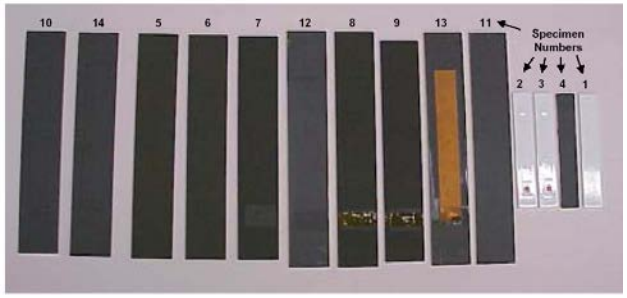	MIL-STD-810F, section 507.4 for salt fog and section 509.4 for humidity	Yes	Yes
5	Riveted joints	Fatigue loading to determine clear data for crack detection and sensor survivability	Multiriveted AL panel	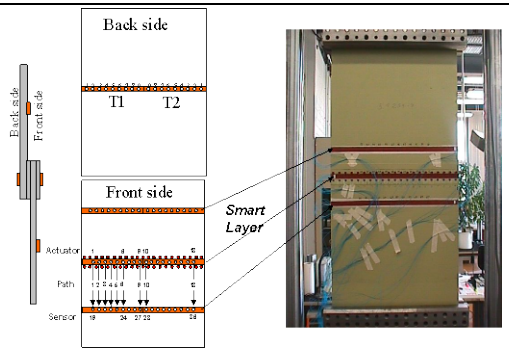	Fatigue testing until failure	Yes	Yes

Table B-1. Results of Survivability and Usability Sensor Tests (Continued)

Test No.	Structure	Objective	Material	Geometry	Tests	Sensors Survived?	Data Usable?
6	Representative airplane part	The goal was to detect crack growth and disbond growth of the bonded repair on the part.	Complex, thick structure made of 2124-T8 aluminum	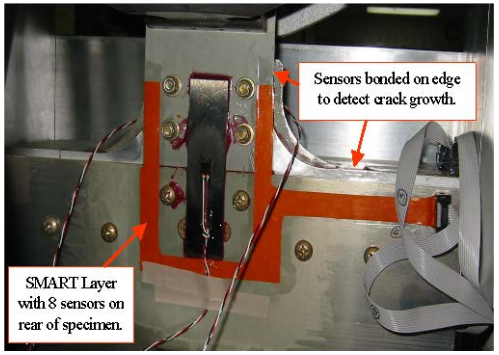	Fatigue cycling until failure	Yes	Yes
7	Multilayered stack-up structures	Determine if useful signals can be transferred through multiple nonbonded structure layers. Determine detectable crack size on the middle plate of a double lap joint using sensors bonded on the top and bottom plates.	AL 7075 T6 double lap joints with Hi-LOK® fasteners	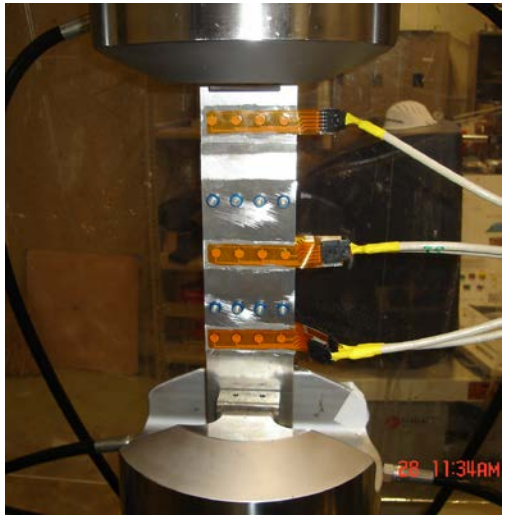	Fatigue cycling until failure	Yes	Yes

B.2 TEST INFORMATION AND DATA.

B.2.1 FATIGUE AND VIBRATION TESTS.

B.2.1.1 Coupon Tests for Survivability During Fatigue for Rotorcraft.

Fatigue tests were previously conducted on materials typically used in rotorcraft structures (i.e. steel, aluminum, and titanium). As part of a U.S. Army program, Acellent conducted fatigue tests on compact tension and dog-bone specimens manufactured with aluminum (Al 2024-T3), titanium (Ti-6Al-4V), and steel (AISI 4340). The goal of the testing was to:

- Ensure survivability of the sensors.
- Determine if clear sensor data can be obtained for crack detection.

B.2.1.2 Compact Tension Tests.

Acellent, Inc. designed and manufactured six compact-tension specimens, two each of Al-2024-T3, Ti-6Al-4V, and AISI 4340 steel. Based on ASTM E 647-00, the dimensions of each specimen instrumented with custom sensor layers are shown in figure B-2. Crack growth versus cycling plots for the Al-2024-T3 and Ti-6Al-4V specimens are shown in figure B-3.

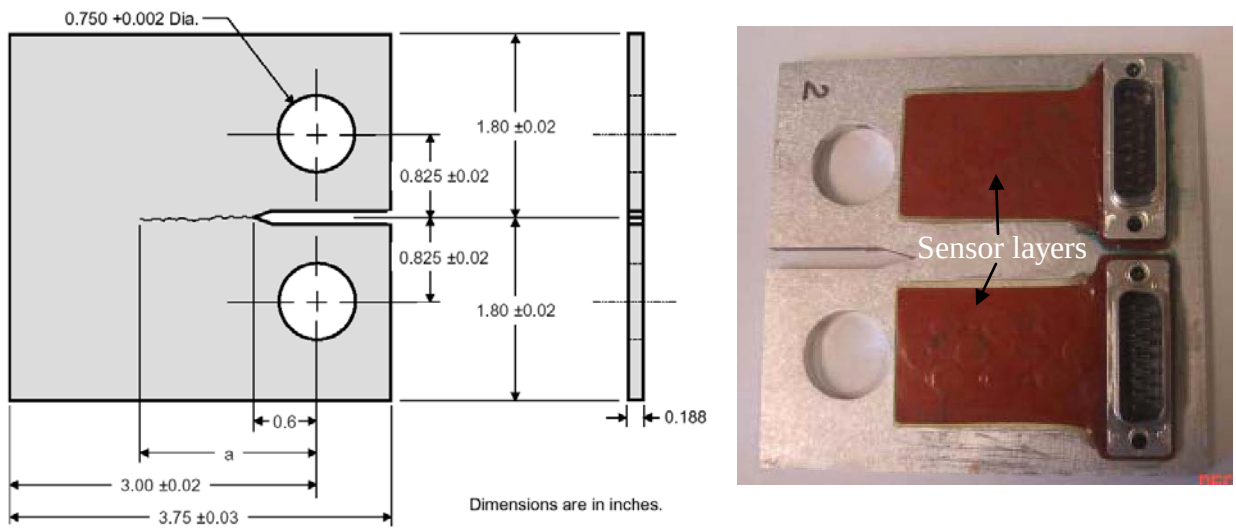

Figure B-2. Compact Tension Specimens

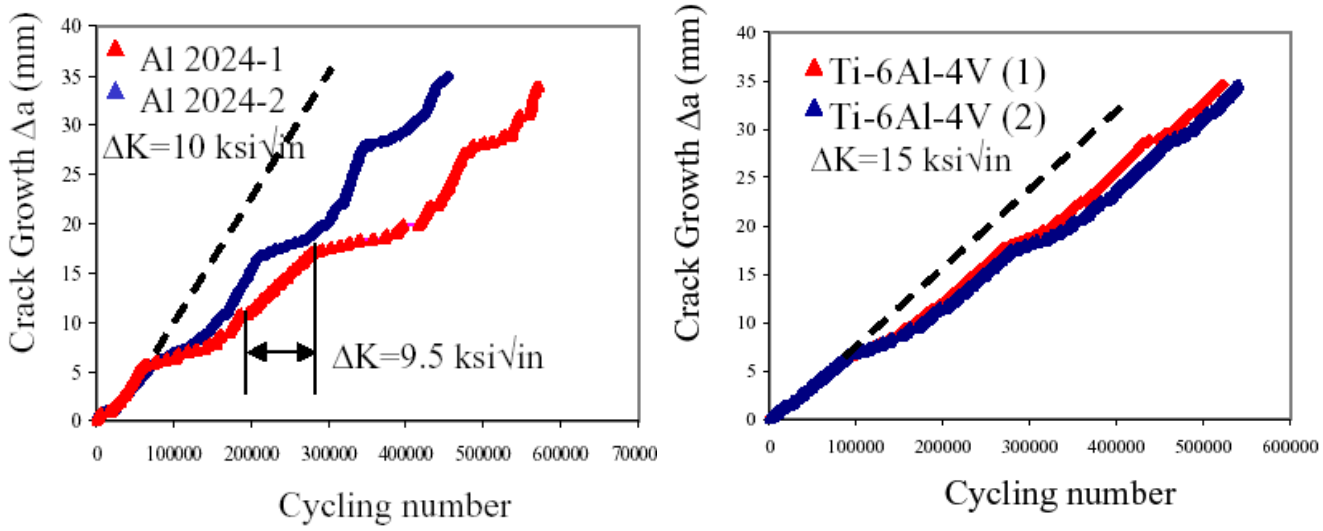

Aluminum Titanium

Figure B-3. Crack Growth vs. Cycles

The tests found that the sensors can survive the fatigue cycling while providing clear data that could be used for damage analysis.

B.2.1.3 Dog-Bone Test Specimens.

The fatigue testing of the dog-bone specimens were conducted to test the sensor survivability due to fatigue loads. Figure B-4 shows the dog-bone test specimens with the sensor layers.

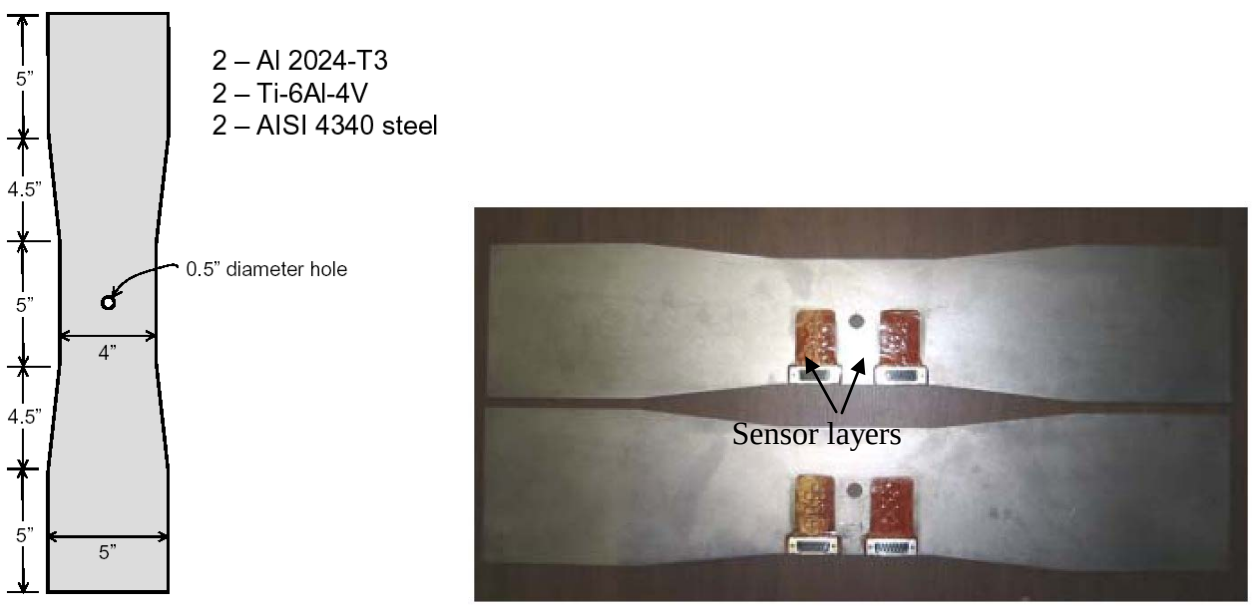

Figure B-4. Dog-Bone Specimens

A 0.5-inch-diameter hole was made in the center, and electrical discharge machining notches were used to help initiate crack growth. During cycling, the fatigue crack growth rate (da/dN) was 2×10^{-6} in/cycle. The rate allows the crack to grow 10 mil in about 10 minutes when the frequency of load is 10 Hz.

The tests demonstrated that the sensors could survive the fatigue loads as well as provide clear data for use in damage detection.

B.2.2 FATIGUE AND VIBRATION TESTING ON PIPELINE.

In collaboration with British Petroleum, the SMART Layer was tested on a Thunder Horse steel pipe sample. The purpose of the tests was to use the SMART technology to detect and monitor the growth of a fatigue crack at the girth weld of a 12.75-inch outer diameter steel pipe with a wall thickness of 1.57 inches. SMART Layers with 30 piezoelectric transducers were manufactured and installed on the pipeline section. The piezoelectric discs are 0.25 inch in diameter and 0.03 inch thick. Two 30-sensor strips were mounted 8 inches apart on either side of the girth weld (figure B-5). The strip locations were chosen to ensure a strong signal from the sensors.

The test was conducted with 400 psi internal pressure and the fatigue cycling ran at ±30 ksi at 27 Hz. Data was collected at specified intervals during the test. The tests were stopped at 13,294,000 cycles because a through-wall crack was observed in the pipe. The system diagnostic image in figure B-5 shows the location of the crack. All the sensors were still functioning when the tests were stopped.

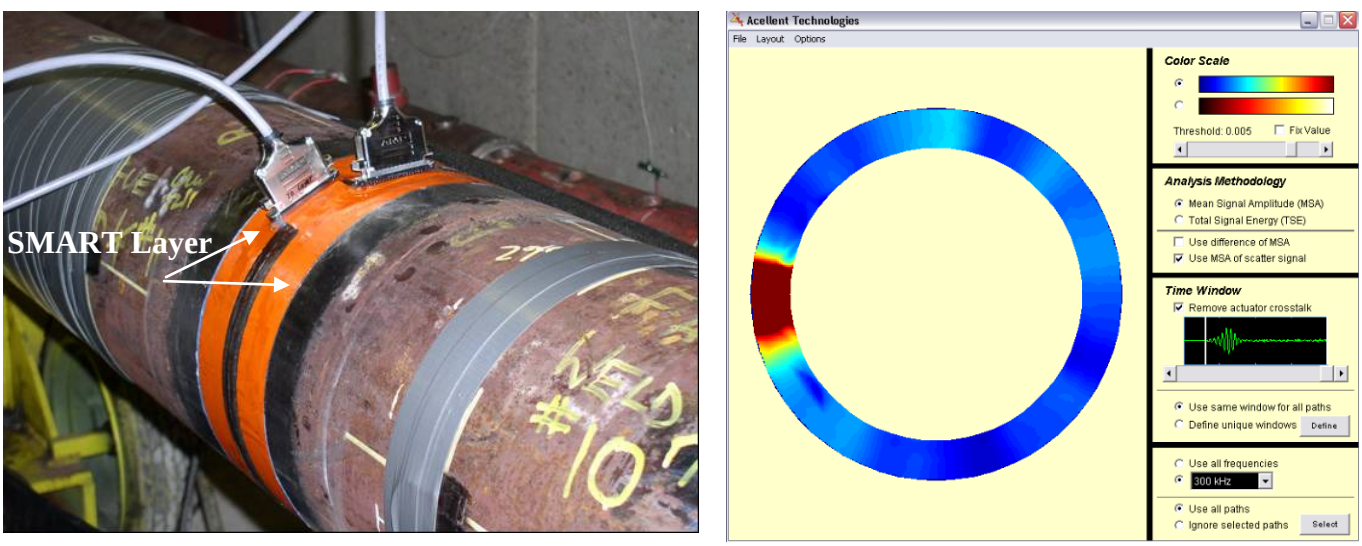

Figure B-5. Pipeline Monitoring

B.2.2.1 Vibration Tests.

The survivability and functionality of the SMART Layer under operating conditions of typical liquid rocket engines, such as cryogenic temperature, vibration loads have been investigated. The tests were conducted at Pratt & Whitney Rocketdyne, Inc. The test environments were derived from operational measurements on large-booster liquid oxygen-hydrogen (LOX-H2) rocket engines during engine hot-fire tests. Measurements of the sensors mounted on an Inconel® duct were taken at ambient and cryogenic temperatures prior to applying the dynamic environments, during full-level vibration tests, and after completion of full-level tests. The defined random and sine vibration environments, which represent an average envelope of the data from the large propellant duct with the highest overall vibration level, is shown in figure B-6.

According to the comparisons of signals before and after the test, there is no degradation in any of the sensors after the vibration and shocks at cryogenic temperature, as shown in figure B-7. The tests conducted during this series demonstrated that the SMART layer could withstand operational levels of vibratory and shock energy on a representative rocket engine duct assembly within a restricted frequency band in laboratory tests.

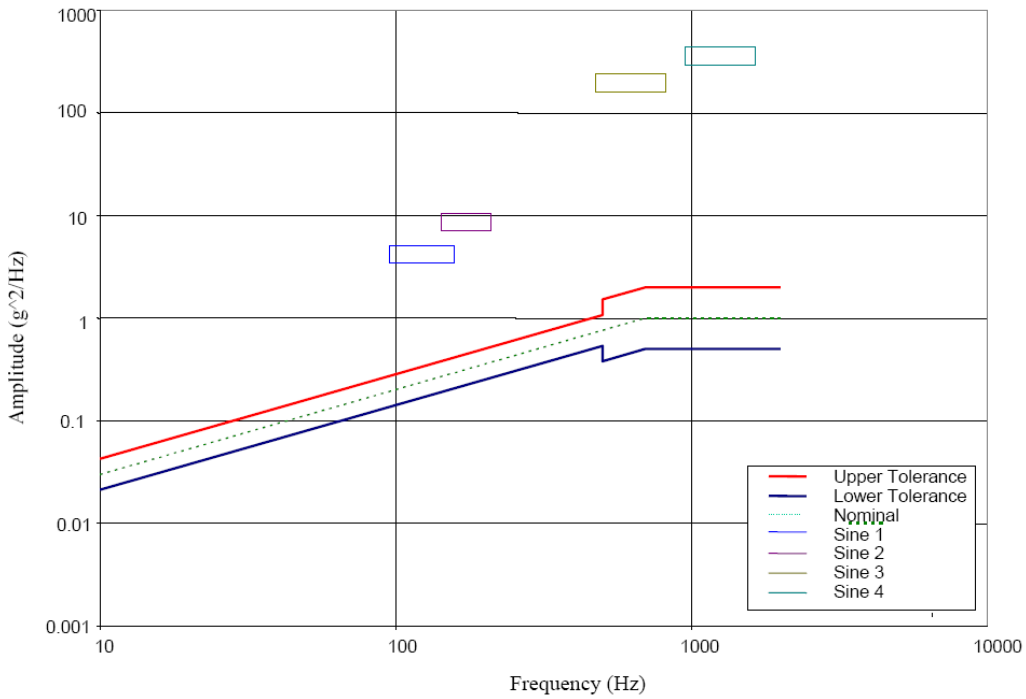

Figure B-6. Vibration Spectrum

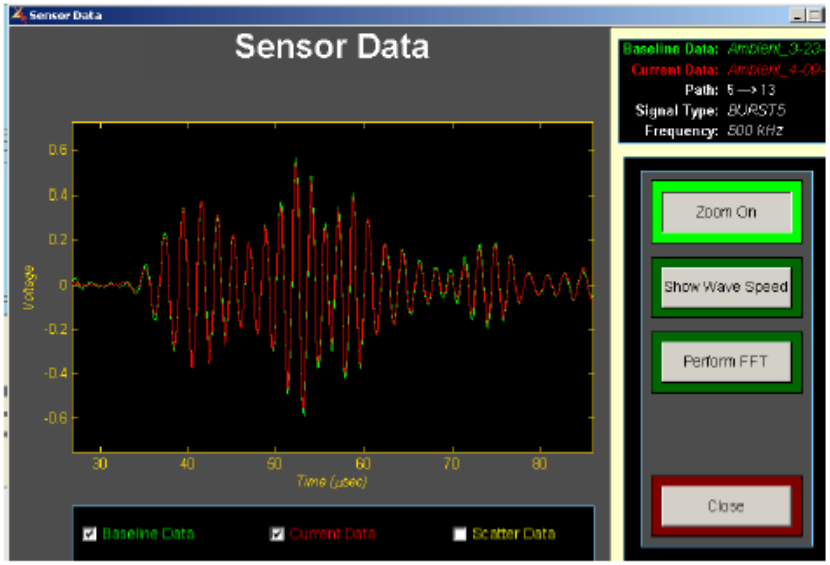

Figure B-7. Comparison of 500 kHz Signals at Room Temperature Before and After the Test

B.2.3 TEMPERATURE TESTS.

Temperature limit tests for the sensor layers were conducted internally at Acellent and through other programs. It was found that the sensor can survive and is operational in the range of -321°F to 340°F .

An example of one test conducted for a program with the U.S. Army is listed here. The specimen used for the testing is shown in figure B-8. Three sensor strips with 2 PZTs on each were mounted on a 12″ x 12″ x 0.080″ aluminum plate. The PZTs disks used in the study are 10 mil thick and 0.25″ diameter. The adhesive used to mount the strips is Hysol® EA 9396. The adhesive was cured at 160°F for 2 hours.

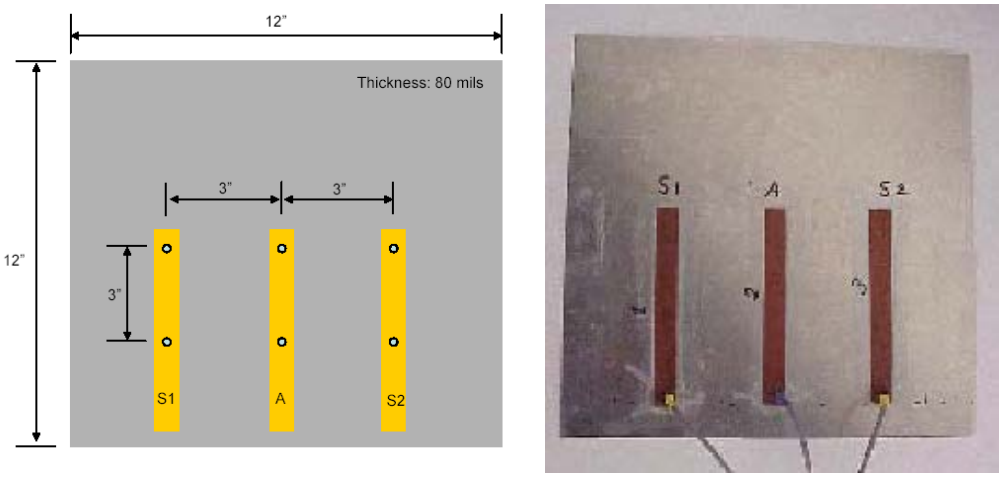

Figure B-8. Specimen With Sensor Layers Used for Temperature Tests

During the test, the PZTs on sensor strip A were used as actuators while the PZTs on strips S1 and S2 were used as sensors. The actuator input signals are 50V five-peak waveforms with frequencies 50 kHz, 100 kHz, 150 kHz, …, 500 kHz.

Figure B-9 shows the comparison of the signals taken at the same temperature, but in two different temperature cycles. The results show that there is no change in signal if the data is collected at the same temperature.

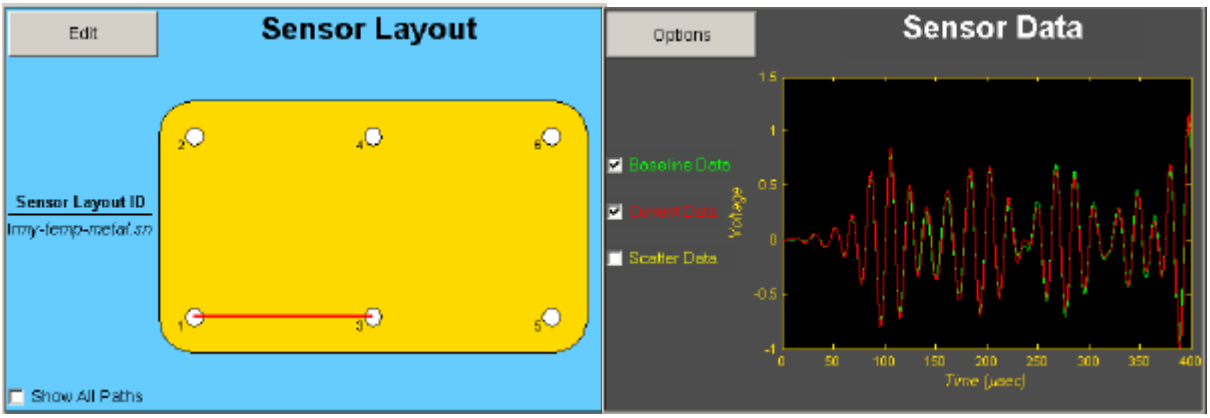

(a) For Path 3-1

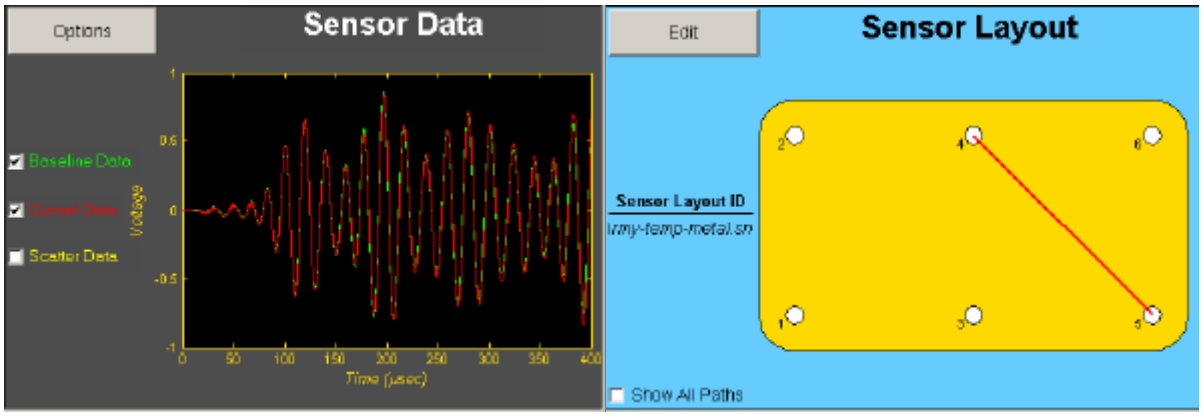

(b) For Path 4-5

(Green line: Signal at 80°F of the first cycle, Red Line: Signal at 80°F of the second cycle)

Figure B-9. Signal Comparisons at 50 kHz for Path 4-5

B.2.4 MOISTURE AND SALT FOG TESTS.

Tests for humidity and salt fog were performed as part of a U.S. Army program. Results from these tests have enormous value in generating confidence in the environmental worthiness and overall durability of the SMART Layer. The purpose of the humidity testing was to determine the resistance of the SMART Layer, adhesive, and exterior coatings to the effects of a warm, humid atmosphere. The tests are for applications in which the damage detection system is likely

to be stored or deployed in a warm, humid environment or an environment in which high levels of humidity occur. Although it is preferable to perform the tests at appropriate natural environment sites, it is not always practical because of logistical, cost, or schedule considerations. Warm, humid conditions can occur year-round in tropical areas, seasonally in mid-latitude areas, and in vehicles and structures subjected to combinations of changes in pressure, temperature, and relative humidity. Other high levels of humidity can exist worldwide.

The salt fog tests were performed to determine the effectiveness of protective coatings and finishes on the SMART Layer. They may also be applied to determine the effects of salt deposits on the physical and electrical aspects of the SMART Layer. The tests are designed to evaluate the effectiveness and quality of protective coatings and finishes for the SMART Layer, and to locate potential problem areas, quality control deficiencies, and design flaws in a relatively short time. In general, these tests are for applications that will experience significant exposure (as opposed to infrequent or irregular) to high levels of salt in the atmosphere.

Three series of tests were conducted, each building on the lessons learned from the previous one. Through each series of testing, the surface preparation and the application of the coatings were improved. The Smart Layer sensors in the third and final series of tests were exposed to the salt fog environment for 1336 hours and continued to function successfully.

At the Army Research Laboratory, the specimens were tested per MIL STD-810F [B-1], section 507.4 for the humidity testing and section 509.4 for the salt fog testing. During the testing, the specimens were visually inspected. If corrosion was observed on one of the SMART Layers, then the corresponding coating was considered not to have passed the test.

A total of 14 new aluminum specimens were prepared. Four were 1″ by 6″, and the other ten were 2″ by 12″. The preparation work was performed at three different locations: Acellent, The Boeing Co., and SMAC. The major purpose for choosing different paint shops and different preparation steps is to determine the effect factors. A photograph of the 14 specimens is shown in figure B-10.

The sensor layers were installed after proper sanding and MIL standard primers were used for protection. Specific primers painted on the layers include:

- MIL-PRF-23377, type 1, Class C2 primer
- MIL-PRF-46168D, type 1, Class H topcoat

After 336 hours of salt fog tests, no disbonding between the sensor layer and the base structure was observed for any of the specimens. The coatings on the specimens survived salt fog exposure with no degradation. The coatings on a few of the specimens exhibited minor degradation, but all of the sensors on all specimens continued functioning and were able to generate and receive usable signals.

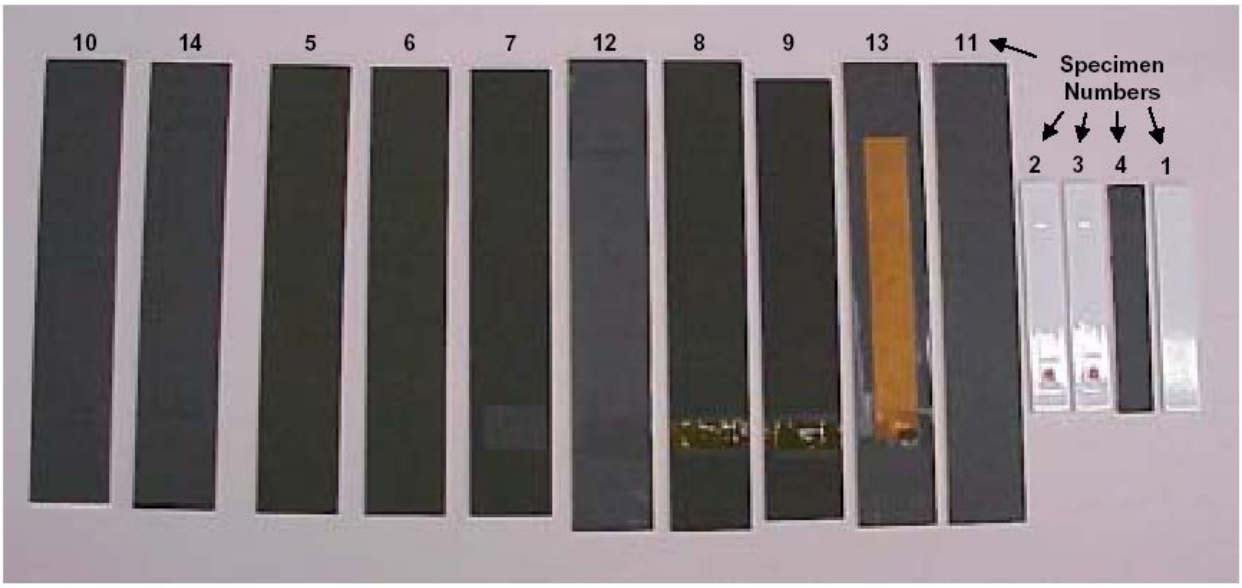

Figure B-10. Specimens for Salt Fog and Humidity Tests

Based on the results, it is clear that, when properly coated, the SMART Layer mounted on the metal specimen can be effectively protected from humidity and salt fog corrosion. It has been shown that the SMART Layers can survive humidity and salt fog exposure with proper surface treatment (sanding or chemical etching), bonding the SMART Layers on the surface with Hysol EA 9396, and using proper coatings (MIL-PRF-23377, type 1, Class C2 primer and painted with a MIL-PRF-46168D, type 1, Class H topcoat).

B.2.5 TESTS ON VARIOUS STRUCTURAL GEOMETRIES.

Tests conducted on typical aircraft structures are presented in this section. The structures are used in all fixed-wing and rotorcraft vehicles. Because of the complexity of the structures in terms of geometry and availability of optimum locations for placement of sensors, data collected from these tests articles may or may not be useful for damage detection.

B.2.5.1 Multiriveted Panels.

Multiriveted aluminium panels, as shown in figure B-11, were tested under uniaxial constant-amplitude fatigue loading to detect crack initiation at the different rivets as well as the following crack propagation. A SMART Layer strip was bonded between the two rivet lines and served as the actuation element. Two more SMART Layer strips were bonded approximately 12 cm above and below the rivet lines and served as sensors, respectively. The actuating piezoelectric elements were then actuated in a sequence using a constant-amplitude actuation signal package that was swept through a frequency band between 100 kHz and 700 kHz. The signals were then recorded by the piezoelectric elements being on the direct straight path as well by the piezoelectric elements being next to them. Measurements with the SMART Layer were done at specified intervals during which load cycling was stopped.

At the beginning of the test, data were recorded that were taken as the reference for the damage-free condition. Any deviation in the sensor signals, which was observed to increase continuously over the number of loading cycles, was considered to result from progressing damage.

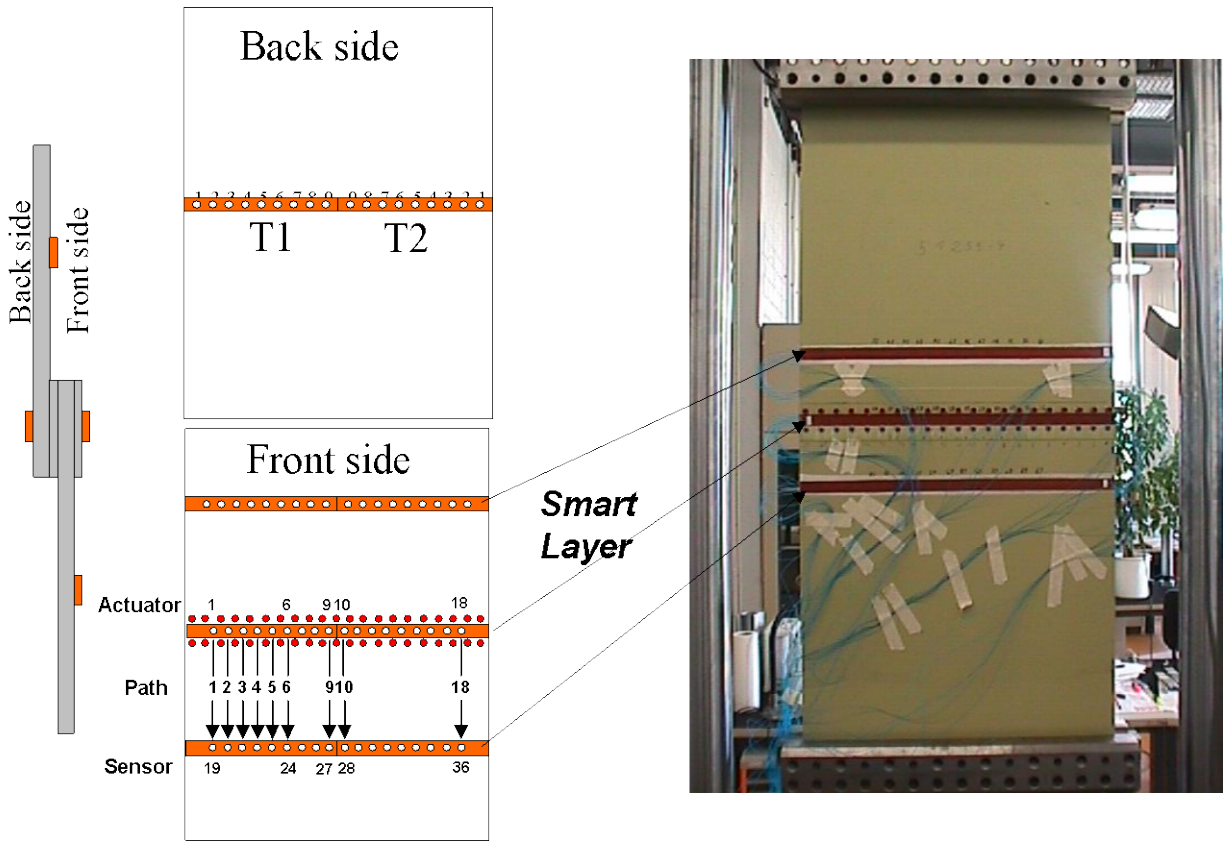

Figure B-11. Riveted Panel in Fatigue Test Using the Smart Layer [B-2]

Data usable for damage detection were obtained from these tests. The sensors also survived the fatigue-to-failure tests for the multiriveted joint panel.

B.2.5.2 Complex Geometries.

As part of a U.S. Air Force/Boeing-funded Structural Health Monitoring for Bonded Repairs program, tests were conducted on a representative airplane part (complex, thick structure) during fatigue cycling. The goal was to detect crack growth and disbond growth of the bonded repair on the part.

Figures B-12 and B-13 show the section of the part where the sensors are mounted on it [B-3]. The test specimens are complex, thick structures made of 2124-T8 aluminum. Two types of specimens were tested, one for crack growth and one for disbond growth. The crack growth specimens had EDM notches at the radii, and the disbond growth specimens had small disbonds created under the composite repair patch. The specimens were subject to cyclic loading to induce

crack growth and disbond growth. A restraining system was used during cycling to reduce the lateral deflections of the test specimen.

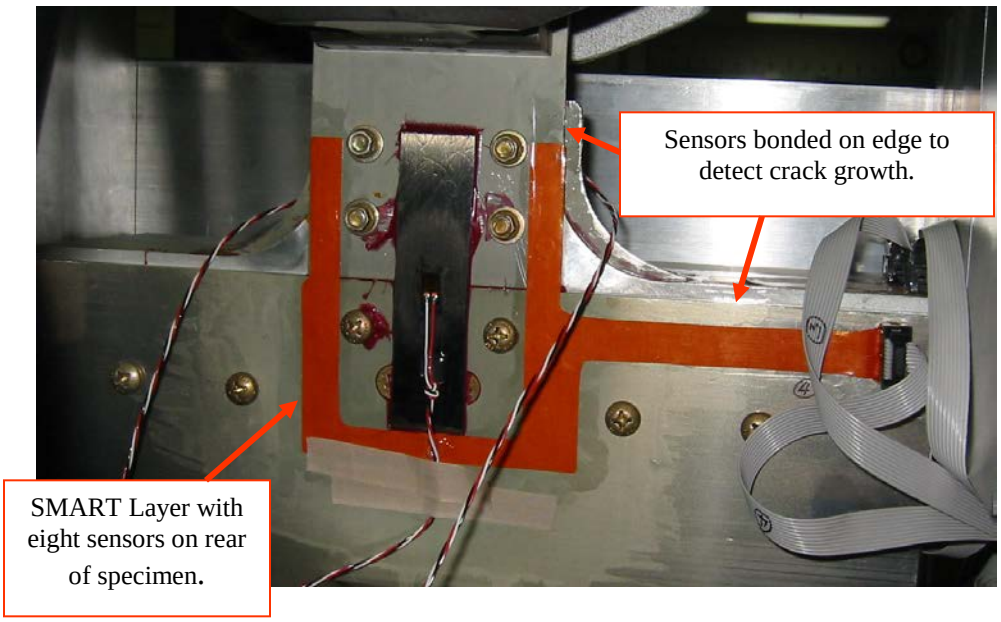

Figure B-12. Sensor Locations on Specimen (Rear View)

Figure B-13. Sensor Locations on Specimen (Front View)

A total of 20 sensors was mounted on each specimen to monitor disbond growth under the composite patch and crack growth on both the left and right sides. Eight sensors on the rear (figure B-12) were used to monitor disbond growth in the composite patch. An additional eight

sensors on the front (in the same locations as those on the rear) were used to test the feasibility of detecting composite disbonds through several interfaces of the assembled (built-up) structure. The remaining four sensors were bonded on the edge of the specimen and used to detect crack growth on both sides (two sensors for the crack on the left and two sensors for the crack on the right).

For the crack specimen, it took over 100,000 cycles to start the cracks. Once the cracks started, they grew steadily and could be tracked both visually and with the sensors. Acellent's system even detected one of the cracks before it was observed visually with the microscope. Figure B-14 shows the damage growth detected versus the cycles.

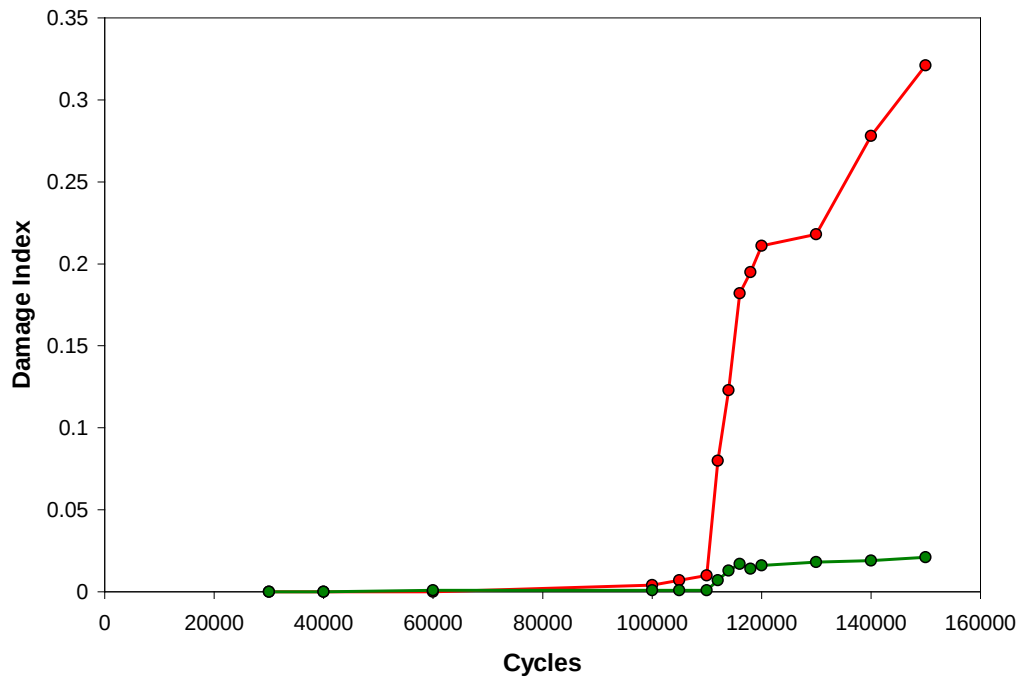

Green = right
Red = left

Figure B-14. Damage Index Curves for the Left and Right Sides of the Component

For the disbond specimen, the cycling loads were set at ±4500 lb for 10,000 cycles, and sensor data was collected every 500 cycles. The loads were increased to ±5000 lb for the next 500 cycles, and then increased again to ±5500 lb for the remainder of the test. The system could show clear changes due to disbond during the test, as shown in figure B-15.

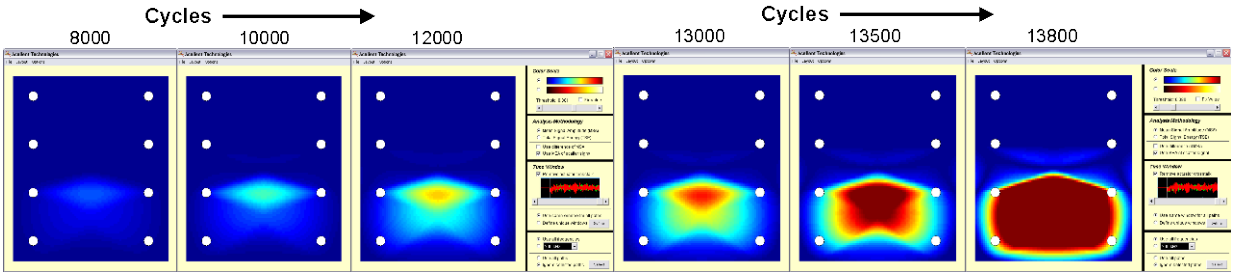

Figure B-15. Disbond Detection

B.2.5.3 Bolted Joints.

Fatigue tests on bolted joint coupon specimens were conducted in collaboration with the Structures Laboratory of Stanford University as part of this current FAA project. There were five SMART Layers mounted on each specimen, as shown in figure B-16.

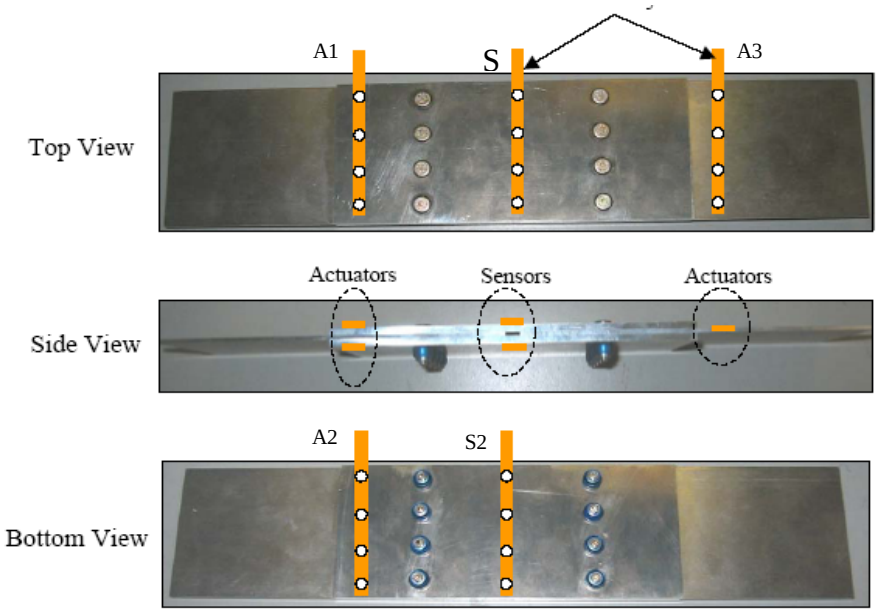

Figure B-16. Test Specimens for Bolted Joint Test

As shown in figure B-17, the MTS machine was used to perform the tests. The fatigue load applied to the specimens was: maximum load = 6000 lb, ratio of minimum load to maximum load = 0.1, frequency of loading =3 Hz.

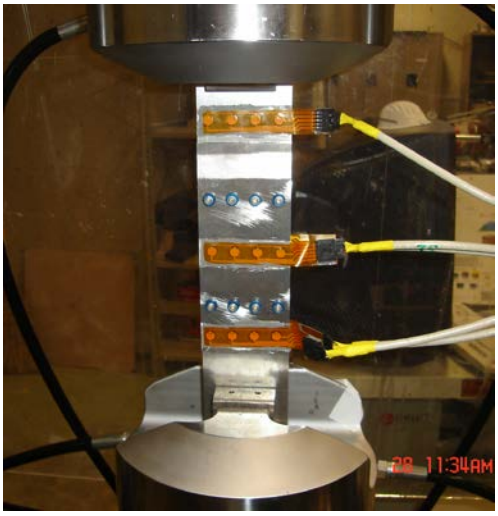

Figure B-17. Test Setup

Before the fatigue test, two sets of baseline data over a range of frequencies (100 kHz – 400 kHz) were taken at the designed minimum load and mean load, respectively. After starting fatigue cycling, the signals were recorded at every 1000 or 2000 cycles until some change of signals. Figure B-18 shows the workspace used for taking data.

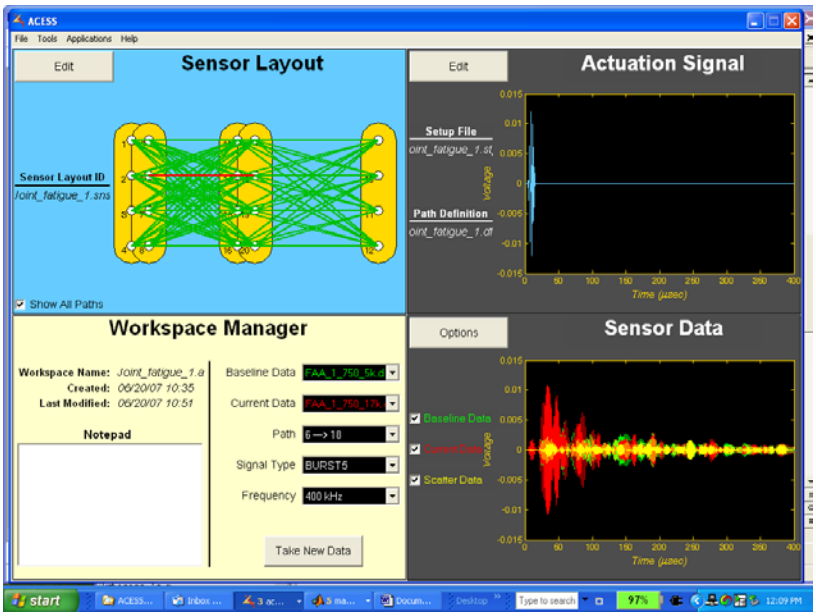

Figure B-18. Workspace of Data Acquisition Software

The signals shown in figure B-19 are from two different paths. Figure B-19 shows a significant difference between the signals taken after 5000 cycles and 17,000 cycles, respectively. This difference change is related to a condition change of the structure near the path. After stopping the test and disassembling the specimen, it was found that the bolt along the path had loosened.

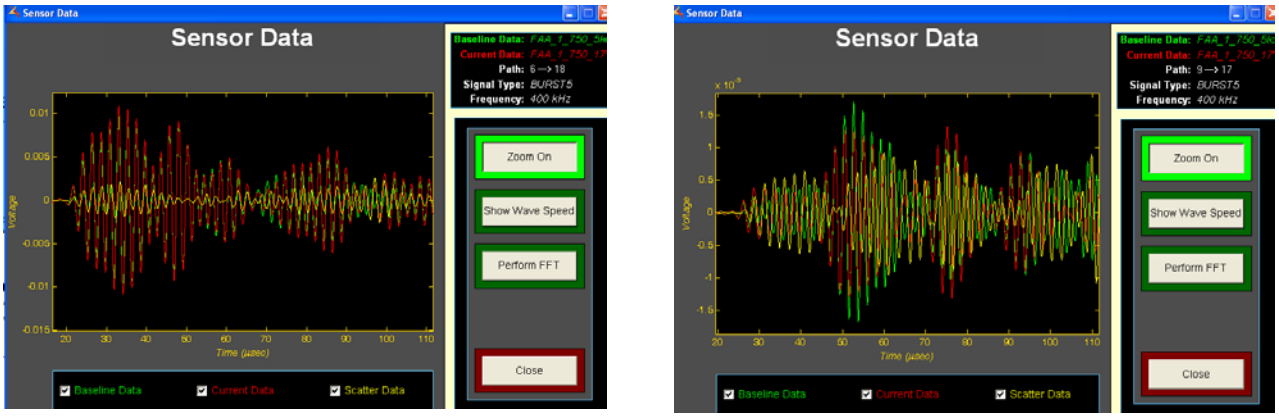

Figure B-19. Typical Signals for Different Paths

The signals from these tests were analyzed and used to determine if there was any crack initiated in the specimens. The specimens were then disassembled to verify if the system correctly detected and located the crack initiation site after a big signal change during the fatigue test.

B.3 SUMMARY.

Table B-1 summarizes previously conducted tests as well as those conducted for this project. The table depicts the survivability and usability of sensors and data.

B.4 REFERENCES.

B-1. MIL-STD-810F, "Department of Defense Test Method Standard for Environmental Engineering Considerations and Laboratory Tests," January 1, 2000.

B-2. Boller, C., Ihn, J.-B., Staszewski, W.J., and Speckmann, H., "Design Principles and Inspection Techniques for Long Life Endurance of Aircraft Structures," *3rd International Workshop on Structural Health Monitoring*, Stanford, California, USA, September 12-14, 2001.

B-3. Beard, J., Kumar, A., Qing, X., Zhang, C., "A Smart Patch System for Monitoring of Bonded Repairs," *5th International Workshop on Structural Health Monitoring*, Stanford, California, USA, September 2005.